LEVEL

AFML-TR-79-4068

STRUCTURAL ASSESSMENT OF INVOLUTES

H. O. Davis and D. F. Vronay

Strategic Systems
Aerojet Solid Propulsion Company
Sacramento, California   95813

June 1979

Final Report
September 1977 - June 1979

AFML/MBM
Air Force Material Laboratory
Wright-Patterson AFB, Ohio   45433

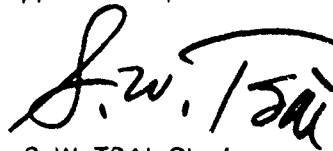D D C
RECEIVED
DEC 11 1979
A

79 12 7 008

NOTICE

When Government drawings, specifications, or other data are used for any purpose other than in connection with a definitely related Government procurement operation, the United States Government thereby incurs no responsibility nor any obligation whatsoever; and the fact that the Government may have formulated, furnished, or in any way supplied the said drawings, specifications, or other data, is not to be regarded by implication or otherwise as in any manner licensing the holder or any other person or corporation, or conveying any rights or permission to manufacture, use, or sell any patented invention that may in any way be related thereto.

This report has been reviewed by the Information Office (OI) and is releasable to the National Technical Information Service (NTIS). At NTIS, it will be available to the general public, including foreign nations.

This technical report has been reviewed and is approved for publication.

N. J. PAGANO, Project Engineer
Mechanics & Surface Interaction Br
Nonmetallic Materials Division

S. W. TSAI, Chief
Mechanics & Surface Interaction Br
Nonmetallic Materials Division

For the Commander

J. M. KELBLE, Chief
Nonmetallic Materials Division

REPORT DOCUMENTATION PAGE		READ INSTRUCTIONS BEFORE COMPLETING FORM
1. REPORT NUMBER AFML-TR-79-4068	2. GOVT ACCESSION NO.	3. RECIPIENT'S CATALOG NUMBER
4. TITLE (and Subtitle) STRUCTURAL ASSESSMENT OF INVOLUTES		5. TYPE OF REPORT & PERIOD COVERED Final rept. Sep 1977 - June 1979 6. PERFORMING ORG. REPORT NUMBER
7. AUTHOR(s) H. O. Davis and D. F. Vronay		8. CONTRACT OR GRANT NUMBER(s) F33615-77-C-5051
9. PERFORMING ORGANIZATION NAME AND ADDRESS Strategic Systems Aerojet Solid Propulsion Company P. O. Box 13400 Sacramento, CA 95813		10. PROGRAM ELEMENT, PROJECT, TASK AREA & WORK UNIT NUMBERS 2420-01-03 01
11. CONTROLLING OFFICE NAME AND ADDRESS Air Force Materials Laboratory (MBM) Wright-Patterson AFB, Ohio, 45433		12. REPORT DATE June 1979 13. NUMBER OF PAGES 151
14. MONITORING AGENCY NAME & ADDRESS(if different from Controlling Office) 155		15. SECURITY CLASS. (of this report) Unclassified 15a. DECLASSIFICATION/DOWNGRADING SCHEDULE

16. DISTRIBUTION STATEMENT (of this Report)

Approved for public release; distribution unlimited.

17. DISTRIBUTION STATEMENT (of the abstract entered in Block 20, if different from Report)

18. SUPPLEMENTARY NOTES

19. KEY WORDS (Continue on reverse side if necessary and identify by block number)

Involute, Cylinder, Laminate, Composite, Behavior Prediction, Mechanical Properties, Carbon/Carbon, Graphite/Epoxy, Elastic, Inelastic

20. ABSTRACT (Continue on reverse side if necessary and identify by block number)

The involute lay-up technique has been utilized for fabrication of ablative and carbon/carbon nozzle components for approximately fifteen years. However, the thermal and structural analyses have always been plagued by the lack of data and, more important, a need for a predictive model. Almost every component designed has a different helix or arc angle and little, if any, ⟶ over

DD FORM 1473   EDITION OF 1 NOV 65 IS OBSOLETE
1 JAN 73

394 703

data existed for each "new" involute configuration. A model for predicting
stress/strain behavior in the cylindrical form using flat laminate mechanical
properties was developed by the Air Force Materials Laboratory. The test
program conducted to verify this model, using empirical results has been com-
pleted. Both a graphite reinforced epoxy and a basic two dimensional carbon/
carbon were tested with variables of arc and helix angles. Based on the lam-
inate properties which were obtained during the test program, predictions were
made for three graphite/epoxy cylinders and fifteen carbon/carbon cylinders
with both uniaxial and combined loading. The cylinders were tested to failure
in axial tension, axial compression, hoop tension, hoop compression, and
clockwise and counterclockwise torsion. The overall predicted strain meas-
urements were in good agreement with the predicted behavior. As expected,
the modeling of the inelastic behavior of the carbon/carbon materials requires
some modifications and interaction to improve the predicted behavior at loads
greater than fifty percent of ultimate strength. However, the model has been
demonstrated to be a useful tool, and it will be used to predict behavior as
new materials and varying arc and helix angles are used in the fabrication
of nozzle components.

FOREWORD

The work described in this final report was performed under Contract
F33615-77-C-5051 by the Strategic Systems Division of the Aerojet Solid
Propulsion Company under the technical direction of Dr. N. J. Pagano (AFML/MBM).

This program can be considered as a part of the continuing efforts by
the Air Force Materials Laboratory to understand and predict the behavior of
C-C involute structures used for rocket nozzle exit cones.

H. O. Davis was the Principal Investigator for this effort. D. F. Vroney,
with the support of Dr. N. J. Pagano, AFML, conducted the analytical studies.
The author gratefully acknowledges the contributions of:

> R. D. Steele - Testing
> K. M. Schalinski - Tool Design
>   and
> George Lucido - Kaiser Aerotech - Fabrication of test
>   articles

The work was initiated in September, 1977, and completed in June, 1979.

Accession For	
NTIS G....&l	✓
DDC TAB	☐
Unannounced	
Justification	
By	
Distribution/	
Availability Codes	
Dist	Avail and/or special
/A	

TABLE OF CONTENTS

FIGURE LIST

FIGURE LIST (cont)

TABLE LIST

TABLE LIST (cont)

APPENDIX

SECTION I

INTRODUCTION

The primary fabrication technique used for cylindrical components, and more specifically exit cones for solid rocket motors, requiring a carbon/carbon material has been the involute layered concept. The involute technique has evolved as a means of positioning layers of material providing a continuous ply orientation from the inside to the outside diameter and from top to bottom. This provides a free standing structural component without overwrap or contained structural backup. Furthermore, with the inherent high temperature capabilities of carbon/carbon materials, the structure functions without insulation except as needed to protect other nozzle and/or chamber components. Alternatives have been evaluated and in some instances tested in rocket motor firings but a fabrication technique to replace the involute concept has not been demonstrated to date. However, failures of composites made by the involute ply orientation during fabrication and also test firings has emphasized the need for better analysis tools. An analysis technique and computer code were developed by the Air Force Materials Laboratory, Reference 1. The program utilizes laminate properties to predict strain and deformation of cylinders fabricated in any involute configuration.

The plies of material in a cylindrical or conical involute section cannot be oriented exactly as a layered laminate. Furthermore, the cylinder or cone with changing axial and cylindrical characteristics in the involute or spiral lay-up orientation presents a difficult problem for prediction of cylinder or cone behavior. The AFML program provides a resolution of the problem for involute cylinders. Selected involute configurations were identified for validation of the computer model in a program started in September 1977 and completed in June 1979.

Reference 1:   Pagano, N.J., "Elastic Response of Rosette Cylinders Under Axi-symmetric Loading" AIAA Journal, Vol. 15, No. 2, Feb. 1977 pp. 159-166

The purpose of this test and analysis program was to verify the capabilities of AFML's computer program to use laminate elastic constants to predict the strain and deformation of involute cylindrical structures when subjected to a variety of individual and combined loading conditions. In addition, the program provides a more comprehensive data base for layered two dimensional (2D) carbon/carbon composites through the testing of laminates, thin wall tubes, and involute cylinders.

The program steps and scope and sequence of major tasks are shown in Figure 1.

Figure 2 describes the involute ply configuration and identifies the terminology used in this report. Two ply patterns are also shown. The ply pattern on the left has a 0 degree helix angle and the one on the right has a 45 degree helix angle.

The objectives of this report are (1) to present the mechanical, physical, and thermal measurements for a graphite unidirectional fabric in an epoxy matrix and bidirectional graphite fabric in a carbonaceous matrix; (2) to compare predicted and measured strains of cylinders in the z and θ planes and 45 degree to the z plane and, (3) to evaluate the effects of non-linear elastic constants on the capability of the program.

Also included in this report are:

1. Descriptions of materials.
2. Processing histories for graphite/epoxy and carbon/carbon materials.
3. Test specimen configurations.
4. Test procedures.
5. Compilation of results.
6. Comparisons of predicted vs measured strain.
7. Evaluations of cylindrical failure mode in relation to measured ultimate strengths.
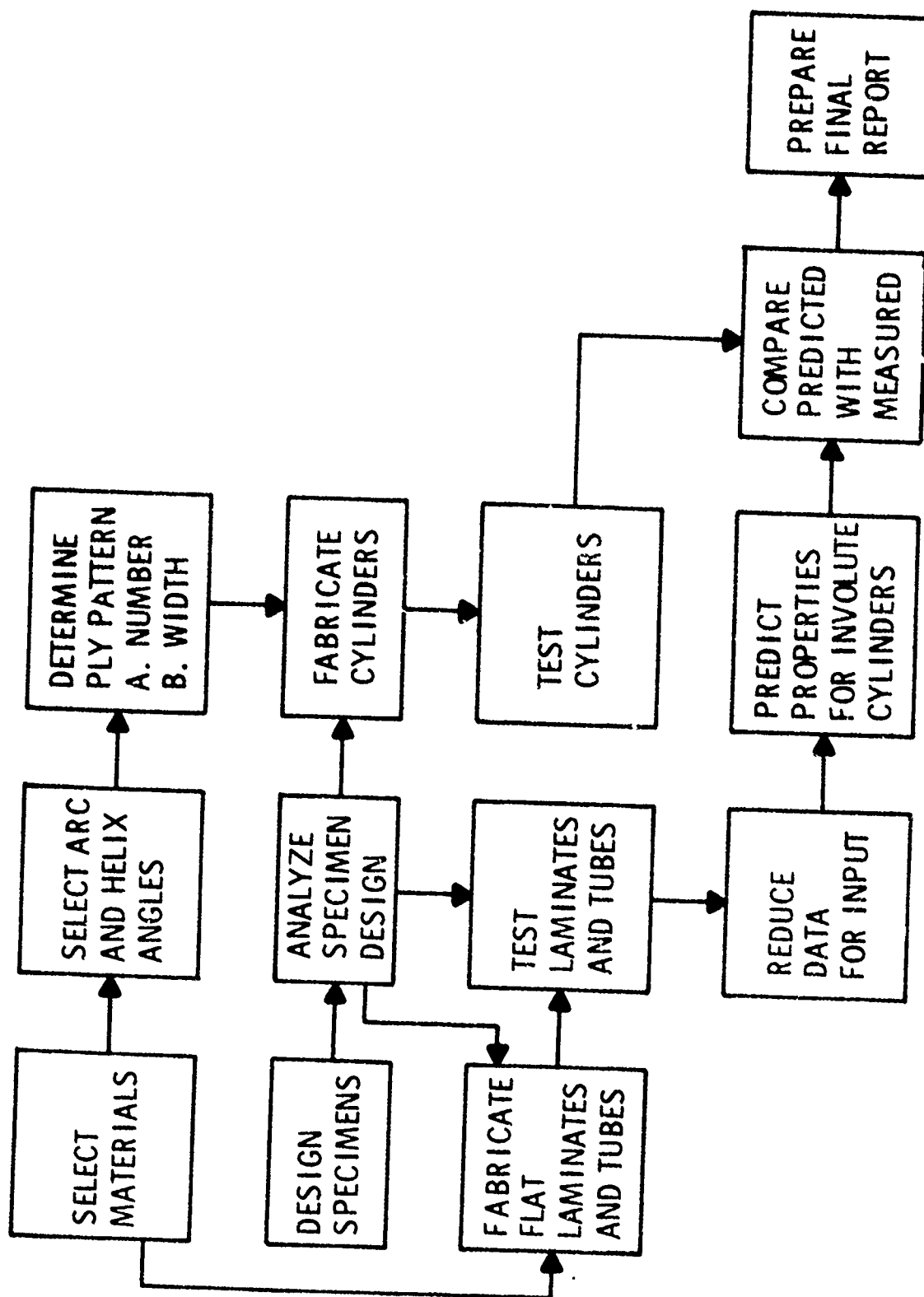
Figure 1. Structural Assessment of Involutes
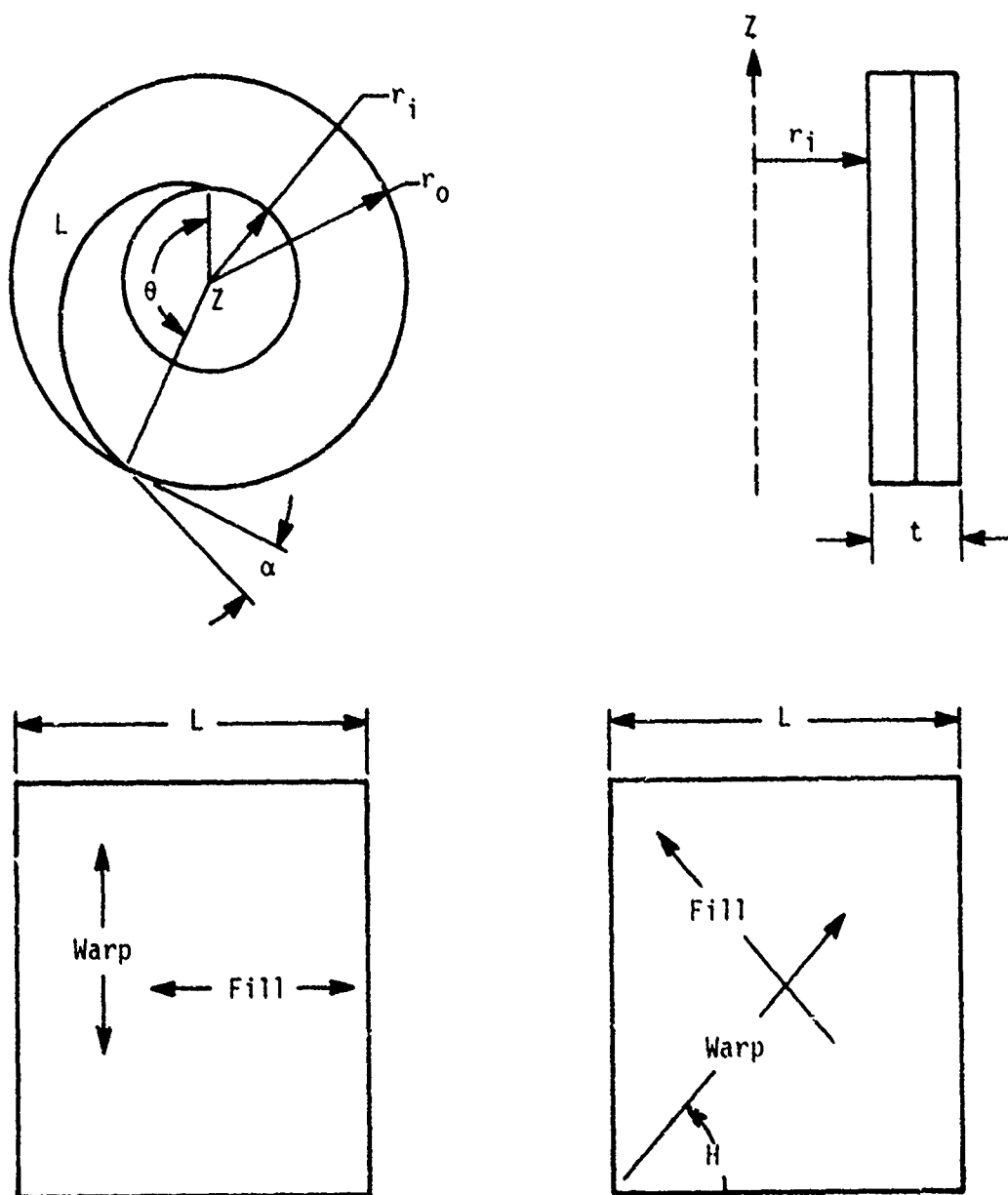
t = Thickness

α = Arc Angle

L = Spiral Length (Ply Width)

θ = Central Angle (Ply Intercept Angle)

H = Helix Angle

r_i = Inside Radius

r_o = Outside Radius

Z = Centerline

Figure 2.   Involute Nomenclature for Cylinders and Cones

SECTION II

SUMMARY

The initial portion of the test program consisted of tension, compression, torsion, and shear testing of graphite/epoxy and resin/pitch WCA fabric reinforced carbon/carbon laminates and thin wall tubes. The carbon/carbon material tested was fabricated by Kaiser Aerotech and is identified as K-Karb 1200. Ultimate strengths in compression, tension, and shear were obtained as well as elastic constants for tension and compression moduli, Poissons ratios, and shear moduli relative to the axes of material symmetry.

The laminate properties shown in Figure 3 were measured and used to predict strain and deformation of cylinders fabricated by the involute process. The tension and compression results from the carbon/carbon laminates are summarized in Table I. The results were in agreement with previous tests of the same material. Density variation for the laminates was less than ± 0.01 grams/cc, indicating a uniform material.

Cylinders were fabricated from both materials using three combinations of involute parameters: 10 degree arc 0 degree helix, 5 degree arc 45 degree helix, and 10 degree arc 45 degree helix. Strain gages were bonded to each cylinder in three equally spaced locations. Axial, circumferential, and 45 degree to warp strain measurements were made for uniaxial and combined loading.

The predicted linear strain behavior for both the graphite/epoxy and carbon/carbon materials produced good agreement with measured results. After the carbon/carbon material became nonlinear at about 75 percent of ultimate strength, the measured strain was significantly greater than predicted. Additional modeling is required using the elastic properties at 75 to 100 percent of ultimate strengths. One nonlinear model for carbon/carbon was demonstrated on one set of 45 degree helix cylinder compression results with good agreement.

Elastic Properties [1], [2]

E_{11}, E_{22}, E_{33}

E_{11}, E_{22}

G_{13}, G_{23}

G_{12}

E_{11}, E_{22}

Ultimate Strength

Laminate

   Tension

   Compression

   Shear

Tubes

   Torsion

   Compression

[1] Properties shown in parentheses were determined in addition to those required for input to the program.

[2] 1 = Warp, 2 = Fill, 3 = Crossply

Figure 3. Test Matrix of Mechanical Properties for the Graphite/Epoxy and Carbon/Carbon Materials

TABLE 1 CARBON/CARBON DATA SUMMARY - WCA REINFORCED

(1.51 gms/cc)

A. Ultimate Strength Properties

Direction of Test	Ultimate Tension, psi	Strain at Failure, Micro in./in.	Ultimate Compression, psi	Strain at Failure, Micro in./in.
Crossply	730	2,600	20,860	25,660
Warp (0°)	9,950	3,910	13,730	5,760
Fill (90°)	5,670	3,900	6,330	4,980

B. Interlaminar Shear Properties

Type Test	Warp psi	Fill psi
Short Beam	3,500	2,400
Rail Shear	2,700	1,800
Notched	1,400	1,100

C. Elastic Properties (Initial Straight Line)

Property	10^6 psi	Poisson Ratios	
E_{11}	2.8	ν_{12}	.037
E_{22}	1.7		
E_{33}	0.7	ν_{13}	.23
G_{12}	0.59		
G_{13}	0.76	ν_{23}	.35
G_{23}	0.60		

SECTION III

TECHNICAL DISCUSSION

The technical discussion is arranged in the same sequence as used to conduct the program. The program was initiated by selecting materials and concluded by comparing predicted versus measured strains. The predictions for uniaxial and combined loading were made prior to testing the cylinders. Laminate testing for the graphite/epoxy and carbon/carbon material was completed prior to initiation of cylinder testing. The selection of a control material was justified in that the test specimens configurations and test procedures were verified prior to testing the primary material, a standard 2D carbon/carbon. Furthermore, the graphite/epoxy exhibited linear behavior to failure, and the carbon/carbon was only linear to approximately 75 percent of ultimate strengths.

The test procedures were based on proven techniques using ASTM standards or other approved methods. The testing to failure of the thin wall cylinders proved not to be satisfactory and produced lower ultimate strengths than the comparable laminate test; however, the elastic constants were equivalent.

The discussion is divided into the following major sections: material selection, processing of laminates and cylinders, mechanical, physical and thermal properties of laminates and thin wall cylinders, testing of cylinders and prediction of cylinder behavior and correlation with measured data.

The laminate and tube test matrix is shown in Figure 4. Rail shear tests, Reference 2, were also measured on graphite/epoxy and carbon/carbon material. Duplicate testing is shown; however, in some cases for compression and tensile moduli, nine test values were obtained. Three values for ultimate strengths were obtained with few exceptions.

Three variations of arc and helix angles of the involute configuration were tested. The complete matrix is shown in Figure 5.

Reference 2: AFML TR-69-311

Material	Graphite/Epoxy	Carbon/Carbon
I. Test Specimen Configuration	A. Plate: 12 x 12 x 0.25 in. B. Plate: 6 x 3 x 3 in. C. Tube: 6 in. long, 2.00 in. ID, 2.125 in. OD	A. Plate: 12 x 12 x 0.25 in. B. Plate: 6 x 3 x 3 in. C. Tube: 6 in. long, 2.00 in. ID, 2.125 in. OD
II. Ply Orientation	0 degrees - All Plates, 6 Tubes 90 degrees - 3 Tubes	0 degrees - All Plates, 6 Tubes 90 degrees - 3 Tubes
III. Uniaxial Loading - Plates, Tubes Deflection and Strain Measurements (Duplicates Required)	• Poisson's Ratio[1] $\frac{F}{W}$, $\frac{CP}{W}$, $\frac{CP}{F}$ (6 Tests) • Shear Modulus: G $G_{1\,2}$, $G_{1\,3}$, $G_{2\,3}$ (6 Tests) • Young's Modulus: E $E_{1\,1}$, $E_{2\,2}$, $E_{3\,3}$ (6 Tests)	• Poisson's Ratio[1] $\frac{F}{W}$, $\frac{CP}{W}$, $\frac{CP}{F}$ (6 Tests) • Shear Modulus: G $G_{1\,2}$, $G_{1\,3}$, $G_{2\,3}$ (6 Tests) • Young's Modulus: E $E_{1\,1}$, $E_{2\,2}$, $E_{3\,3}$ (6 Tests)
IV. Coefficient of Thermal Expansion Measurement - Plates (Duplicates Required)	Room Temperature to 350°F (6 Tests) Warp Fill Crossply	Room Temperature to 4500°F (6 Tests) Warp Fill Crossply

V. Ultimate Strength - Uniaxial Loads
(Triplicates Required)
	Plates
	• Shear - Interlaminar (6 Tests)
	  · Short Beam
	  · Notched
	• Tension (6 Tests)
	  · Warp
	  · Crossply
	• Compression (6 Tests)
	  · Warp
	  · Fill
	
	Tubes
	• Axial Compression (6 Tests)
	  · Warp
	  · Fill
	• Clockwise Torsion (3 Tests)
		Plates
		• Shear - Interlaminar (6 Tests)
		  · Short Beam
		  · Notched
		• Tension (9 Tests)
		  · Warp
		  · Fill
		  · Crossply
		• Compression (9 Tests)
		  · Warp
		  · Fill
		  · Crossply
		
		Tubes
		• Axial Compression (6 Tests)
		  · Warp
		  · Fill
		• Clockwise Torsion (3 Tests)

(1) Denominator indicates load direction axis.   W = 1 - Warp axis
F = 2 - Fill axis
CP = 3 = Crossply axis

Figure 4. Laminate and Tube Test Matrix

Material	Graphite Epoxy	Carbon/Carbon
I. Test Specimen Configuration	Cylinders: 8 in. long, 4.0 in. ID, 5.0 in. OD (3 pcs)	Cylinders: 8 in. long, 4.0 in. ID, 5.0 in. OD (15 pcs)
II. Arc/Helix Matrix Test Specimen Distribution	Arc Angle OD Helix Angle: 0° — 5°: 1 ea, 10°: 1 ea 45° — 5°: 1 ea, 10°: 1 ea	Arc Angle OD Helix Angle: 0° — 5°: 5 ea, 10°: 5 ea 45° — 5°: 5 ea, 10°: 5 ea

III. Uniaxial Loading Deflection and Strain Measurements (Duplicates Required)	• Axial Loading
	  · Tension (6 Tests)
	  · Compression (6 Tests)
	• Torsion
	  · Clockwise (6 Tests)
	  · Counterclockwise (6 Tests)
	• Hoop Tension (6 Tests)
		• Axial Loading
		  · Tension (6 Tests)
		  · Compression (6 Tests)
		• Torsion
		  · Clockwise (6 Tests)
		  · Counterclockwise (6 Tests)
		• Hoop Tension (6 Tests)

IV. Combined Loading Deflection and Strain Measurements (Duplicates Required)	• Axial Tension/Internal Pressure (6 Tests) • Axial Compression/Internal Pressure (6 Tests) • Clockwise Torsion/Internal Pressure (6 Tests) Reduced Gage Section Thickness: t = 0.075 in.	• Axial Tension/Internal Pressure (6 Tests) • Axial Compression/Internal Pressure (6 Tests) • Clockwise Torsion/Internal Pressure (6 Tests) Reduced Gage Section Thickness: t = 0.250 in.
V. Ultimate Strength - Uniaxial Loads[1]	• Axial Compression (3 Tests)	(see table below)

Number of Tests, Arc/Helix Angles — Carbon/Carbon Ultimate Strength:

	10°/0°	5°/45°	10°/45°
• Axial Compression	1	1	1
• Axial Tension	1	1	1
• Hoop Tension (Internal Pressure)	1	1	1
• Torsion - Clockwise		1	1
• Torsion - Counter-clockwise		1	1
	4	5	5

(1) Cylinders previously used to measure strain and deflection below proportional limit.
(2) Total Tests = 152 this page

Figure 5. Involute Cylinder Test Matrix

A. MATERIALS SELECTION

Two materials were required to conduct the evaluation of the computer program. Although the program was directed primarily toward carbon/carbon materials, a material which could be readily fabricated with lower cost and more ideal behavior was needed as a control material. A graphite/epoxy material which had a high anistropy, warp to fill, was selected as the composite material to verify the capability of the computer program to predict elastic response. The material selected is a 4 to 1, warp to fill ratio, fabric containing T-300 1000 filament yarn, a product of Union Carbide. The fabric was woven and impregnated by Fiberite Corporation, Winona, Minn. The material was designated ASPC 3431/934. The woven fabric had been previously evaluated and was chosen for the epoxy system because of its excellent mechanical properties with phenolics.

The certification data for the lot of material used is presented below:

Certification Data for ASPC-3431/34

Date of Manufacture	11-7-77
Lot Number	A8-058.
Resin Solids, %	41
Volatile Content %	0.8
Filler	None
Laminate Flow, % (100 ps)	21.5
Short Beam Shear, psi	
Warp	14,750
Fill	7,130
Flexure Strength, psi	
Warp	240,210
Fill	67,210
Flexure Modulus, psi x 10^{-6}	
Warp	16.7
Fill	5.2
Yarn	Thornel T-300 1000 filament - Grade WYP 90-1/a

Thread Count, yarns/in.

Warp	56
Fill	14
Weave	8 Harness Satin
Resin	Fiberite 934
Cured Ply thickness, in.	0.0062

These data were obtained prior to initiation of fabrication of laminates or cylinders.

The carbon/carbon material was selected based on its wide usage in current high performance solid rocket nozzles, plus the considerable amount of existing data for both laminate and involute structures. The reinforcement is the fabric normally used in low modulus intermediate density two dimensional (2D) carbon/carbon structures. The fabric was impregnated by Fiberite Corporation to make their standard Karbon 408 graphite/phenolic material system. The description of the material and the certification properties of the material used are shown below:

Certification Data for K408

Date of Manufacture	11-2-77
Lot Number	A8-042
Resin Solids, %	32.6
Volatile Content, %	3.0
Filler	Not Reported
Laminate Flow, % (100 psi)	14.8
Short Beam Shear (Warp) psi	3140
Dowel Shear, psi	2870
Flexure Strength (Warp) psi	30590
Flexure Mod (Warp) psi x 10^{-6}	1.9
Fabric	WCA

Weave	Square (Plain)
Thread Count, Yarns/Inch	
Warp	27
Fill	21
Filaments/Yarn Bundle	1440

Other suppliers of these types of materials are available within
the industry. Some fabricators use alternate and interchangeable sources of
resin for making the low modulus carbon/carbon composites; the reinforcement is
generally WCA. The interchangeability of sources is desirable; however, the
only accepted approvals for verification as to equivalency is structural, ther-
mal, and erosive behavior in the use environment.

B. PROCESSING OF LAMINATES, TUBES, AND CYLINDERS

The size and number of laminates, tubes, and cylindrical billets
was determined based on the requirements of the test matrices shown in Fig-
ures 4 and 5. The total test materials consisted of:

<div align="center">

MATERIAL

</div>

	No.	Graphite/Epoxy Size, in.	No.	Carbon/Carbon Size, in.
Laminates	2	12 by 12 by 0.25	2	12 by 12 by 0.25
	2	6 by 3 by 3	2	6 by 3 by 3
Tubes	6	6 long by 2.008 ID and 2.126 OD	9	6 long by 2.008 ID and 2.126 OD
Involute Cylinders	3	8 long by 4.016 ID and 4.803 OD	15	8 long by 4.016 ID and 4.803 OD

1. Graphite/Epoxy

The graphite/epoxy laminates and cylinders were processed by
Kaiser Aerotech, San Leandro, California. The cure pressure was 100, +5, -0

psi, and the final cure phase was for 120, +15, -0 minutes hold at 350, +10, -0°F. The heating rate was 2 to 3°F per minute with a step hold at 250°F for 65, +5, -0 minutes. The laminates, tubes, and cylinders were processed by the same cycle. However, the first attempt to fabricate cylinders from the high flow angle material produced wrinkles in the ply arc angle as shown in Figure 6. The material was not sufficiently stiff in the fill direction to prevent wrinkling. The cylinders were refabricated by staging the material at 180°F for 20 minutes prior to cutting plies and laying-up in the female mandrel. The staging produced a more rigid ply which slipped at the ply interface rather than binding and wrinkling. Ply spacing lines were also placed on the mandrel in order to better control the ply location. The plies were debulked as a unit. It was not necessary to allow for shrinkage; however, the cylinders were made about 0.250 in. excess in the cylinder wall and machined to final configuration.

There was no other difficulty encountered in making the laminates, tubes, and cylinders.

The radiographic and visual inspection indicated satisfactory laminates, tubes, and cylinders by the processes utilized. Further discussion of quality is contained in the test data section. The critical control paramaters were verification of the following.

a.   Material type and lot number.

b.   Ply shape and warp/fill direction.

c.   Number of plies.

d.   Staging of material.

e.   Vacuum 24 in. Hg

f.   Cure/pressure cycle.

g.   Finish dimensions.

h.   No delaminations or wrinkles.

The number of plies, ply width, and arc angle (average shown) for each of the three graphite/epoxy cylinders were verified by using the method described in Reference 1.
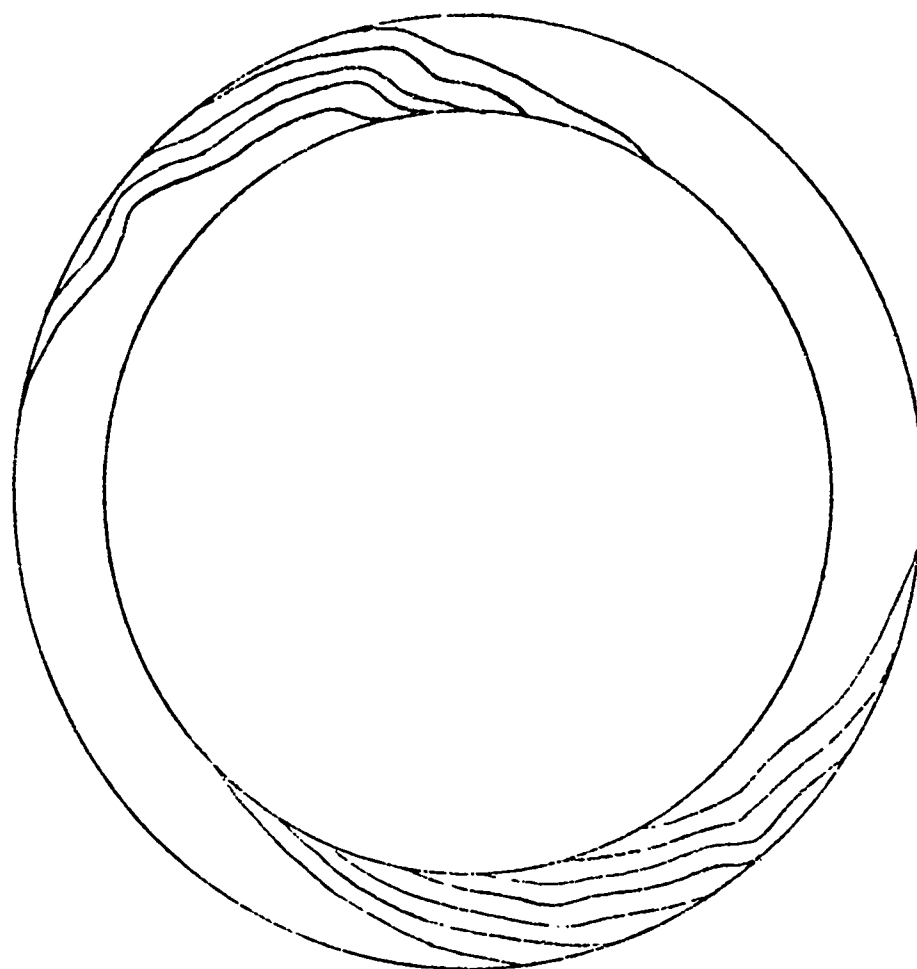
Figure 6.   Discrepant Graphite/Epoxy Cylinder
Showing Ply Pattern Wrinkles

The helix and arc angles for the cylinders were selected to provide a rigorous test of the AFML model, i.e., high arc angles and maximum helix angles. The matrix for the graphite/epoxy is shown in Figure 5.

The number of plies were as follows:

Average Arc Angle, degrees	Helix Angle, degrees	Number Of Plies
5	45	172
10	45	324
10	0	324

The actual and calculated ply width for the 5 degree arc angle cylinder was 7.9 in. for the as-cured billet which was 4.0-in. ID and 5.3-in. OD. The ply width for the 10 degree arc angle was 4.2-in. for the as-cured billet.

2.   Carbon/Carbon

The carbon/carbon laminate, tubes, and cylinders were produced by standard carbon/carbon processing. The process for carbon/carbon structures requires many more steps than the graphite/epoxy. However, the initial process of compaction (debulking) and cure are similar. The processing steps for the carbon/carbon are shown in Figure 7.

All of the compacting (debulking) for the laminates, tubes, and cylinders occurred during the cure/pressure cycle. The cure/pressure cycle included a final cure temperature of 310 ± 10°F at a cure pressure of 200 ± 10 psi. Some of the processing steps, including heating and cooling rates, are considered proprietary by the fabricator. The process temperatures and heating rates were approved prior to fabrication. The maximum temperature and minimum time at conversion temperatures are shown as follows:
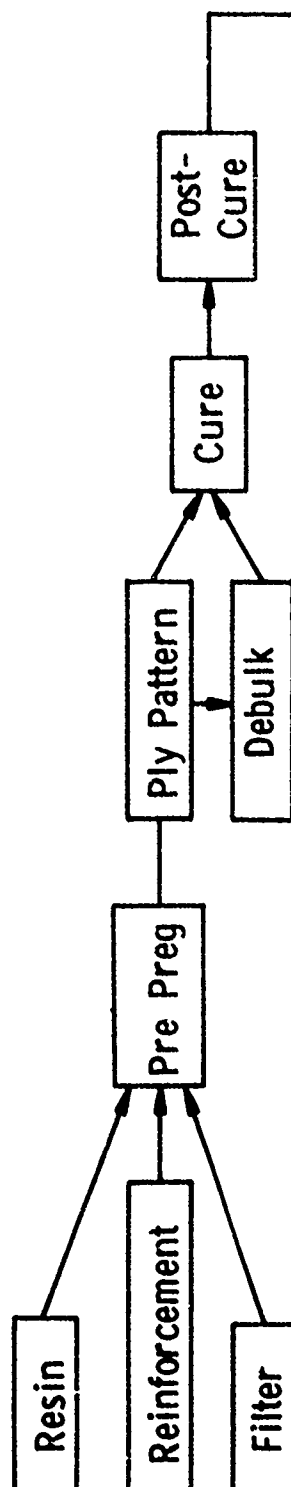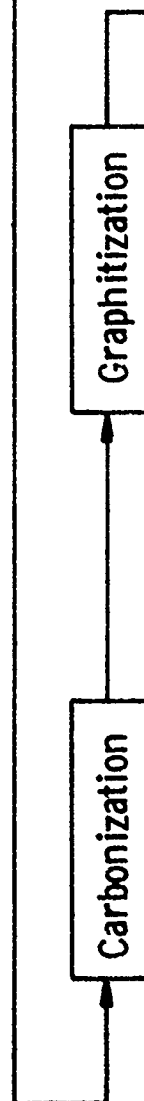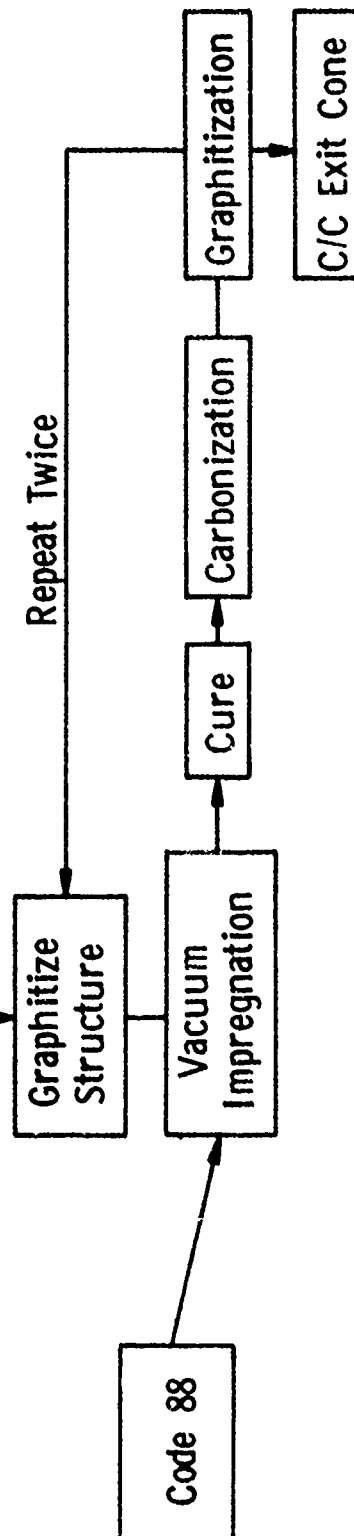
Figure 7. Processing Steps for Production of Carbon/Carbon Material

Process	Maximum Temperature Range °F	Time at Maximum Temperature, hr
Postcure	500 +25, -0	24
Carbonization	1500 +50, -0	4
Graphitization	4500 ± 100	4

The maximum temperature for the conversion process of the Code 88 impregnation also consists of a graphitization cycle at 4500 ± 100°F with a minimum hold of 30 minutes.

All process steps are considered critical to achieving the final required specific gravity of 1.50 minimum. The following major checks and verification were made during the processing of the carbon/carbon laminates, tubes, and cylinders

a. Material identification and lot number

b. Ply dimensions and warp/fill orientation

c. Bagging material and bleeder thickness

d. Ply pattern location and orientation in mold

e. Vacuum 24-in. Hg minimum and cure pressure cycle

f. Removal of surface glaze

g. Weight and dimensions

h. No wrinkles after cure – no delaminations after each process step.

i. Postcure cycle – temperature limits

h. Carbonization cycle – temperature limits

j. Graphitization cycle – temperature limits

k. Impregnation cycle

l. (1) Temperature
   (2) Pressure
   (3) Time

m. Conversion cycles for Code 88

n. Final density

o. Final radiograph inspection for delamination

There were anomalies reported for dimensions on the tube specimens. Seven of the nine tubes had to be refabricated. Graphite sleeve rounding fixtures were used in the inside diameter of the tubes and cylinders. The tubes were made from spliced gore patterns to achieve ply orientation parallel to the surface with arc angle 1 degree. The laminates and cylinders were within the specified dimensions.

C. MECHANICAL AND THERMAL PROPERTY MEASUREMENT

1. Mechanical

A structural analysis was conducted on each test specimen configuration using a conventional two dimensional finite element program. Each of the test specimen configurations shown in Appendix A was analyzed during loading. The properties necessary for the prediction of cylinder behavior are shown in Figure 3. Some of the Poisson's ratios and the moduli were measured in tension and compression; however, the computer code does not discriminate between tension and compression data. The additional properties determined are also included in Figure 3. Additions are shown in parentheses. Ultimate strengths were obtained in tension, compression, torsion, and shear. Initial stress strain measurements were made at least once prior to failure for the elastic constants. All compression specimens were partially loaded and unloaded in tension (approximately 50 percent of ultimate load) prior to the partial and ultimate loading in compression. This has added scope to the program to verify moduli from the identical specimen and eliminate the possible effect of non-uniform material. There were no significant differences between results from the tension only specimens and the tension/compression specimens.

The graphite/epoxy and carbon/carbon specimens had the same configuration except for short beam shear testing. The carbon/carbon specimen was 0.4-in. thick and the graphite/epoxy was 0.250-in. thick. Thicknesses were calculated to produce shear failures rather than tension or compression failures in bending for each of the materials.

a. Graphite/Epoxy

A summary of the average graphite/epoxy mechanical property measurements is shown in Table 2. The values are nominal or average values. All mechanical property measurements are shown in Table 3. The values obtained were as expected with the exception of the very good warp properties of the ASPC 3431/34. The ultimate warp tensile strength was 190,000 psi and the ultimate warp compression was 140,000 psi. This compares favorably with unidirectional tape tensile of approximately 200,000 psi. Furthermore, the fabric provides 40,000 psi fill tensile and 70,000 psi fill compressive strength.

Three types of shear tests were conducted. The average values ranged from 5,000 to 14,400 psi in the warp direction and from 3,600 to 7,000 psi in the fill direction. The low value of 7,000 psi (warp) for the rail shear is not consistent with the other results. The test samples are suspect, possible damage before test or during assembly into the rail shear fixture. The samples were radiographically inspected and no discrepancies could be isolated prior to starting specimen assembly. There was not sufficient material for retest as a result of the material usage for making cross ply tensile specimens.

All of the laminate specimens were checked for fiber volume and resin content and void volume. The values obtained are shown below:

Test Panel	Specific Gravity	Resin Solids, %	Fiber Volume, %	Void Content, %
TP 3431-101-1	1.57[1]	36.9	55.81	-0.376
	1.57	36.5	56.24	-0.318
	1.60[2]	-	-	-
TP 3431-103-3	1.60	31.4	61.7	-0.386
TP 3431-102-2	1.62	31.6	61.5	-0.899
TP 3431-103-3	1.61	30.4	62.8	-0.490

(1) Values were from edge of panel

(2) Taken from center of test panel and is more representative of specimens tested

TABLE 2. SUMMARY OF MECHANICAL PROPERTIES FOR GRAPHITE/EPOXY LAMINATES AND TUBES

TYPE TEST		PSI
TENSILE		
	WARP	190,000
	FILL	41,500
COMPRESSION ULTIMATE		
	WARP	140,000
	FILL	70,000
SHEAR-ULTIMATE		
RAIL		
	WARP	7,000
	FILL	7,000
NOTCHED		
	WARP	6,000
	FILL	3,600
SHORT BEAM		
	WARP	14,400
	FILL	6,600
TUBE COMPRESSION		
	WARP	85,000
	FILL	

TYPE TEST		PSI X 10^{-6}
TENSILE MODULUS		
	WARP	16.5
	FILL	5.1
COMPRESSION MODULUS		
	WARP	16.4
	FILL	5.1
SHEAR MODULUS		
	G_{12}	1.15
	G_{23}	0.65
	G_{13}	0.7

POISSONS RATIO

$\nu_{12} = 0.04$

$\nu_{13} = 0.06$

$\nu_{23} = 0.023$

TABLE 3. MECHANICAL PROPERTIES OF GRAPHITE/EPOXY LAMINATES AND TUBES (SHEET 1 OF 2)

Type Load	Specimen Identification	Fabric Loading Direction	Ultimate Strength psi	Initial Modulus 10^6 psi	Poissons Ratio, v_{12}	Poissons Ratio, v_{21}	Poissons Ratio, v_{31}	Poissons Ratio, v_{32}	Strain at Failure Micro - in./in.
Tension	TP 101-1	Warp	183,600	16.4	0.107				10,600
	TP 101-2	Warp	194,200	17.9	0.144				10,500
	TP 101-3	Warp	193,200	17.3	0.125				10,600
	TP 101-1		NTF(1)	17.1	0.099				
	TP 101-3		NTF	17.0	0.120				
	TP 101-1		NTF	17.4	0.108				
	TP 101-2		NTF	15.9	0.130				
	TP 101-3		NTF	17.0	0.140				
	TP 101-4		NTF	17.0	0.122				
	TP 101-5		NTF	15.1	0.091				
	TP 101-6		NTF	-	0.135				
	Average		190,000	16.6 16.8	0.127 0.121				10,560
Tension	TP 102-1	Fill	42,130	5.0		0.045			9,500
	TP 102-2	Fill	40,330	5.0		0.045			7,850
	TP 102-3	Fill	42,130	5.0		0.030			9,400
	TP 102-1	Fill	NTF	5.16		0.039			
	TP 102-2	Fill	NTF	4.93		0.037			
	TP 102-7	Fill	NTF	5.0		0.044			
	TP 102-8	Fill	NTF	4.9		-			
	TP 102-9	Fill	NTF	5.5		0.039			
				5.4		0.032			
	Average		41,500	5.1		0.039			8,920
Tension	TP 103-1	Crossply	2,060	1.9			0.056	0.230	1,120
	TP 103-2	Crossply	-	-			-	-	
	TP 103-3	Crossply	NTF	1.3			0.05	0.195	1,400
	TP 103-1			1.7			0.07	0.270	
	TP 103-2			-			-	-	
	TP 103-3			1.6			0.07	0.23	
	Average		2,180	1.63			0.062	0.23	1,260

(1) NTF - Not to Failure

Page 29

Type Load	Specimen Identification	Fabric Loading Direction	Ultimate Strength psi	Initial Modulus 10^6 psi	Poissons Ratio, ν_{12}	Poissons Ratio, ν_{21}	Poissons Ratio, ν_{31}	Poissons Ratio, ν_{32}	Strain at Failure Micro - in./in.
Compression	TP 101-4	Warp	129,400	15.7	0.105				8,150
	TP 101-5		143,200	15.6	0.105				9,500
	TP 101-6		146,200	16.3	0.129				8,900
	TP 101-4		NTF	15.6	0.102				
	TP 101-5		NTF	16.9	0.087				
	TP 101-6		NTF	15.8	0.129				
	Average		140,000	16.0	0.10				8,850
Compression	TP 102-7	Fill	70,900	4.9		0.025			15,000
	TP 102-8	Fill	73,700	5.0		0.014			-
	TP 102-9	Fill	73,300	5.4		0.024			16,000
	TP 102-7		NTF	5.1		0.025			
	TP 102-8		NTF	-					
	TP 102-9		NTF	5.0		0.033			
	Average		73,000	5.1		0.024			15,500
Interlaminar Shear	Short Beam 1	Warp	15,070						
	2	Warp	13,810						
	3	Warp	14,510						
	Average		14,400						
	Short Beam 1	Fill	6,210						
	2	Fill	6,330						
	3		7,280						
	Average		6,600						
	Rail Shear 101-6W	Warp	7,700(2)	G_{13} 0.67					
	101-6F	Fill	NTF	G_{23} 0.65					
	Notched 101-7W	Warp	6,295(3)						
	101-8W		3,202(3)						
	101-9W		3,552(3)						
	Average		6,300						

(2) Apparent damage to specimen near attaching point. Did not effect strain measurements.
(3) Specimen loaded without side supports, not to specification.

TABLE 3. MECHANICAL PROPERTIES OF GRAPHITE/EPOXY LAMINATES AND TUBES (SHEET 3 OF 3)

Type Load	Specimen Identification	Fabric Loading Direction	Ultimate Strength psi	Initial Modulus 10^6 psi	Poissons Ratio, v_{12}	Poissons Ratio, v_{21}	Poissons Ratio, v_{31}	Poissons Ratio, v_{32}	Strain at Failure Micro -in./in.
Interlaminar Shear (cont)	Notched 102-4F	Fill	3,740						
	102-5F		3,715						
	102-6F		3,345						
	Average		3,600						
Torsion Shear	Tube-Warp Warp Axial								
	2A-105-1-W	Shear 12	18,580	1.1					
	2A-101-1-W	Shear 12	19,110	1.16					
	Average		18,800	1.1					
	2A-105-1	Shear 21	NTF	1.14					
	2A-102-1	Shear 21	NTF	1.18					
	Average			1.16					
	Tube-Fill Axial								
	2C-101-1	Shear 21	NTF	0.90					
	2C-103-1	Shear 21	NTF	0.95					
	Average			0.92					
Compression	Tube								
	2A-101-1	Warp	85,700	14.9					
	2A-102-1	Warp	NTF	15.4					
	2A-103-1	Warp	87,600	16.9					
	2A-103-1W	Warp	NTF	16.5					
	2A-103-1	Warp	79,880	13.6					
		Warp	NTF	14.1					
	Average		86,650	15.4					
	2C-101-1	Fill	52,650	5.3					
	2C0103-1	Fill	62,080	3.6					
	2C-103-1	Fill	NTF	4.5					
	2A-104-	Fill	56,230	4.5					
			NTF	4.3					
	Average		57,000	4.4					

The calculations for fiber volume and void content were made using 1.76 as the specific gravity of the graphite filament and 1.30 for the resin matrix. The negative void contents are observed quite often for high modulus graphite reinforced laminates. The calculated number is based on a nominal specific gravity. A negative void content is indicative of a low void panel.

A photograph of a tube with and sleeves attached (bonded with epoxy) for torsion and compression testing of the thin wall tubes is shown in Figure 8. Strain gages for axial, hoop and 45 degree measurements are shown bonded in place for test. Three of the tube specimens (configuration) shown in Appendix A) were tested in compression. The average value obtained was 85,000 psi, or approximately one half of the laminate test results.

The thin wall tubes, shown in Appendix A, were designed primarily to obtain the G_{12} shear modulus and to have a backup compression test. The tube was satisfactory for obtaining G_{12} but did not produce ultimate compression strengths comparable to the laminate uniaxial test (configuration in Appendix A). The tube data recorded in Table 3 produced warp compression values approximately 40 percent lower than the values produced by dogbone type specimens, 85,000 psi compared to 140,000 psi. Similarly, the tube fill compression values were approximately 20 percent of the values produced by the dogbone specimens, 57,000 psi compared to 73,000. Although the specimens were analyzed and determined to have satisfactory thickness to gage length dimensions, apparently some buckling occurred. Observation of the failure surface after test showed delamination, separation of plies, and a crushed interface.

The torsion specimens with warp in the axial direction produced a fill tensile failure with the failed surface parallel to warp yarns. The test plan scope did not include torsion tests to failure for tube specimens with the fill in the axial direction.

The tensile and compression failures were characteristic of high modulus graphite fabric reinforced epoxy, Reference 3.

An example of the stress/strain curve for a compression and tensile failure of a laminate is shown in Figures 9 and 10. The strain gages were aligned with the warp surface (axial), fill surface (tang.) and cross ply surface. These strain measurements were used to determine ν_{13} and ν_{12}.

An example of the stress/strain curve for determination of G_{12} (tube specimen) is shown in Figure 11.

The variation of the test results was within that normally obtained for graphite fabric reinforced epoxies. However, the variance was not determined for this test program because of the low frequency of tests with the exception of the elastic moduli for tension and compression.

b.   Carbon/Carbon

The primary emphasis of the laminate and tube testing phase was directed toward obtaining representative values for the carbon/carbon laminates. A summary of the average elastic properties obtained is shown in Table 4. The property measurements obtained include shear modulus G_{12} and G_{21}. Poisson's ratios ν_{21}, ν_{31} were obtained for initial (approximately 50 percent of ultimate) loading of the tensile test.

All of the test results, Table 5, compare favorably with those previously reported for the carbon/carbon material, Reference 4. The density of the laminates varied from 1.50 to 1.51 gm/cc. The ultimate

Reference 3:   MX Upper Stage Motor Advanced Development Program, Volume XI, Part 2, Material Properties, Composites, Plastics, Elastomers

Reference 4:   MX Upper Stage Motor Advanced Development Program, Volume XI, Part 1, Material Properties, Carbon/Carbon
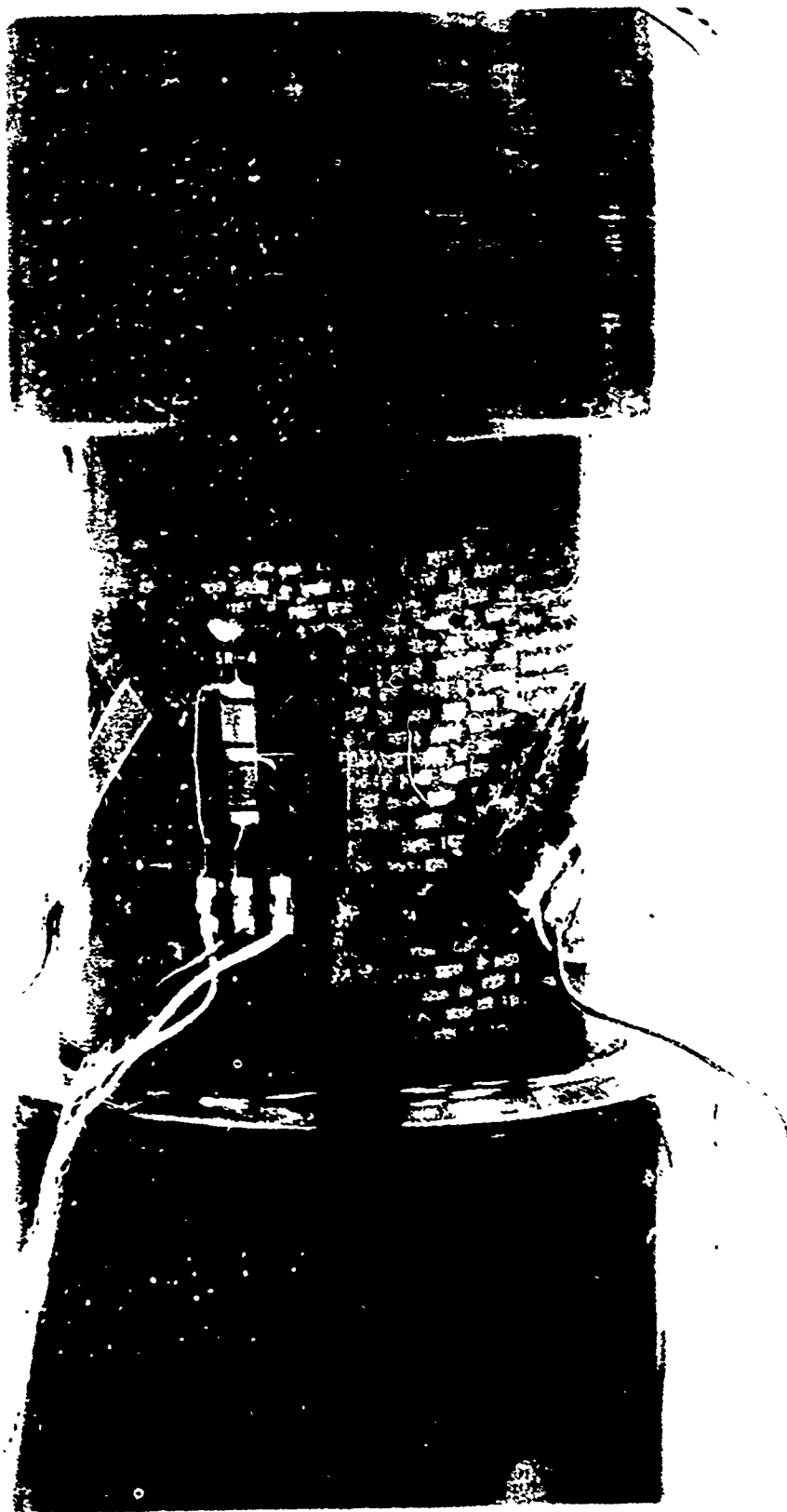
Figure 8. Graphite/Epoxy Tube with Strain Gages and Sleeve Attachment Bonded Ready for Test

TP 102 #7 COMPRESSION TO FAILURE

STRESS, PSI x 10,000
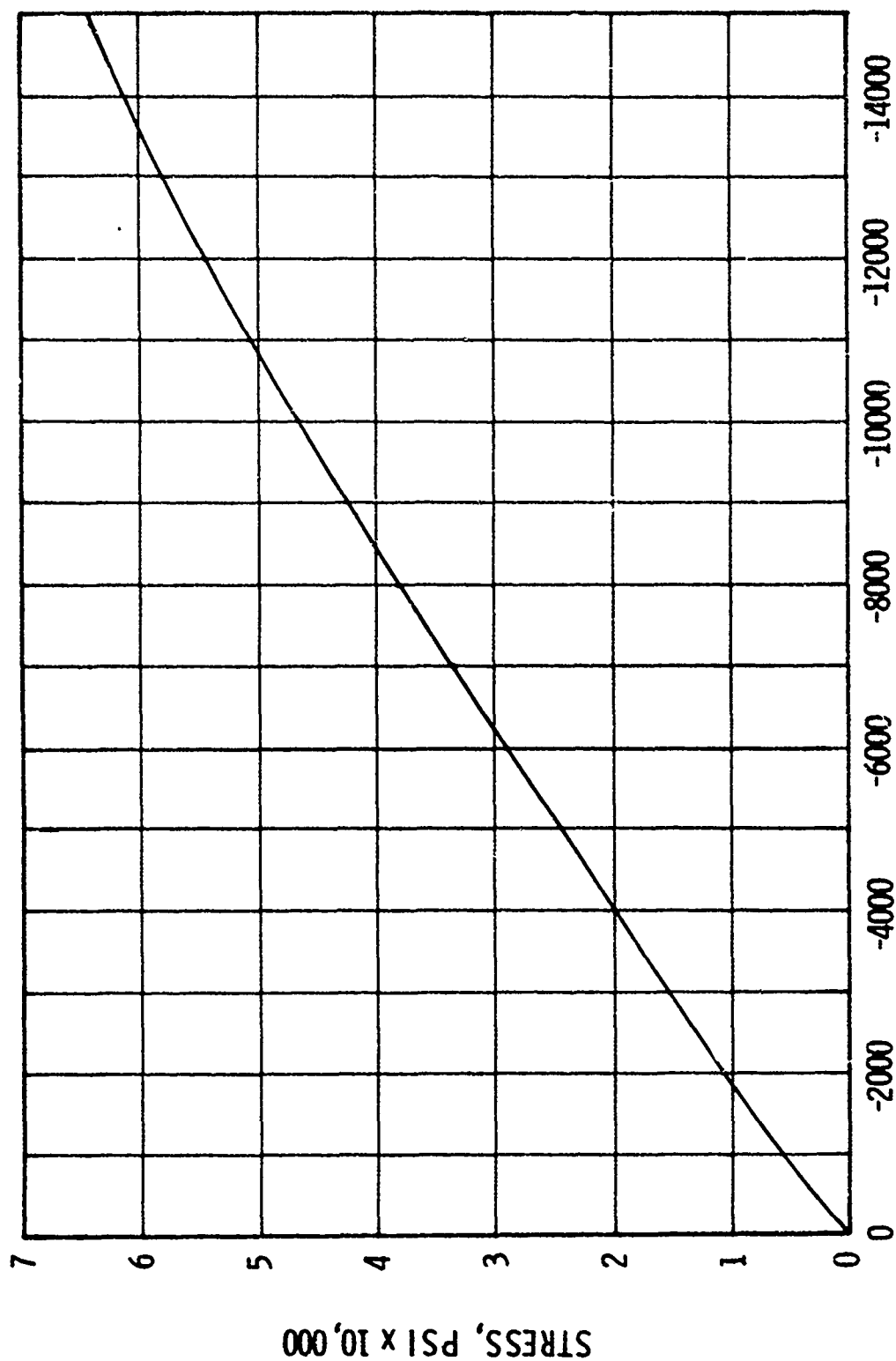
STRAIN (MICRO-IN/IN)

Figure 9. Typical Stress/Strain Curve for Graphite/Epoxy Fill Compressive Test to Failure

TP 101 #1 TENSILE TO FAILURE

STRAIN (MICRO-IN/IN)

STRESS, PSI x10,000
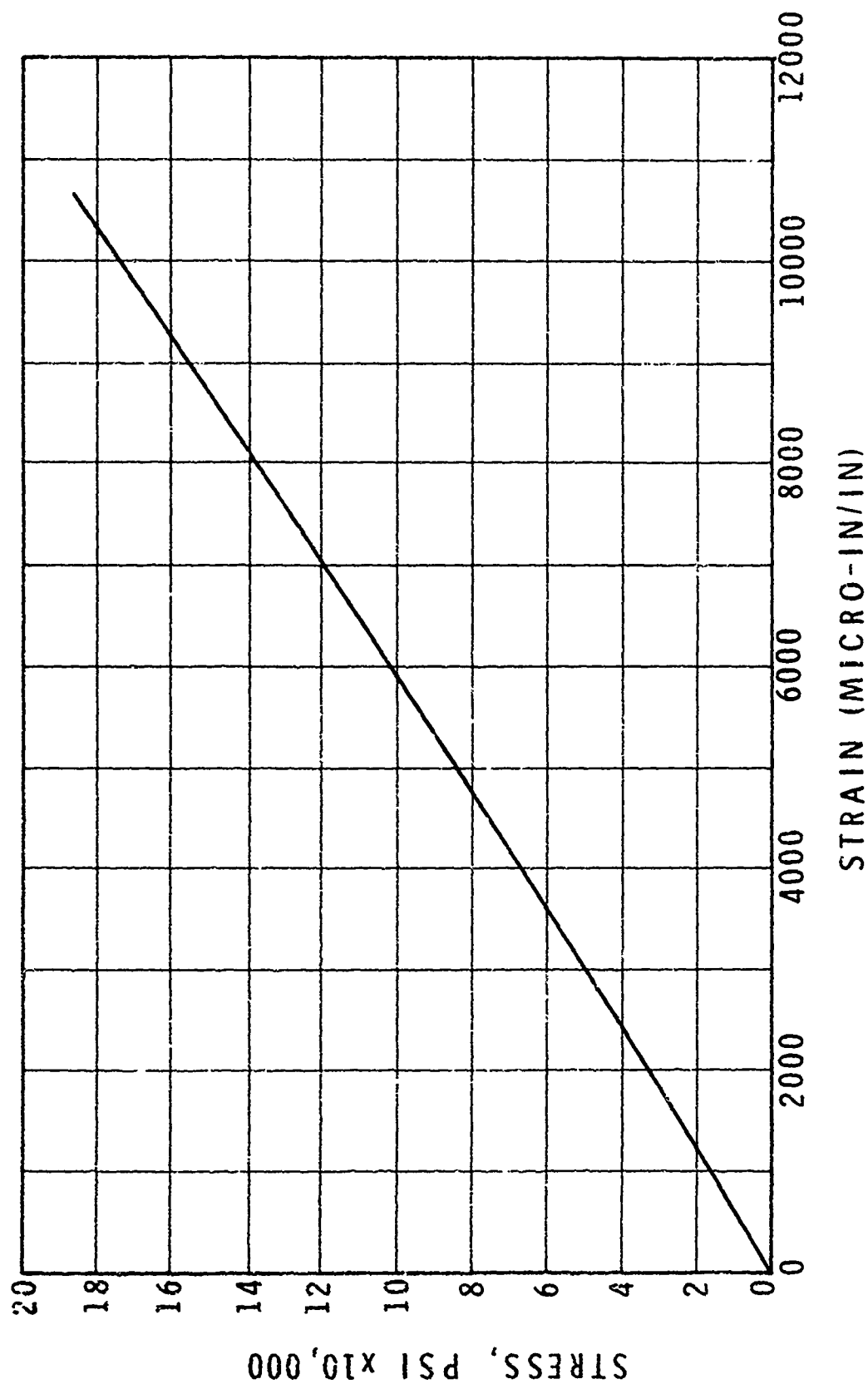
Figure 10. Typical Stress/Strain Curve for Graphite/Epoxy Tensile Loaded to Failure

Page 36
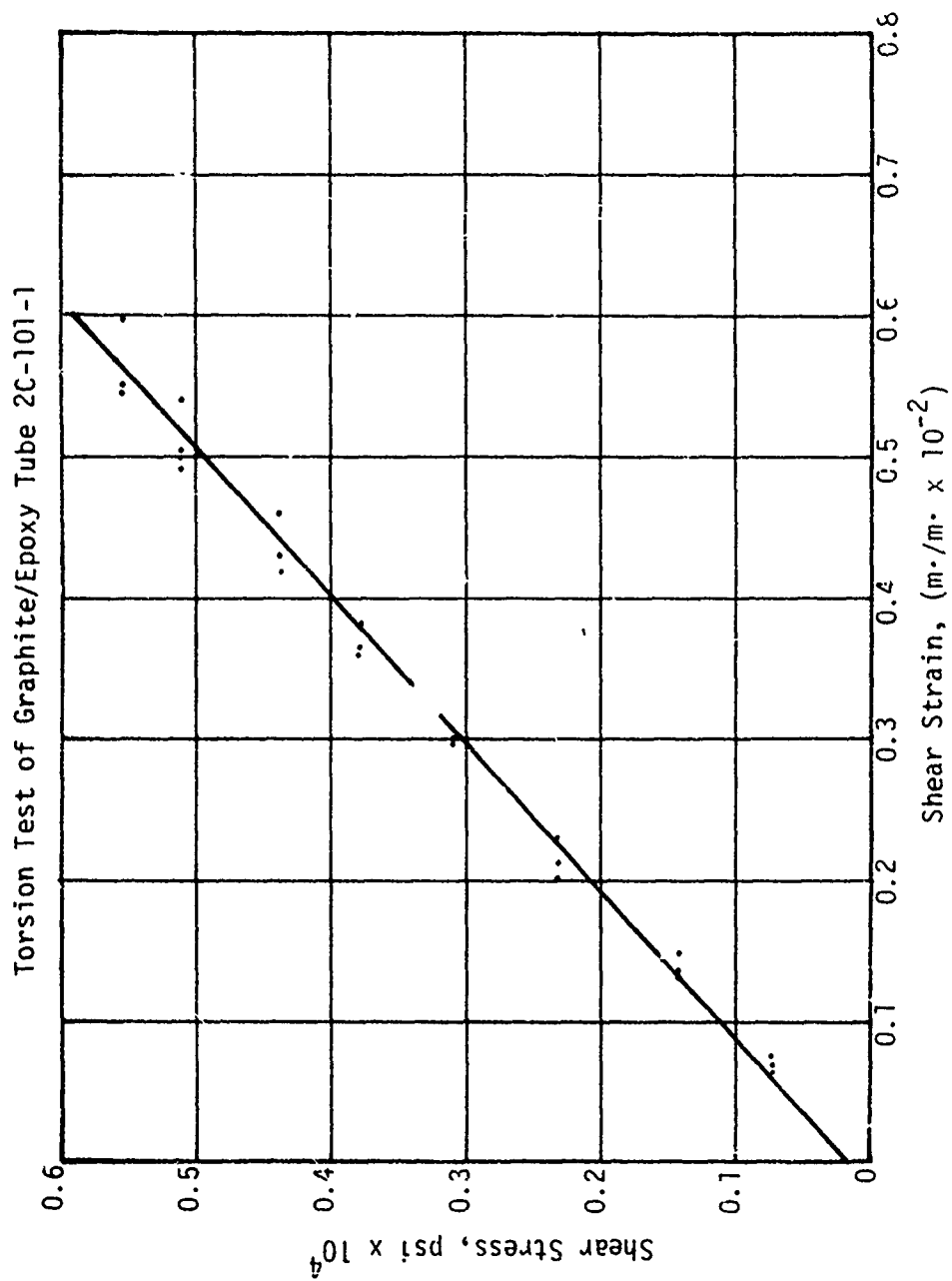
Figure 11. Typical Stress/Strain Curve for Shear Modulus Determination – G_{12}

TABLE 4. ELASTIC CONSTANTS USED FOR ITERATIV [1] PREDICTIONS

TYPE LOAD	ELASTIC CONSTANT	INITIAL STRAIGHT LINE (2)	SECANT 75% OF ULTIMATE	SECANT AT ULTIMATE
Tension	E_{11}	2.8	2.6	2.5
	E_{22}	1.7	1.51	1.4
	E_{33}	.625	.41	0.3
Compression	E_{11}	2.8	2.5	2.4
	E_{22}	1.7	1.57	1.33
	E_{33}	0.75	0.68	0.82
Tension	ν_{13}	0.185 / 0.125 [3]		
	ν_{23}	0.29 / 0.25 [3]		
	ν_{12}	0.065 / 0.072 [3]	.057	.055
Compression	ν_{13}	.23	.283	.58
	ν_{23}	.35	.565	0.90
	ν_{12}	.037	.05	.065
Shear	G_{12}	.59	.3	.3
	G_{21}	.56	–	–
	G_{13}	.76	.721	.65
	G_{23}	.65	.61	.55

(1) Initial moduli and Poisson's ratios taken from initial straight line portion of stress/strain curves. Secant moduli and Poisson's ratio taken at 75% and 100% of ultimate stress.

(2) Tension, compression and shear modulus of elasticity are given psi x 10^{-6}.

(3) These values were obtained from the compression specimens which were loaded in tension less than 50 percent of ultimate prior to failure in compression.

TABLE 5. MECHANICAL PROPERTIES OF CARBON/CARBON LAMINATES AND TUBES (SHEET 1 OF 4)

Type Load	Specimen Identification	Primary Fabric Loading Direction	Ultimate Strength psi	Initial St. Line Modulus 10^6 psi	Poissons Ratio ν_{12}	ν_{21}	ν_{31}	ν_{13}	ν_{32}	ν_{23}	Strain at Failure microin.
Tension	129-TW-1	Warp	9,450	2.7	0.096			0.14			3,780
	129-TW-2		10,710	2.6	0.84			0.14			4,285
	129-TW-3		9,690	2.9	0.069			0.095			3,680
	129-TW-1		NTF(1)	3.0	0.061						
	129-TW-2			2.8	0.062						
	129-TW-3			2.7	0.052						
	129-TCW-1			2.7	0.072						
	129-TCW-2			2.9							
	129-TCW-3			2.8							
	129-TCW-1			3.0	0.053						
	129-TCW-2			2.4	0.05						
	129-TCW-3			2.9	0.058						
	Average		9,950	2.8	0.066			0.125			3,915
Tension	130-TF-1	Fill	5,400	1.7						0.26	3,550
	130-TF-:		5,890	1.45						0.28	5,000
	130-TF		5,720	1.7						0.24	3,150
	130-TF-1		NTF	1.8						0.22	
	130-TF-2			1.5						0.39	
	130-TF-3			1.7						0.16	
	130-TCF-1			1.7		0.22					
	130-TCF-2			1.5		0.13					
	130-TCF-3			2.2		0.06					
	130-TCF-1			1.6		0.23					
	130-TCF-2			1.7		0.17					
	130-TCF-3			1.85		0.05					
	Average		5,670	1.7						0.25	
Tension	127-1	Cross Ply	760	0.61			0.010		0.10		2,600
	127-2		610	0.51			0.0125		0.09		2,019
	127-3		820								
	Average		730	0.56			0.011		0.1		2,310

TABLE 5. MECHANICAL PROPERTIES OF CARBON/CARBON LAMINATES AND TUBES (SHEET 2 OF 4)

Type Load	Specimen Identification	Primary Fabric Loading Direction	Ultimate Strength psi	Initial St. Line Modulus 10^6 psi	Poissons Ratio						Strain at Failure microin.
					12	21	31	13	32	23	
Compression	129-TCW-1	Warp	13,760	2.7	0.04			0.22			
	129-TCW-2		14,100	2.9	0.061			0.30			
	129-TCW-3		13,320	2.8	0.087			0.19			
	129-TCW-3			2.8				0.21			
	Average		13,725	2.8	0.063			0.23			
Compression	130-TCF-1	Fill	6,450	1.7		0.14				0.29	
	130-TCF-2		6,380	1.6		0.16				0.39	
	130-TCF-3		6,170	1.8		0.27				0.36	
	130-TCF-2			1.7		0.23				0.34	
	130-TCF-3			1.9		0.11				0.37	
	Average		6,330	1.74		0.18				0.35	
Compression	128-1	Cross Ply	22,260	0.818			0.074		0.132		23,200
	128-2		20,160	0.721			0.057		0.100		27,800
	128-3		20,150	0.72			0.057		0.14		26,000
	Average		20,860	0.75			0.063		0.12		25,660
Interlaminar Shear	Short Beam 128-1	Warp	3,618								
	128-2		3,413								
	128-3		3,545								
	Average		3,530								
	Short Beam 128-1	Fill	2,506								
	128-2		2,326								
	128-3		2,478								
	Average		2,435								

TABLE 5. MECHANICAL PROPERTIES OF CARBON/CARBON LAMINATES AND TUBES (SHEET 3 OF 4)

Type Load	Specimen Identification	Primary Fabric Loading Direction	Ultimate Strength psi	Initial St. Line Modulus 10^6 psi	ν_{12}	ν_{21}	ν_{31}	ν_{13}	ν_{32}	ν_{23}	Strain at Failure microin.
Interlaminar Shear (cont)	Rail Shear										
	128-1	Warp	2,700	G_{13} 0.78							
	128-2		2,106	G_{13} 0.74							
	Average		2,700	0.76							
	Rail Shear										
	127-1	Warp	1,994	G_{23} 0.65							
	127-2		1,784	G_{23}							
	Average		1,890	0.65							
	Notched										
	129-1	Warp	1,417								
	129-2		1,326								
	129-3		1,511								
	Average		1,420								
	Notched										
	130-1	Fill	940								
	130-2		1,290								
	130-3		1,244								
	Average		1,155								
Torsion	Tubes Warp	Shear 12									
	Axial										
	3-103-1		3,457	G_{12} 0.5							
	3-101-1		3,778	0.64							
	3-105-1		3,227	0.56							
	3-104-1		NTF	0.6							
	3-106-1		NTF	0.61							
	3-102-1		NTF	0.63							
	Average		3,490	0.59							

TABLE 5. MECHANICAL PROPERTIES OF CARBON/CARBON LAMINATES AND TUBES (SHEET 4 OF 4)

Type Load	Specimen Identification	Primary Fabric Loading Direction	Ultimate Strength psi	Initial St. Line Modulus 10^6 psi	Poissons Ratio						Strain at Failure microin.
					ν_{12}	ν_{21}	ν_{31}	ν_{13}	ν_{32}	ν_{23}	
Torsion (cont)	Tubes Fill Axial	Shear 21									
	4-103-1		NTF	G_{21} 0.56							
	4-101-1		NTF	NA							
	4-102-1			NA							
	Average			0.56							
Compression	Tubes Warp Axial	Warp	8,610	2.5	0.095						3,900
	-3-102-1		8,810	2.52	0.09						3,800
			8,805	2.4	0.1						4,500
				2.6	0.10						
				2.8	0.1						
				2.6	0.09						
	Average		8,740	2.6	0.095						4,070
	Tubes Fill Axial	Fill	5,530	2.2		0.082					2,710
	-4-101-1R		4,860	1.8		0.11					3,250
	-4-102-1R		5,730	1.5		0.07					5,450
	-4-103-1	NTF		2.3		0.11					
	-4-101-1R			1.8		0.11					
	-4-102-1R			1.3		-					
	-4-103-1										
	Average		5,370	1.8		0.097					3,800

(1) NTF

tensile strengths ranged from 9,000 to 10,700 psi. The warp compressive
strength was slightly higher ranging from 13,000 to 14,100 psi.

The fill tensile and compressive strengths were slightly
lower than previously reported (Reference 4). The average fill tensile was
5,700 psi and the average fill compressive was 6,300 psi. Ultimate tension
and compression results with the strain at failure are shown in Table 6. The
maximum variation for strain at failure was the fill tension with variation
ranging from 0.3 to 0.5 percent. It is assumed that this is characteristic,
based on review of reported data for similar materials. An example of a
stress/strain curve in tension for the carbon/carbon material is shown in
Figure 12. The shape of the curve indicates stress/strain behavior becoming
nonlinear at about 50 percent of ultimate.

The changes in moduli and Poisson's ratio at 75 percent
of ultimate load and 100 percent of ultimate load are also shown in Table 4
along with initial straight line determinations. These values were used as
the input for analysis to improve predictions of strain for cylinder tested
to ultimate compression. The v_{13} and v_{23} values were not obtained at 75 and
100 percent of ultimate for tensile loading. The initial values were obtained
on the compression specimens. The tensile specimens did not have strain
gages in the cross ply direction.

The cross ply moduli in compression increased with load.
All other moduli decreased with load. The increase in modulus is attributed
to the compacting, which occurs in the porous matrix. As the load compacts
the material, a rather high strain (2 percent at failure) is obtained. The
porosity is reduced, and the reinforcement is loaded in intralaminar rather

Page 43

TABLE 6. MEASURED ULTIMATE STRESSES AND STRAIN AT FAILURE FOR CARBON/CARBON MATERIAL

Panel Designation	Direction of Test	Specimen Number	Ultimate Strength psi	Strain in Micro Inches at Failure
130	Crossply Tension	1	760	2,600
	Crossply Tension	2	610	----*
	Crossply Tension	3	820	2,019
130	Crossply Compression	1	22,260	23,200
	Crossply Compression	2	20,180	27,800
	Crossply Compression	3	20,150	26,000
130	Fill Tension	1	5,400	3,550
	Fill Tension	2	5,890	5,000
	Fill Tension	3	5,720	3,150
130	Fill Compression	1	6,450	6,100
	Fill Compression	2	6,380	5,350
	Fill Compression	3	6,170	4,500
129	Warp Tensile	1	9,453	3,780
	Warp Tensile	2	10,710	4,285
	Warp Tensile	3	9,690	3,680
129	Warp Compression	1	13,760	6,075
	Warp Compression	2	14,100	5,900
	Warp Compression	3	13,320	5,300

* Data calibration questionable
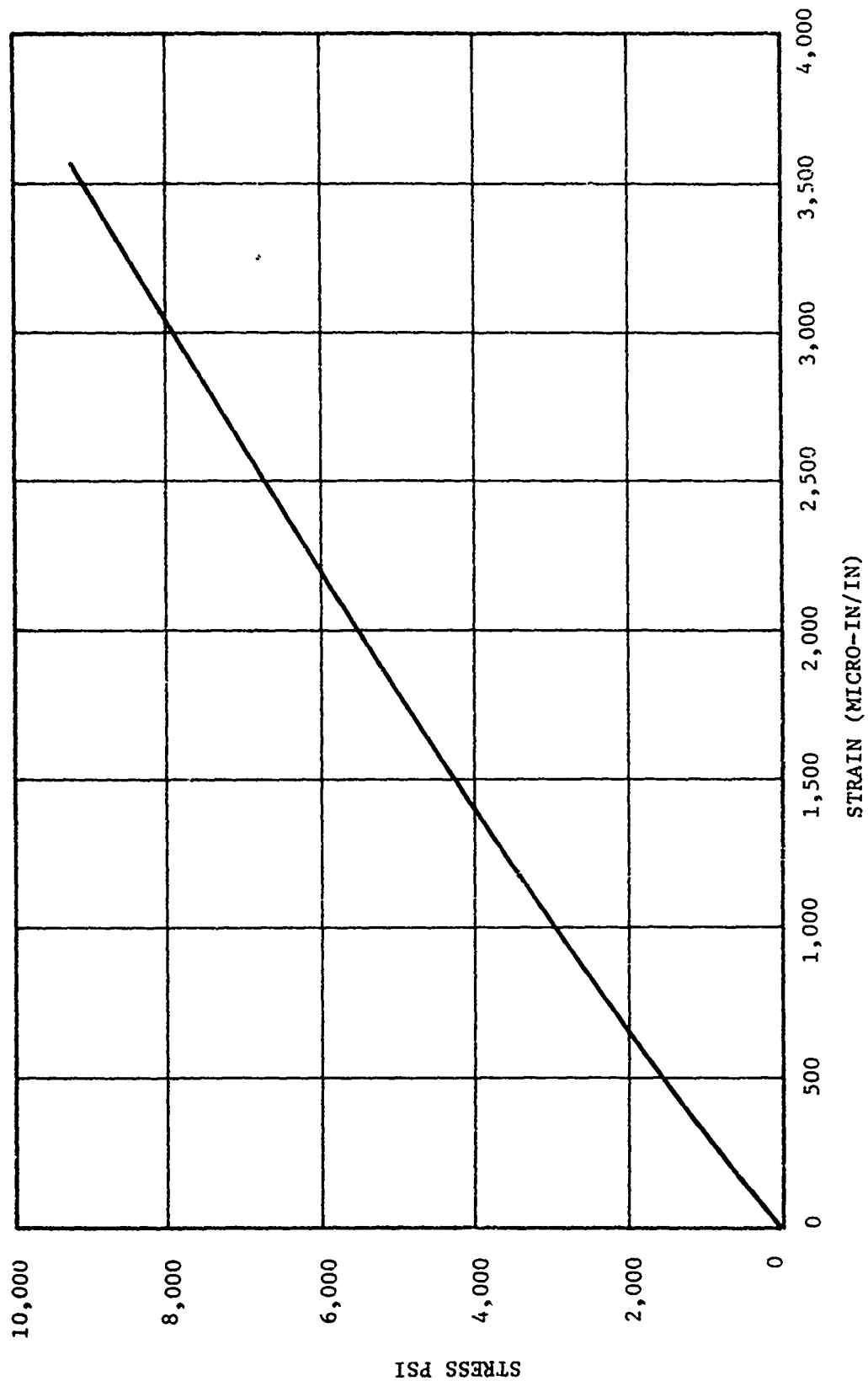
Figure 12. Typical Stress/Strain for Carbon/Carbon Tensile Loading – Warp Direction

Page 45

than interlaminar shear, and the material becomes more rigid with load. The compression ν_{13} and ν_{12} also increase with load. The initial value was 0.23 and increased to 0,58 at failure for ν_{13}.

All values obtained for initial straight line moduli, Poisson's ratios, and ultimate strengths are contained in Table 5.

A typical stress/strain curve for determination of initial shear modulus, G_{12}, is shown in Figure 13. All shear data were plotted, and G_{12} was calculated for the initial straight line as well as for 75 percent of ultimate to failure. The G_{12} shear moduli decreased from 0.6×10^{6} psi to 0.3×10^{6} psi.

A typical stress/strain curve for the carbon/carbon material loaded to failure in compression is shown in Figure 14. Average modulus values decreased from 2.8 to 2.5×10^{6} psi at failure.

c.   Tube Versus Laminate Data

The graphite/epoxy and carbon/carbon tube test in compression produced lower values than the laminate test for the warp or fill direction. The variation for the graphite/epoxy is discussed above. For the carbon/carbon the axial compression tube values were almost 4,000 psi lower than the laminate warp direction. However, the fill values were approximately the same (5,340 psi average for the tubes and 5,760 psi average for the laminates).

Based on these empirical results, it appears that the failure mode was the same for the fill specimens but not for the higher strength warp. It is likely that buckling occurred in the tube specimens where the warp is in the primary load direction.

Page 46
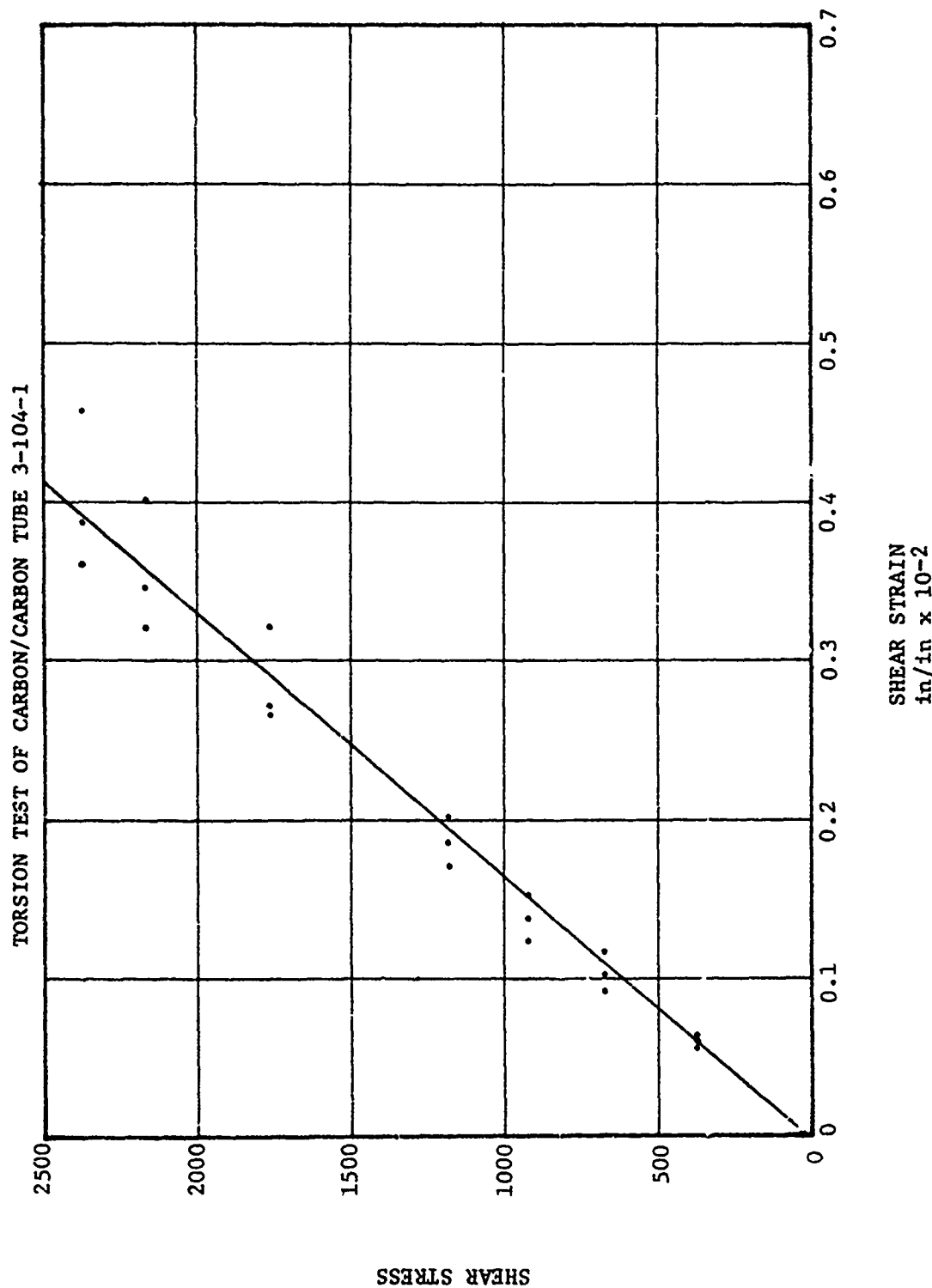
Figure 13. Typical Stress/Strain Curve for Shear Modulus Determination – G_{12}
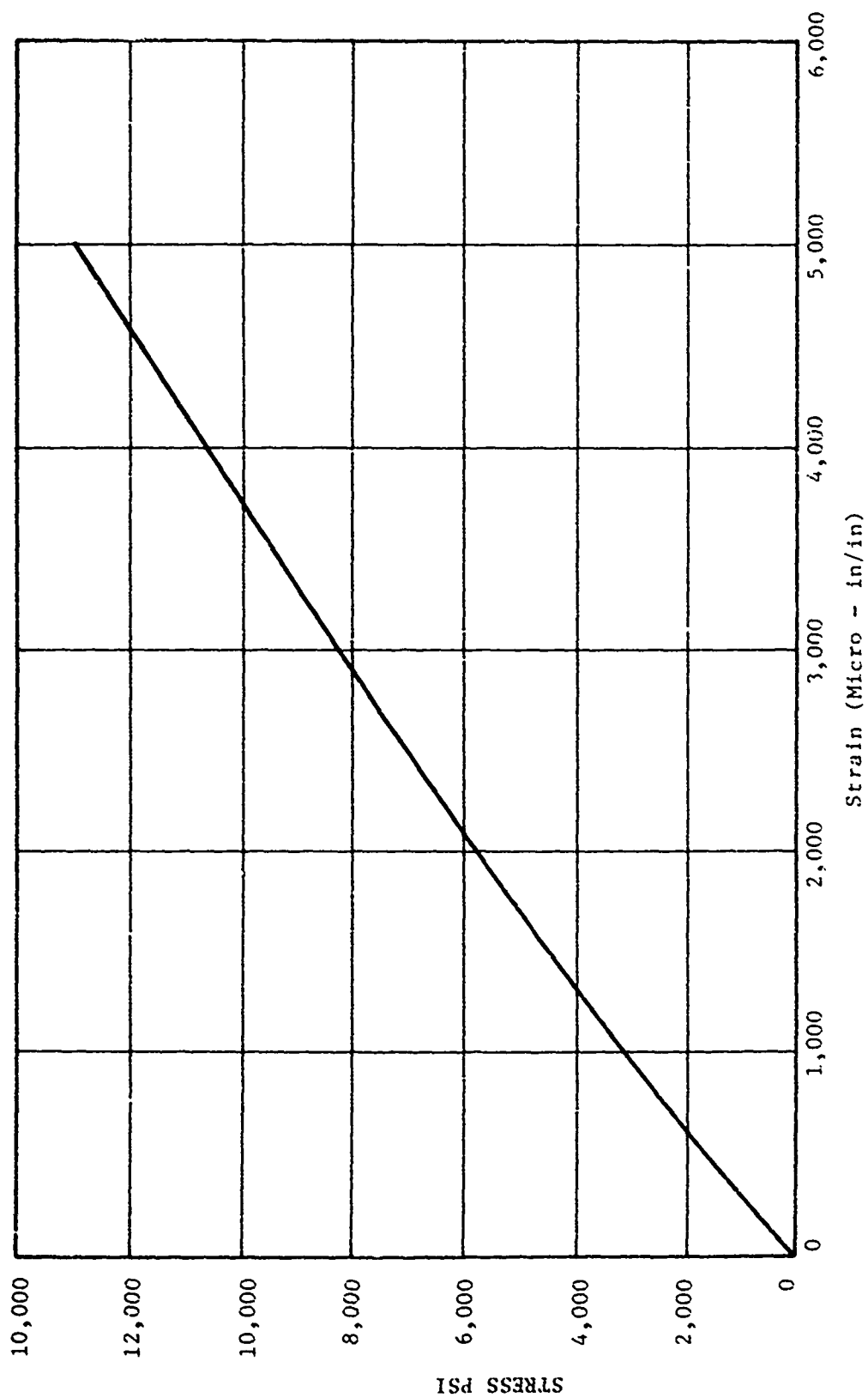
Figure 14. Typical Stress/Strain Curve for Carbon/Carbon Compression Loading to Failure – Warp Direction

The moduli and Poisson's ratio from laminates and tubes were in much better agreement. The tube moduli and Poisson's ratio were not used for prediction of behavior for the cylinders. However, it appears that either laminate or tube data could be used. For example, the warp modulus was 2.6×10^6 psi from the tubes and 2.8×10^6 psi for laminates. Fill modulus was 1.8×10^6 psi for the tubes compared to 1.74×10^6 psi for the laminates. The average Poisson's ratio ν_{12} from the tubes was 0.095, and from the laminate was 0.063. The tube ν_{21} was 0.097 compared to 0.18 from the laminates.

The tubes provided the only source for the G_{12} and G_{21} as well as the ultimate shear strength in torsion. All test results are listed in Table 5. The ultimate shear strength of 3490 psi is similar to the reported through fabric shear strength of 3800 psi, Reference 5.

d.   Physical Property Measurement

The physical properties of selected specimens from laminates and tubes were documented. In general, results were satisfactory. One of the test specimens from the graphite/epoxy laminate had a relative low fiber volume percentage; however, all the mechanical properties taken from this laminate were satisfactory. There were no anomolies recorded for the carbon/carbon laminates and tubes which were tested.

(1)   Graphite/Epoxy

The specific gravity, resin solids, fiber volume, and void content were determined on five specimens. With the exception of test panel 101, the results were satisfactory. The results are shown in Section III C. Specific gravity was below 1.60 for TP 101, and the percent resin was high, 36 percent. Apparently, the area tested did not bleed resin as well as the remaining samples. Tensile, compression, and shear specimens

---

Reference 5:   Data Reported by G. Lucido, Kaiser Aerotech, Telephone Conversation, February 1979.

Page 49

were taken from this laminate. The values obtained did not indicate an un-
satisfactory test panel. The retest for specific gravity produced a value
of 1.60. This indicates an edge effect on the test panel designated 101
with the outside edge being high in resin. This could have been produced
by either a lack of pressure or resin bleed during cure. It is not believed
that mechanical properties were taken from material with the high resin con-
dition.

(2) Carbon/Carbon

A specific gravity for carbon/carbon laminates and
tubes ranged from 1.50 to 1.51. The range of values and density distribution
for the 3 in. thick laminates was also 1.50 to 1.51. Density distribution was
determined by slices from the 3 in. thick laminates.

Typical photomicrographs of the 3 in. thick lam-
inates were also taken for documentation of the matrix/reinforcement char-
acteristics. These photomicrographs were also used for comparison to a
typical section of a carbon/carbon involute cylinder. The photomicrographs
are shown in Figures 15 and 16. The typical void pattern in low density car-
bon/carbon was observed throughout the samples mounted for photomicrographs.

One of the contributing factors to the lower
strength and modulus in the fill direction is also shown by Figures 15 and 16.
The fill yarns have the typical greater bend height and smaller radius. This
results from the greater shrinkage of the fill yarns during the conversion
processing from rayon to graphite.

e. Thermal Expansion

Thermal expansion measurements in the warp, fill, and
crossply directions were made for both the graphite/epoxy and carbon/carbon

Figure 15. Carbon/Carbon Photomicrographs 100X Showing Bend in Fill Yarns and Voids (Dark Areas) in Warp Yarn Matrix - Typical

Figure 16 Carbon/Carbon Photomicrographs 100X Showing Bend in Warp Yarn and Voids (Dark Areas) in Fill Yarn Resin Matrix - Typical

materials. The temperature range for the graphite/epoxy was RT to 350°F and RT to 5000°F for the carbon/carbon materials. A quartz dilatometer was used for the graphite/epoxy and for the carbon/carbon up to 1500°F. The carbon/carbon specimen was also evaluated from RT to 5000°F in a graphite dilatometer.

The results are presented in Figure 17 through 24. Curves are plotted as unit thermal expansion (in./in.) versus temperature (°F). As expected the greatest thermal expansion is in the crossply direction for both the graphite/epoxy and carbon/carbon material.

The effects of weave, concentration of warp and fill yarns, and type of matrix were demonstrated in the values obtained. For example both weave and yarn concentration effects are shown in comparing warp to fill unit thermal expansion for the graphite/epoxy. At 350°F the unit thermal expansion for the fill direction (Figure 17) is 5.5 times the warp direction (Figure 18). The warp to fill weave count is four to one. The crossply unit thermal expansion (Figure 19) at 350°F is 45 times that of the warp. All three unit thermal expansion curves are shown in Figure 20.

The carbon/carbon anisotropy in thermal expansion is not great. At 4500°F the fill is only slightly higher than the warp and the crossply unit thermal expansion is only 1.6 times that of the warp direction. The warp thermal expansion is shown in Figure 21 and, the fill in Figure 22. The crossply specimen thermal expansion peaked at 4500°F (maximum process temperature) and started to shrink as shown in Figure 23. This behavior of slope change for thermal expansion is characteristic of carbon/carbon materials when the maximum process temperature is exceeded. The change is evidence of additional crystalline structure change at the higher temperature. The comparative unit thermal expansion for the carbon/carbon material is shown in Figure 24.
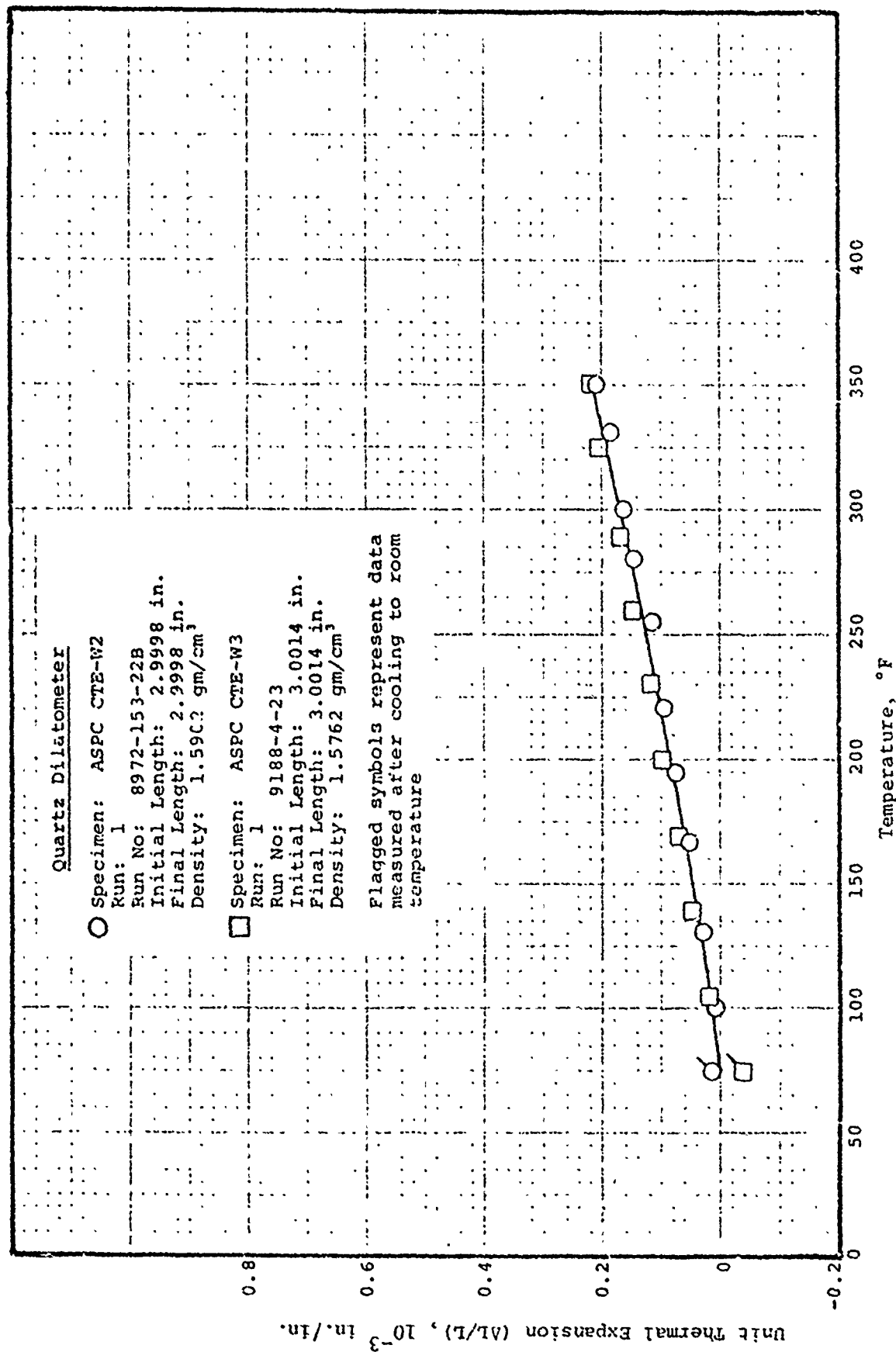
Figure 17. Unit Thermal Expansion of Aerojet 3441/934 Graphite Epoxy in the Warp Direction

Quartz Dilatometer

○ Specimen: ASPC CTE-W2
Run: 1
Run No: 8972-153-22B
Initial Length: 2.9998 in.
Final Length: 2.9998 in.
Density: 1.5902 gm/cm³

□ Specimen: ASPC CTE-W3
Run: 1
Run No: 9188-4-23
Initial Length: 3.0014 in.
Final Length: 3.0014 in.
Density: 1.5762 gm/cm³

Flagged symbols represent data measured after cooling to room temperature

X-axis: Temperature, °F
Y-axis: Unit Thermal Expansion (ΔL/L), 10⁻³ in./in.

Page 53

Figure 18. Unit Thermal Expansion of Aerojet 3431/934 Graphite Epoxy in the Fill Direction
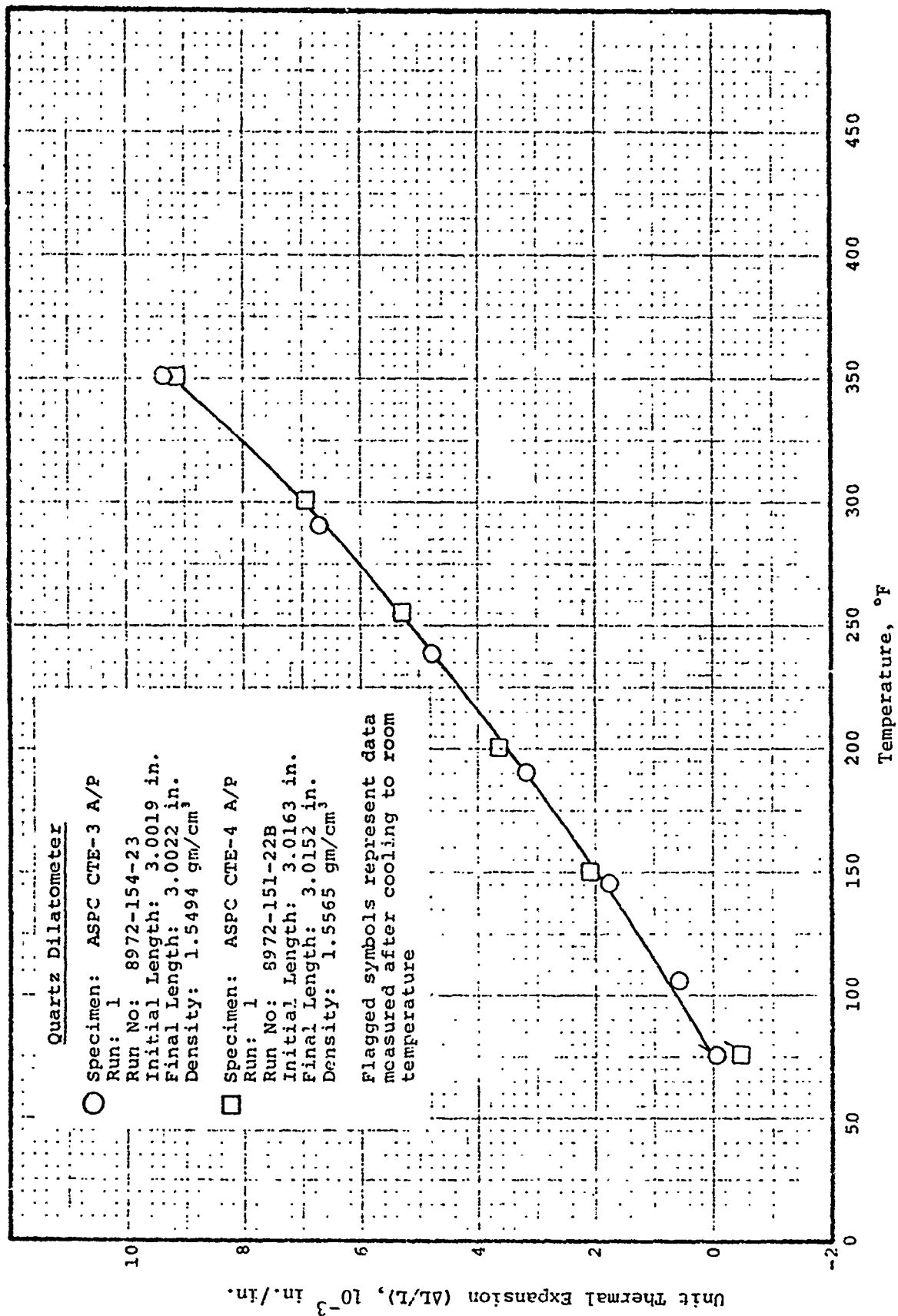
Figure 19. Unit Thermal Expansion of Aerojet 3431/934 Graphite Epoxy in the Crossply Direction
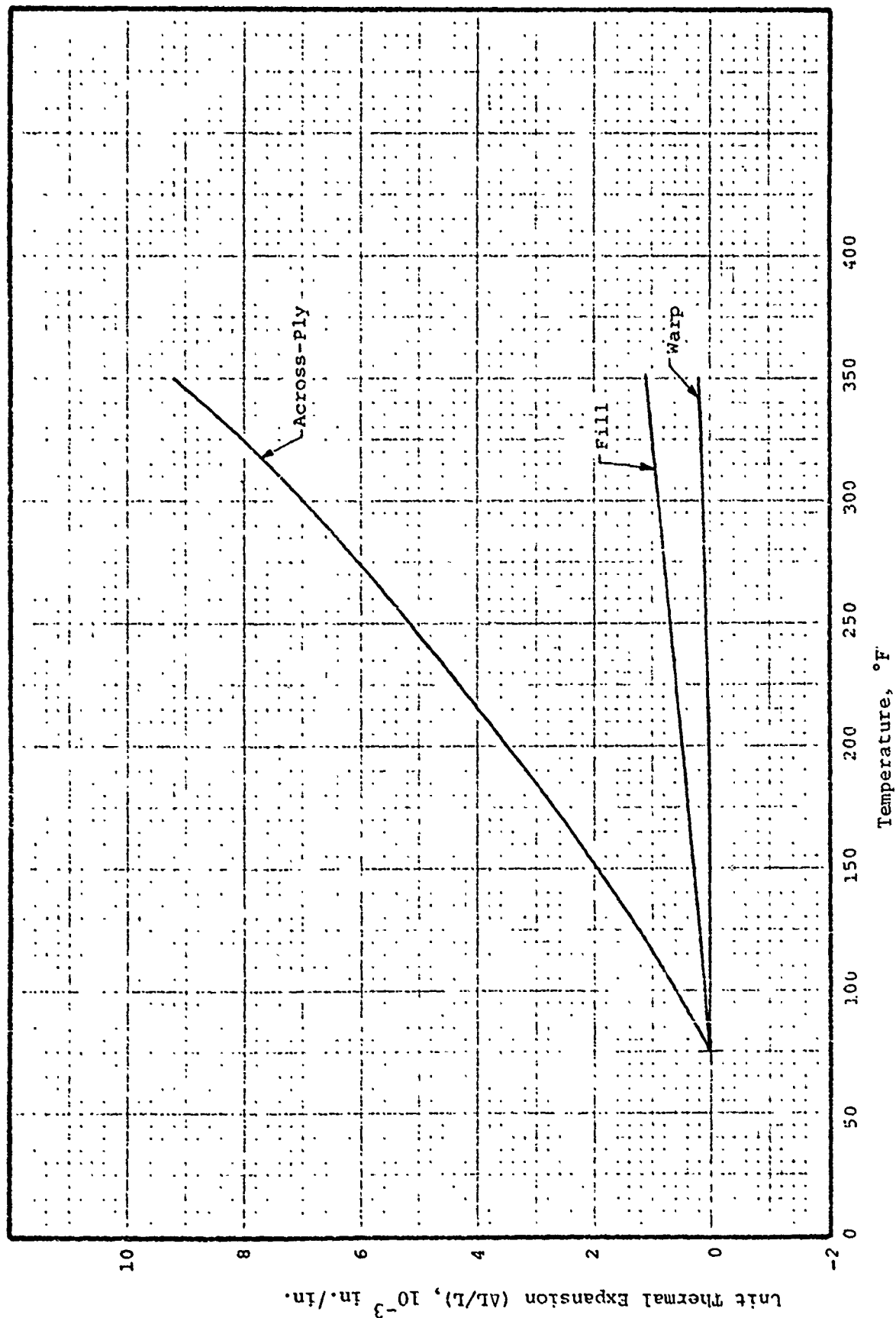
Figure 20. Comparison of Unit Thermal Expansion of Aerojet 3431/934 Graphite/Epoxy between the Warp, Fill, and Crossply Directions
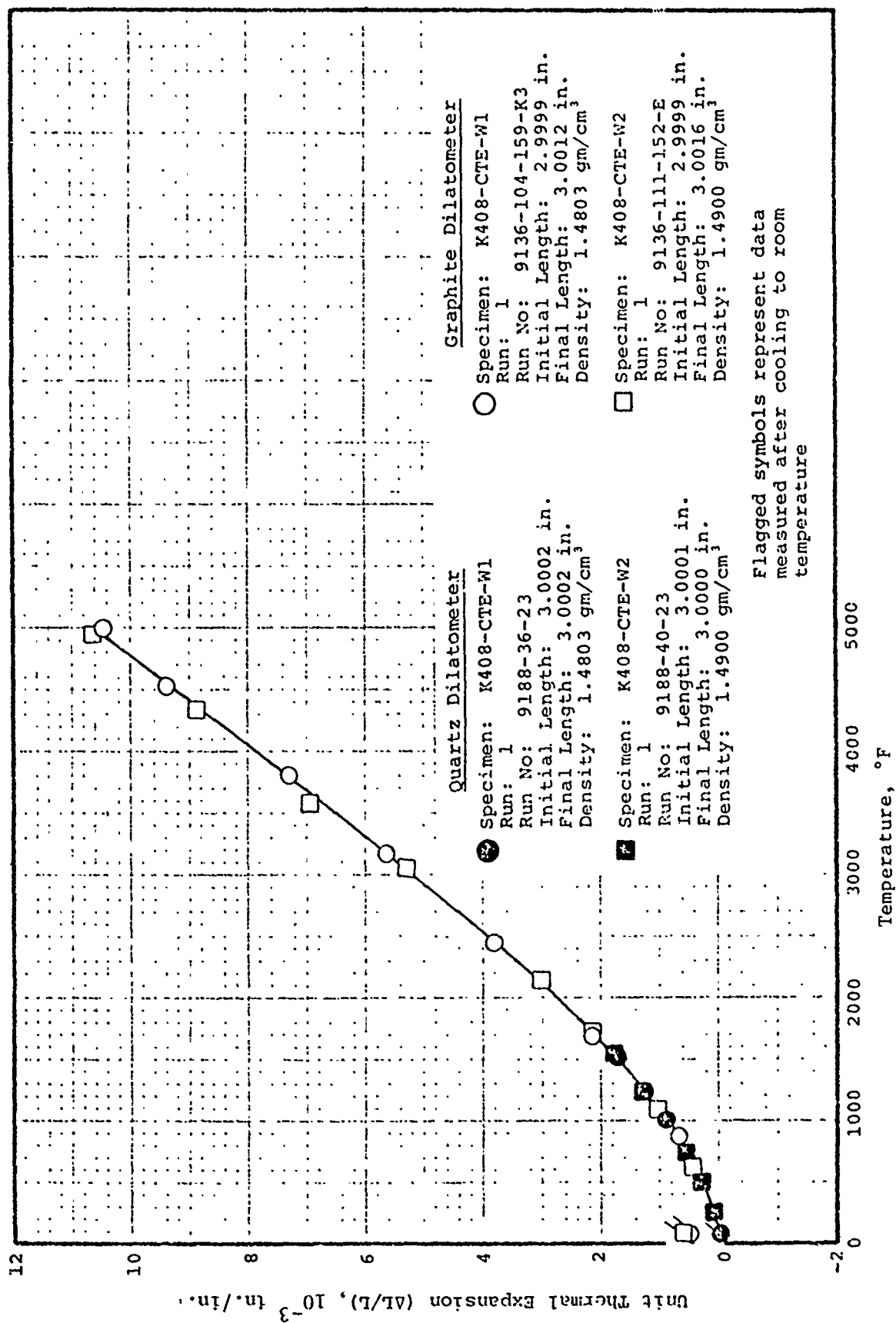
Figure 21. The Unit Thermal Expansion of K408 Carbon/Carbon in the Warp Direction
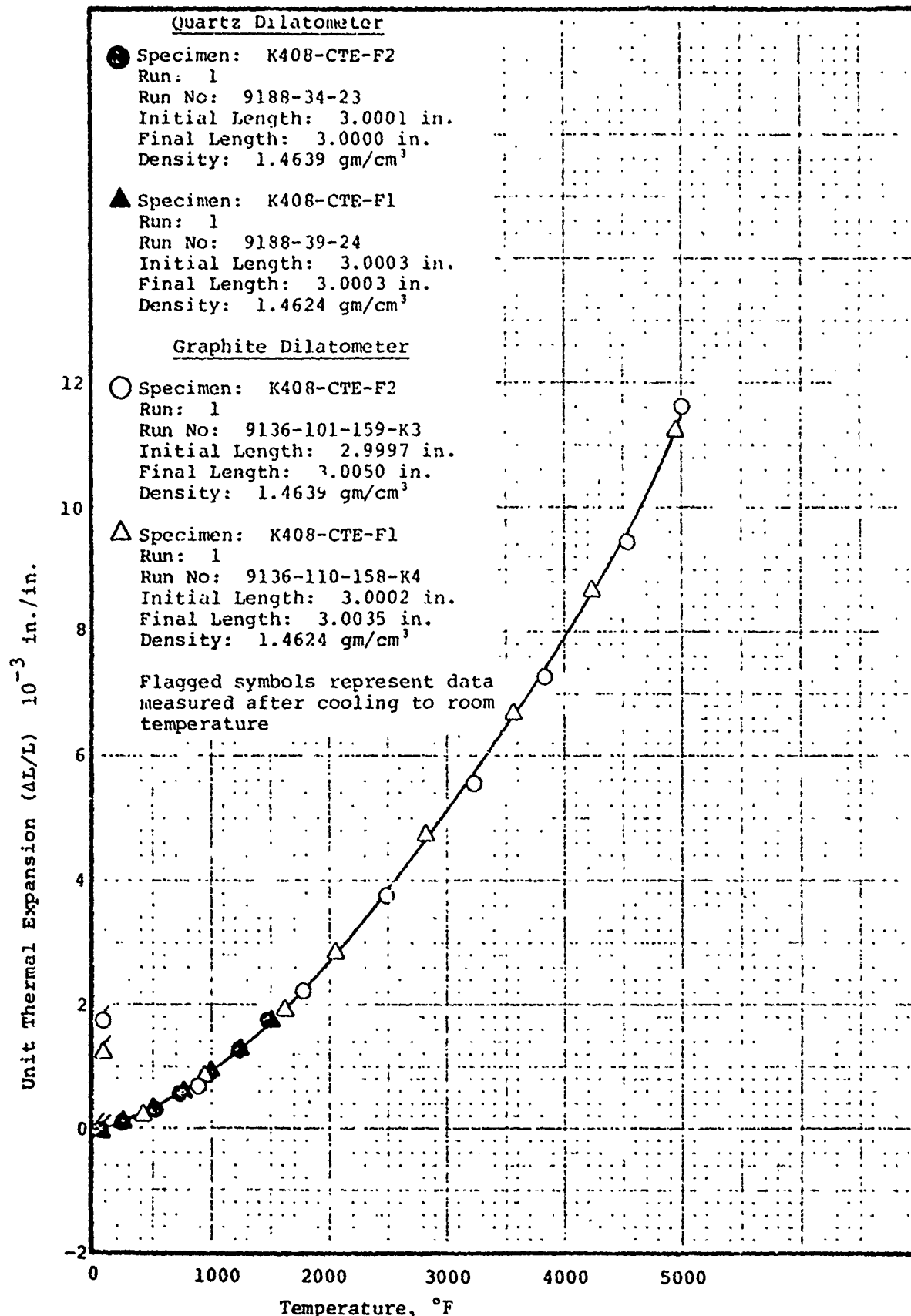
Figure 22. The Unit Thermal Expansion of K407 Carbon/Carbon
in the Fill Direction
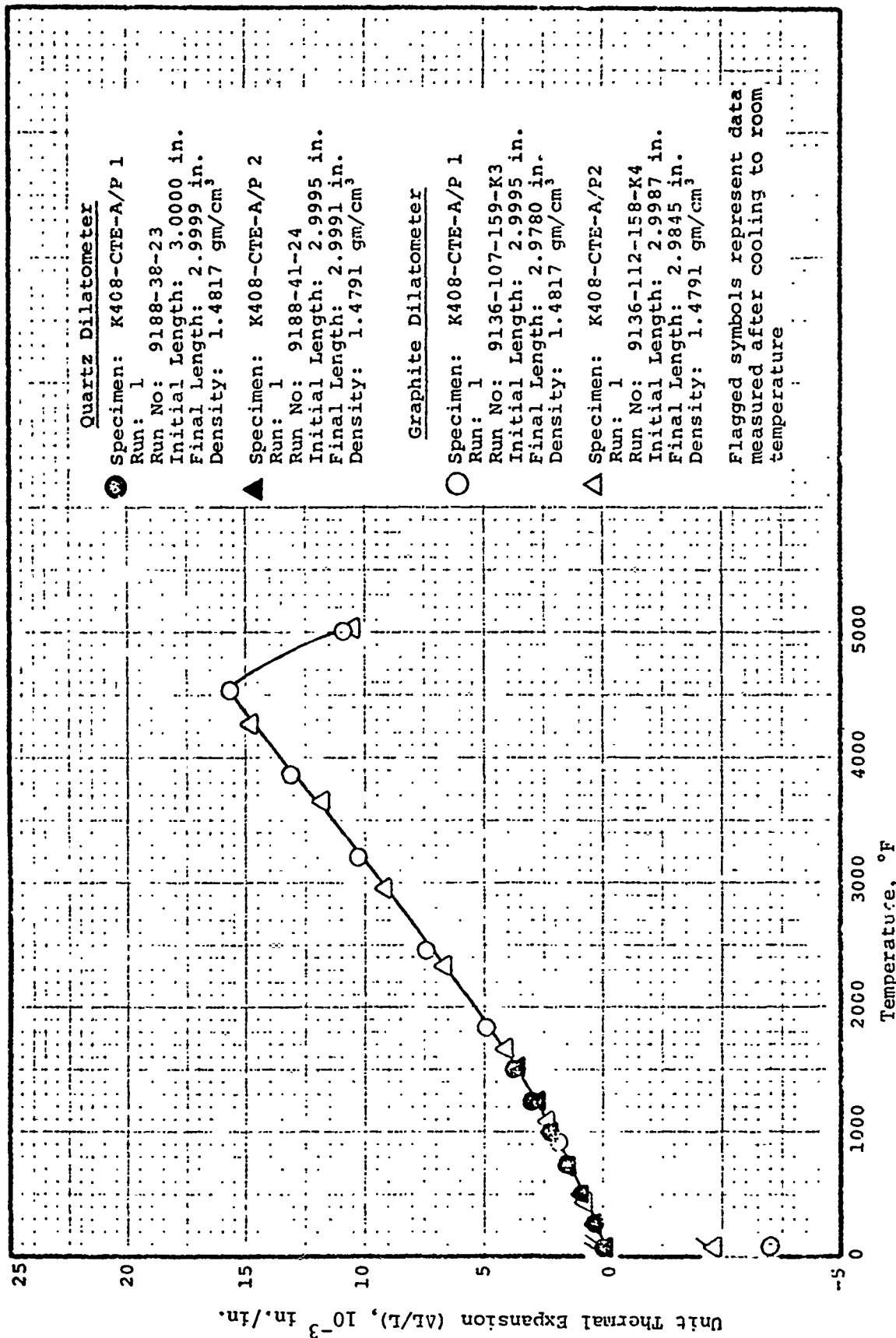
Figure 23. The Unit Thermal Expansion of K408 Carbon/Carbon in the Cross-Ply Direction
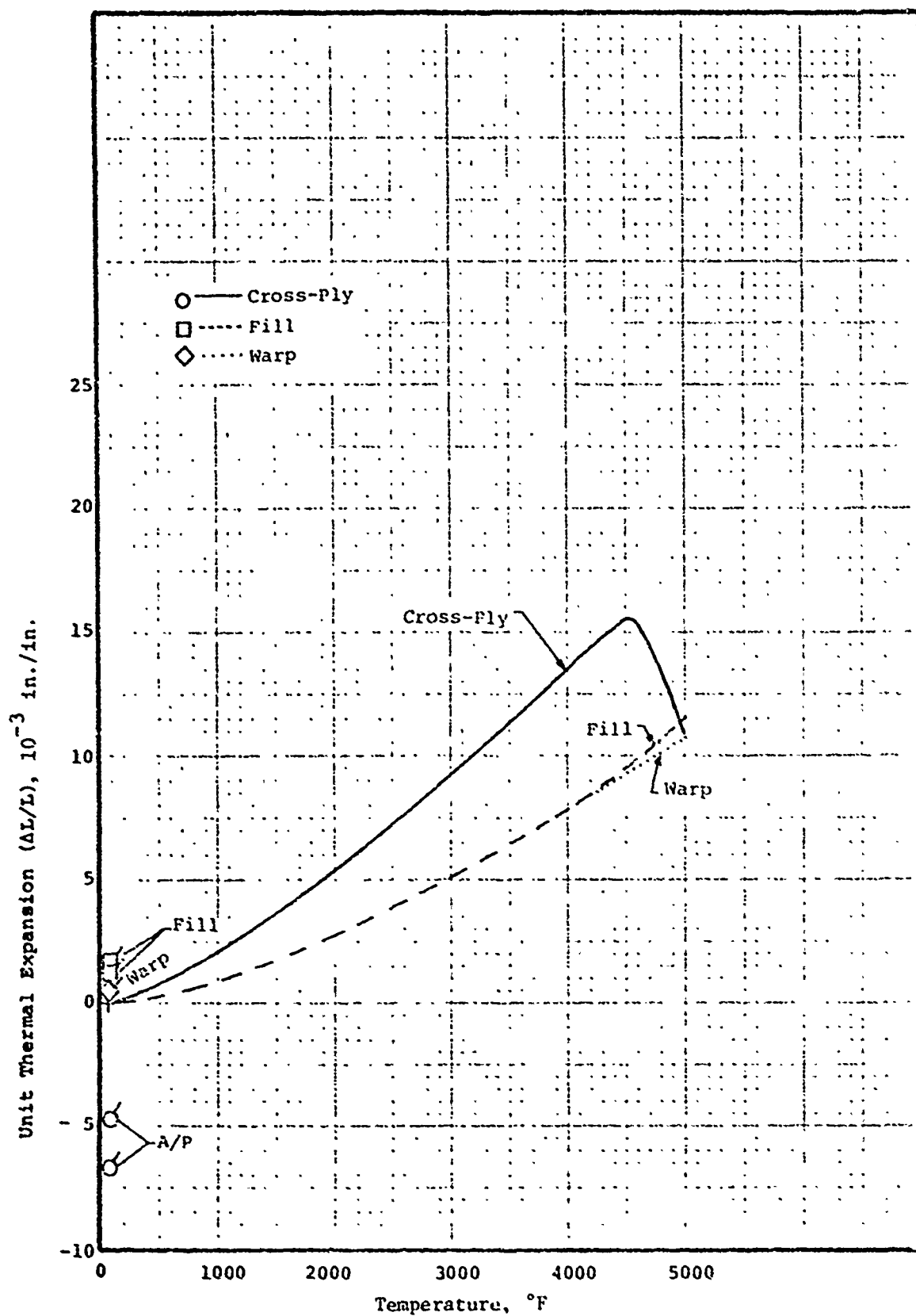
Figure 24. Comparison of Unit Thermal Expansion of K40S Carbon/Carbon between the Warp, Fill, and Cross-Ply Directions

Page 60

f.   Observation of Failed Surfaces

The method selected to document . ? condition of the failed shear surfaces was photographs using a scanning electron microscope at the University of California at Davis, California. These and otner photographs were also observed in a stereo setup using two photographs taken of the same area at different angles. The depressions and fiber or resin surfaces can be better isolated by this technique. A graphite/epoxy rail shear surface magnified 1000 times is shown in Figures 25 and 26. Figure 25 shows the failed resin surface with imprint (striation) from the fiber surface and irregular tensile failed surface of the resin. The fiber surface striations are across the photograph, left to right. There is some resin debris on the surface.

The warp yarn surface is shown in Figure 26. The tensile failure of the resin is shown in the left-handed side of the photograph, top to bottom. The right-hand side shows broken yarns at the shear surface; shear load was right to left on the photograph. Small particles of resin debris are also shown on the failed surface.

The shear surface of the carbon/carbon rail shear is shown in Figures 27 and 28. Figure 27 shows warp filaments (two failed) and imprint of the filament. The texture of the imprint is indicative of a sheath around the filament which is less porous than the majority of the matrix. The matrix does not have the characteristic appearance of tensile failure as shown by the graphite/epoxy resin.

The fill filament surface is shown in Figure 28. At the extreme left side of the photograph is a filament broken in the axial plane. The filaments appear to have matrix material attached to the crenolated surfaces in varying thicknesses. Although not shown, it was observed that some warp yarns have completely failed in tension. Fill yarns tended to be partially missing where they were on the failed shrface, indicating some shear

Page 61
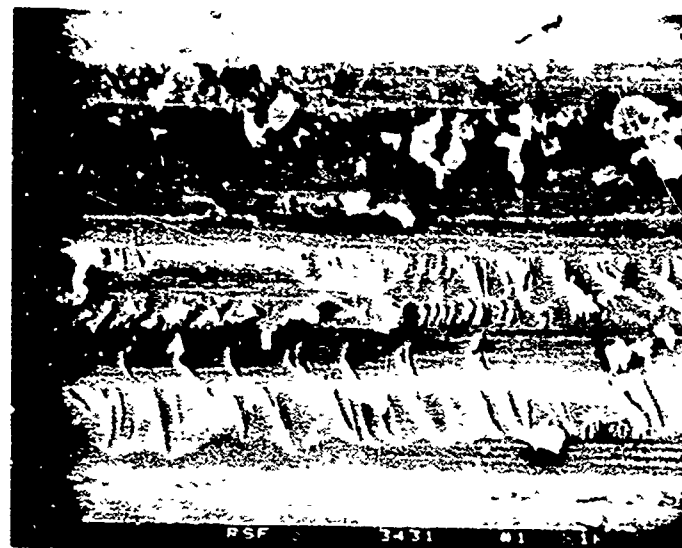
Shear Plane

Figure 25. Failed Shear Surface of Graphite/Epoxy Fill Rail Shear
Specimen Showing Imprint of T-300 Filaments (Fill
Direction) and Characteristic Resin Surface. Loose
Particles are Resin Debris (100X SEM).
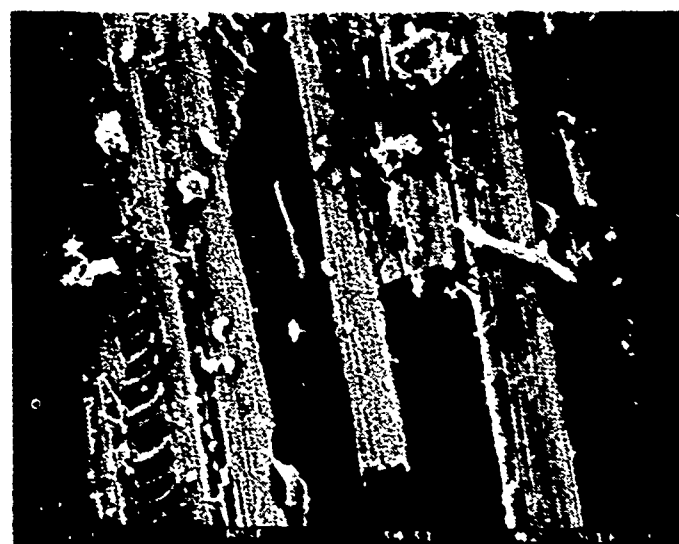
Shear Plane

Figure 26. Failed Shear Surface of Graphite/Epoxy Fill Rail Shear
Specimen Showing Broken Warp Filaments (Transverse of
Shear Plane) and Characteristic Resin Surface, Left Side
Between Filaments (100X SEM).
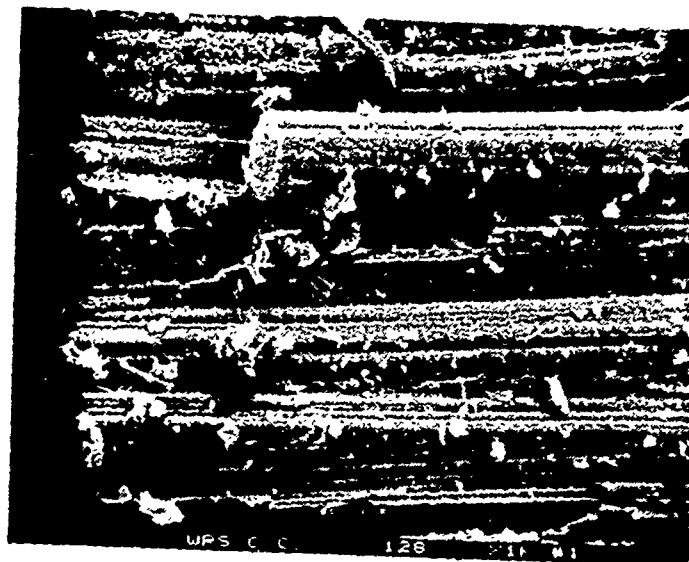
Figure 27. Failed Shear Surface of Carbon/Carbon Warp Rail Shear
Specimen Showing Characteristic Filaments and Filament
Imprints in Matrix. Loose Particles are Matrix Debris
(1000X SEM).
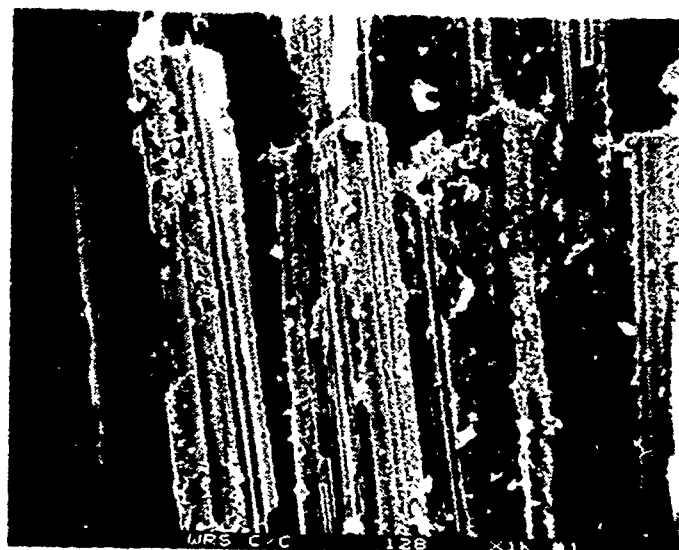
Figure 28. Failed Shear Surface of Carbon/Carbon Warp Rail Shear
Specimen Showing Broken Fill Filaments and Matrix Material
Attached to the Filament Surfaces.

Page 63

load through or into the yarn bundle. This is characteristic of nested fabrics tested in interlaminar shear, but it could not be determined if the yarn damage occurred after failure or at initial failure.

D. TESTING OF CYLINDERS

The graphite/epoxy and carbon/carbon involute cylinders were tested in accordance with the matrix shown in Figure 5. The deflection and strain measurement for the uniaxial loading was duplicated for:

1. Axial tension
2. Axial compression
3. Torsion
   a. Clockwise
   b. Counterclockwise
4. Hoop Tension

Figure 29 shows the relationship of the warp and fill orientation to the strain gage indications. The 45-degree gage was parallel to the fill yarn for all 45 degree helix tests. Strain gages were located at 0, 120 and 240 degrees for all testing. The ply orientation in relation to the clockwise and counterclockeise torsion testing is also shown in Figure 29. Torsion loading was applied at the top of the cylinder. The combined loading included the following:

1. Axial Tension/Internal Pressure
2. Axial Compression/Internal Pressure
3. Clockwise Torsion/Internal Pressure

As for the uniaxial testing, the combined loading testing was conducted on at least two cylinders.
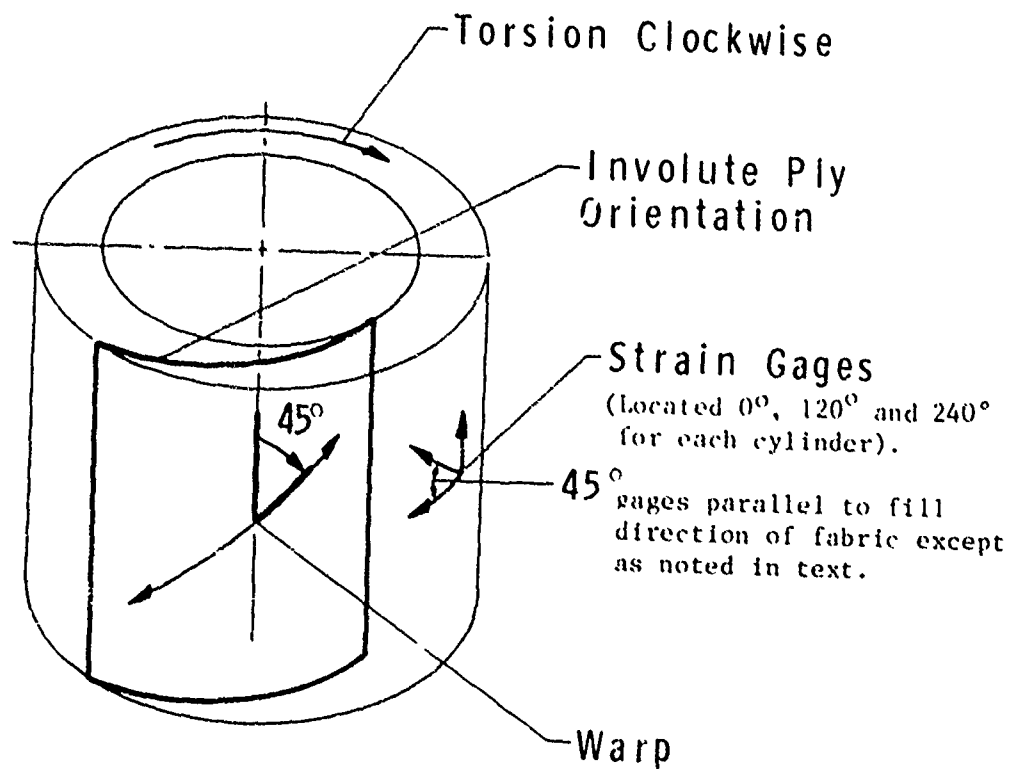
Figure 29. Strain Gage Location and Warp/Fill Orientation
for 45° Helix Cylinders

Three cylinders were used for all of the graphite/epoxy testing. There were 15 cylinders of the carbon/carbon materials, five each of the (1) 10 degree arc/45 degree helix, (2) 5 degree arc/55 degree helix and (3) 10 degree arc/0 degree helix. Two of the graphite/epoxy cylinders were tested to failure, and all 15 of the carbon/carbon cylinders were tested to failure.

The cylinders were machined to contour as shown in Appendix A. Steel sleeves were bonded to both ends ID and OD of the cylinders using a trowelable epoxy adhesive. The sleeves were then placed in a drill fixture and eight 0.625 in. dia holes were drilled through the steel sleeves. These holes were used for shear pin attachment to the holding fixture for compression, tension, and torsion testing. A photograph of the torsion test fixture with a cylinder assembled for test is shown in Figure 30. The test setup shown in Figure 30 was also used for torsion and internal pressure. The gas inlet tube is attached at the bottom of the fixture.

All loads applied to the cylinders with exception of the internal pressure testing were applied through the pins and sleeves bonded to the ends of the cylinders. To obtain uniform strain for tension and compression loading, specimens were preloaded, and adjustments were made in the pin fit-up prior to test. Additional cylinder length would reduce the pin fit-up and alignment problem.

The internal pressure was applied through a rubber bag inside the cylinder.

The loading for compression, tension, torsion, and internal pressure was in incremental steps. Strain measurements were read from each of the nine strain gages by a data acquisition system prior to applying the next increment of load. The readout required maintaining the cylinder under a constant load for approximately 15 seconds prior to applying the next increment of load.
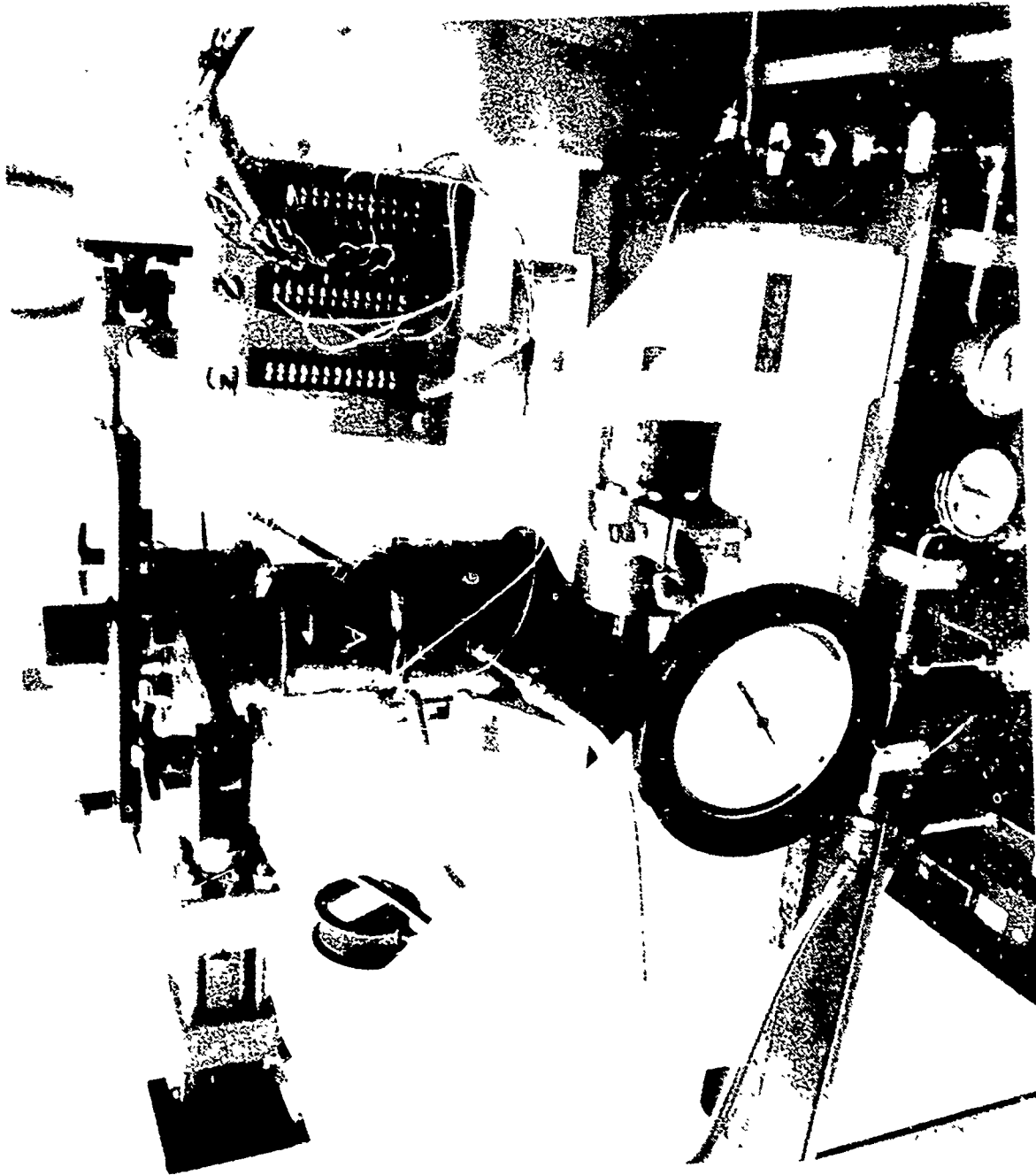
Figure 30. Torsion Test Fixture with Assembled Carbon/Carbon Cylinder Ready for Test with Attached Strain Gages

1. Graphite/Epoxy

The test plan previously discussed is shown in Figure 5.
Each specimen was loaded twice per test plan. Two of the graphite/epoxy
cylinders, 5 degree arc/45 degree helix and 10 degree arc/45 degree helix,
were tested to failure in compression. The ultimate strengths were very low
compared with the warp compressive strength. The ultimate strengths were
26,700 and 27,000 psi, respectively, for the 10 degree arc/45 and 5 degree
arc/45 helix degree cylinders. A buckling failure (possible shear) with
cross ply delamination was the observed failure mode for the 10 degree arc
specimen and to a lesser degree for the 5 degree arc specimen. The calcu-
lated modulus for the compression and tension loading of the 10 degree arc
0 degree helix cylinder was approximately 2.0×10^6 psi lower than for the
laminates or tubes. Based on these results it is assumed the same low vol-
ume factors existed for the 0 degree helix cylinder as for the 45 degree
helix cylinders discussed below. The measured strains for the uniaxial and
conbined loading are presented in Section E.

Predicted warp-fill shear stress at failure was 13,500 warp-
fill for both cylinders which is near the warp-fill allowable of 17,200 psi.
A significant factor which affected both ultimate strength and modulus was
the high resin content/low fiber volume of the cylinders. The following
average values were obtained from the 10 degree arc/45 degree helix sample.

Property	Value
Density, gm/cc	1.56
Fiber Volume, %	53.00
Resin Solids, %	39.60
Void Content, %	0.500

There was low void content, indicating good compaction dur-
ing the cure/pressure cycle, but the fiber volume was low, and the resin con-
tent was high. These values indicate less resin bleedout during cure than was

obtained for the laminates and tubes. The average density for the laminates and tubes was 1.61 with a fiber volume of 61 percent.

The resin staging, discussed in Section B, used to prevent wrinkling of the graphite/epoxy plies apparently reduced the normal resin bleedout during cure. A review of the results indicates the low fiber volume affected the strain results for the 10 degree arc/0 degree helix and produced the lower modulus for the cylinder.

A graphic comparison of the measured versus predicted axial strain for hoop tensile testing of a graphite/epoxy cylinder is shown in Figure 31. Agreement is good; however, the measured strain is higher and increasing at a faster rate per unit load than the model prediction.

A predicted versus measured strain for the combined internal pressure and axial tension loading provides a very good agreement for the axial strain as shown in Figure 32. The remainder of the predicted versus measured comparisons for the graphite/epoxy are shown in tabular form in Section E.

2. Carbon/Carbon

The carbon/carbon cylinders were also tested in accordance with the test plan shown in Table 7. The reuse of cylinders for strain measurements was minimized for the carbon/carbon cylinders. The strain measurements are contained in tabular form in Section E. Agreement of predicted with measured strain is also discussed in the analysis section; however, some graphic comparisons are presented in the following discussion.

The density determinations from a sampling of the carbon/ carbon cylinders indicate a somewhat lower density than that measured for the

TABLE 7. TEST PLAN FOR CARBON/CARBON CYLINDERS

Cylinder Serial No.	Uniaxial	Combined	Ultimate
1153769-1-101-1 A	Ten., Comp.	Ten/Press, Comp/Press	Comp.
1153769-2-101-1 B	" "	" " " "	Tension
1153769-3-101-1 C	" "	" " " "	Comp.
1153769-1-102-1 A$_1$	Ten., Comp, Press.	Ten/Press, Comp/Press	Tension
1153769-2-102-1 B$_1$	" " "	" " " "	Comp.
1153769-3-102-1 C$_1$	" " "	" " " "	Tension
1153769-1-103-1 A$_2$	Pressure	CW TOR/Pressure	Pressure
1153769-2-103-1 B$_2$	"	" "	Pressure
1153769-3-103-1 C$_2$	"	" "	Pressure
1153769-1-104-1 A$_3$	CW TOR	CW TOR/Pressure	CCW TOR
1153769-2-104-1 B$_3$	" "	" "	CCW TOR
1153769-3-104-1 C$_3$	" "	" "	CCW TOR
1153769-1-105-1 A$_4$	CCW TOR	CW TOR/Pressure	CCW TOR
1153769-2-105-1 B$_4$	" "	" "	CCW TOR
1153769-3-105-1 C$_4$	" "	" :	CCW TOR

A = 5° Arc 45° Helix
B = 10° Arc 0° Helix
C = 10° Arc 45° Helix
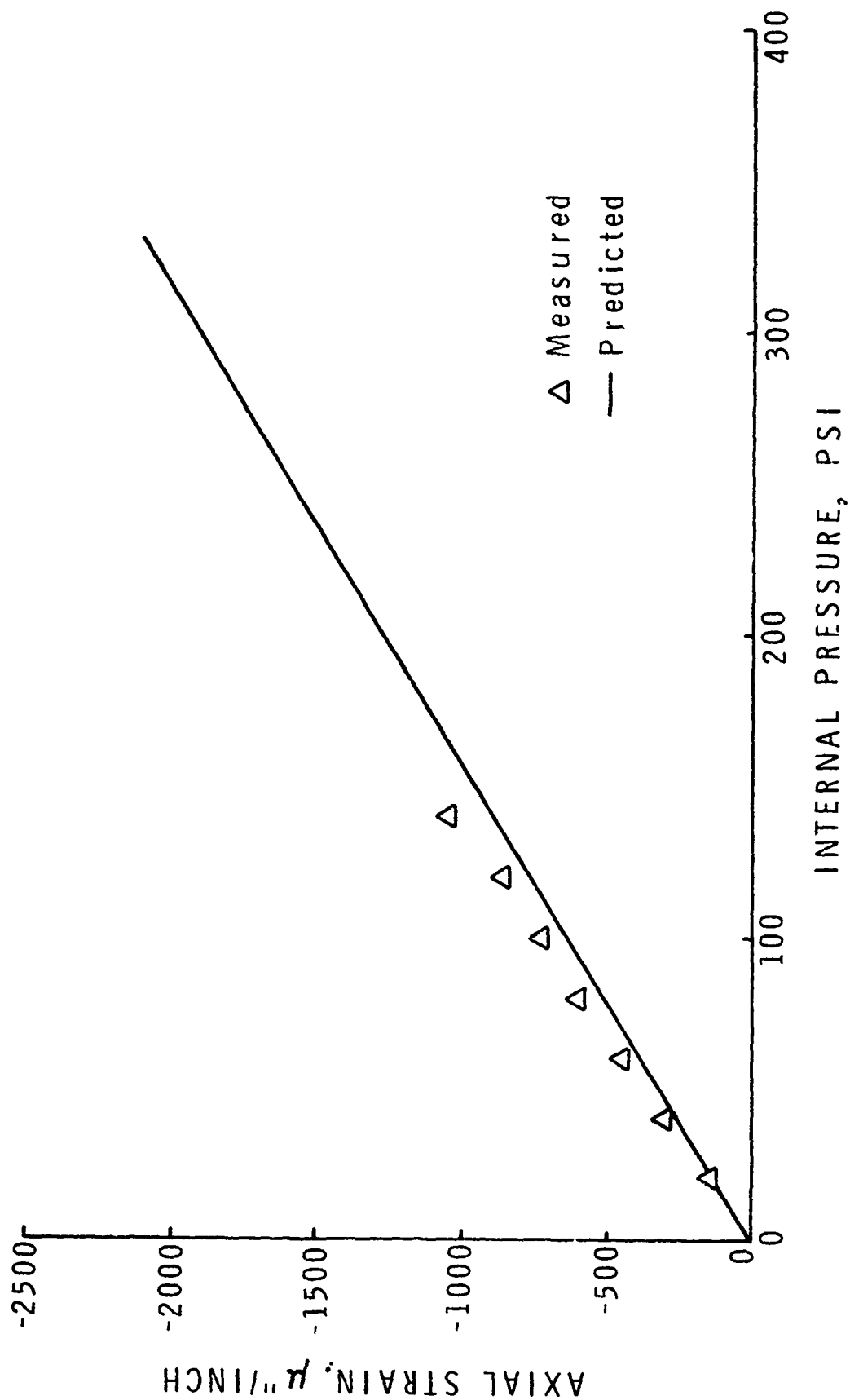
Figure 31. G/E, Internal Pressure vs Axial Strain, 10° Arc, 45° Helix

Page 71
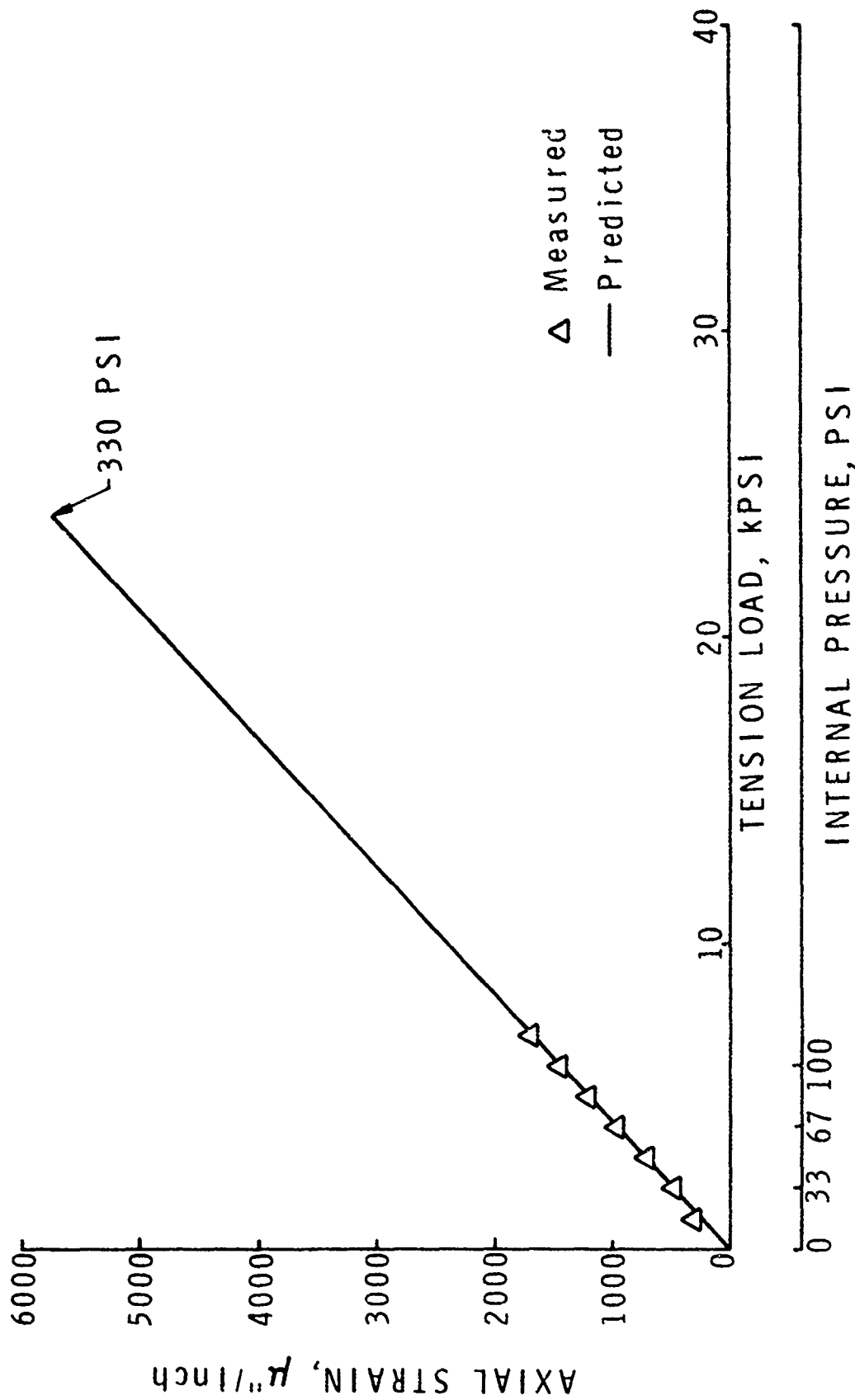
Figure 32. G/E, Tension/Pressure vs Axial Strain, 10° Arc, 45° Helix

Page 72

laminate. A value of 1.48 gm/cc was obtained from the test cylinders compared to 1.50 and 1.51 from the carbon/carbon test laminates. Previous comparisons of cones and laminates have shown equivalent densities. The cause of the slightly lower density could not be determined; however, the effects on mechanical properties were not considered significant based on previous tests of the carbon/carbon material, Reference 4. A reasonable density tolerance to be expected is +0.02/-0.02 gm/cc. The tolerance estimate is based on experience and not a controlled experiment.

Figure 33 shows a cylinder assembled and ready for testing. Loading of the carbon/carbon cylinders was in increments, allowing for data collection at each load. Slightly higher ultimate strengths would possibly have been obtained for a continuous load to failure.

The ultimate strength values for the carbon/carbon cylinders are listed below for each of the three involute variations.

Type Test	Involute Arc, Degrees	Variation, Degree Helix	Ultimate Strength, psi
Tension	10	0	7777
	5	45	6880
	10	45	7197
Compression	10	0	11340
	5	45	7750
	10	45	7720
Torsion-Clockwise	10	0	4064
(Shear Stress)	5	45	6885
	10	45	5214
Torsion	10	0	4445
Counter-Clockwise	5	45	6057
(Shear Stress)	10	45	7407
Hoop Tensile	10	0	4985
	5	45	NA
	10	45	5303

Page 73
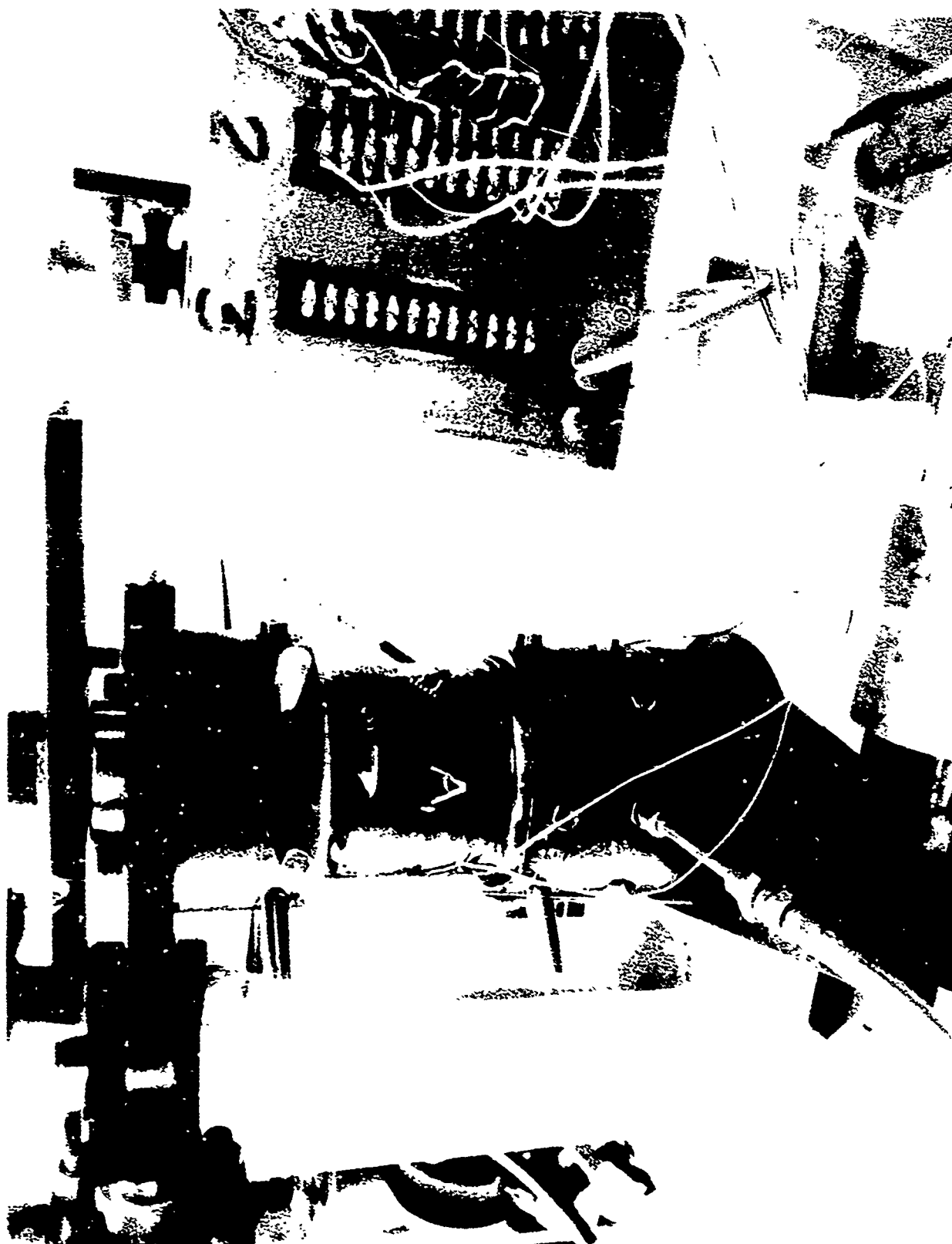
Figure 33. Carbon/Carbon Test Cylinder Assembled for Combined Torsion/internal Pressure Loading

All of the measured stresses at failure are also shown in
Table 18 in Section E. Based on limited previous test data, the ultimate
strengths indicate acceptable values were obtained for all cylinders, with
the exception of two cylinders. The hoop tensile (internal pressure) speci-
men for the 5 degree arc/45 degree helix was damaged subsequent to the inter-
mediate test loading, and no value for ultimate hoop tensile strength was ob-
tained. In addition, the axial tensile test of the 10 degree arc/0 degree
helix produced a low ultimate strength, 7777 psi, compared with 9950 psi av-
erage for the laminate test in the warp direction. This was the first cyl-
inder tested in tension, and difficulties were encountered in obtaining good
alignment as evidenced by the large variation, approximately 15 percent, in
the axial strain gage indications. There was only one specimen per each type
of ultimate test; therefore, a determination of the effect of misalignment
could not be ascertained. All subsequent tests were aligned to control
strains within 10 percent prior to loading for data collection.

A photograph of the tensile failure of 5 degree arc/45 de-
gree helix specimens is shown in Figure 34. The failure surface parallel to
the warp yarns is more uniform than on the opposite side parallel to the fill
in the fill yarns. However, it can only be postulated that failure initiated
at this point. Another failure mode could have been initial failure of both
warp and fill yarns and propagation along the 45 degree helix on both sides
of the cylinder. Figure 29 was used as a reference of the warp-fill orien-
tation for comparison with the failed surfaces.

A failed axial compression specimen is shown in Figure 35.
The failure appears to have been typical shear with some delamination evident.
Occurrence of delamination prior to initial failure is not likely because of
the predicted low interlaminar shear cross ply tension. The buckling that
was observed on the graphite/epoxy was not evident. The predicted failure
modes are shown in Table 18.

Figure 34. Tensile Failure 5° Arc/45° Helix Showing Some Tensile Failure Parallel to Helix Angle (piece on left is top of cylinder)

Figure 3   Axial Compression Failure, 10° Arc/0° Helix, Typical Shear Surfaces and Strain Gages at 120° Location

A failed hoop tensile (internal pressure) specimen is shown
in Figure 36. Characteristically, approximately one half of the specimen
was blown out and broken into pieces at failure. The failed pieces were also
delaminated. Some of the remaining failed surfaces are also interlaminar
separations.

All three types of involutes tested in torsion are shown in
Figures 37 through 39. Figure 37 is a 10 degree arc/45 degree helix. Figure
38 is a 5 degree arc/45 degree helix, and Figure 39 is a 10 degree arc/9 de-
gree helix. Each of the photographs shows different failure patterns. The
limited experience in testing carbon/carbon cylinders in torsion makes it
difficult to draw valid conclusions about the specimen appearances and the
complicated loading. There appears to be some delamination (separation be-
tween plies) for all of the specimens. Separation between plies was also
present, but to a lesser extent, in the 10 degree arc/0 degree helix specimen.
The failure shown in Figure 39 appears to be tensile failure of the fill
yarns. (The same failure characteristic was observed on one of the graphite/
epoxy tube torsion degree tests, Section C.) The most likely failure mode
for the 0 degree helix cylinder is warp-fill shear failure as shown in
Table 18. Both of the 45 degree helix cylinders had high fill fiber tension
stress, Table 18. The effects of variation in the helix angle are discussed
in Section III, D.5.

Two of the cylinders were sectioned to verify the warp and
fill direction specified. Photomicrographs of the sectioned cylinders are
shown in Figures 40 and 41. Observation of the cross sectioned cylinders
verified that the warp/fill relation was as specified and as reported by the
fabricator. Rough measurements of the helix angles both from the sectioned
pieces and surface condition indicate warp and fill helix was 45 ± 5 degrees.
It is not believed that it would be possible or practical to obtain cylinder
lay-ups with closer tolerances on the helix angles. Some distortion of the

Figure 36. Hoop Tensile Failure, 10" Arc/45" Helix Showing both between Ply and Crossply Failed Surfaces — Failed Pressure Bag Inside Cylinder

Figure 37. Torsion Test Failure Section, 19° Arc/45° Helix Showing Failure at OD Surface Following Approximate Helix Angle

Figure 38. Torsion Test Failure Section, 5° Arc/45° Helix Showing Delamination Propagating Along Center of Wall Thickness

Figure 39. Torsion Test Failure Section, 10° Arc/45° Helix Showing Failure through Fill Yarns – Strain Gages at 240°

Figure 40.   Photomicrograph of a Cross Section Approximately Parallel to
              Fill Direction 5 degree Arc 45 degree Helix Cylinder.   Torsion
              Failure.

Figure 41.   Photomicrograph of a Cross Section Approximately Parallel to
              Warp Direction, 10 degree Arc 45 degree Helix.   Torsion Failure.

fill yarn exists in the as processed condition. The fill yarns are not al-
ways perpendicular to warp yarns in the as graphitized fabric. Furthermore,
some distortion results from handling during the prepeg operation as the
fabric is passed through the resin and drying ovens.

The matrix contains irregular voids (density is 1.45 gm/cc)
that extend into, and in some cases, through the yarn bundles. In Figures
40 and 41 the dark areas are voids, gray areas are matrix, and the light
irregular shapes are ends of graphite filaments. The white areas, continuous
from right to left, are fill yarns in Figure 40 and warp yarns in Figure 41.
This is characteristic of the 2D carbon/carbon material in both laminates and
cylinders. The appearance of the matrix that encapsulates the yarn bundle
was very similar to the cross section of the test laminates which were pre-
viously discussed and shown in Figures 15 and 16.

The measured and predicted ultimate strength values for all
cylinders are contained and discussed in Section E. Selected, predicted, and
measured values were also plotted and are discussed herein. The agreement
for predicted and measured strain is very good for the axial compression
test of the 0 degree helix cylinder as shown in Figure 42. The measured
strain is only slightly higher at failure.

Conversely, the agreement at failure for the compression
testing of a 45 degree helix is very poor as shown in Figure 43. However,
the agreement is satisfactory up to approximately 75 percent of ultimate. A
method that improves the prediction is discussed in Section E. Another com-
parison of predicted versus measured strain, at 45 degrees to load, is shown
in Figure 44. The agreement is adequate up to 50 percent of ultimate, but
deviates significantly above 50 percent.
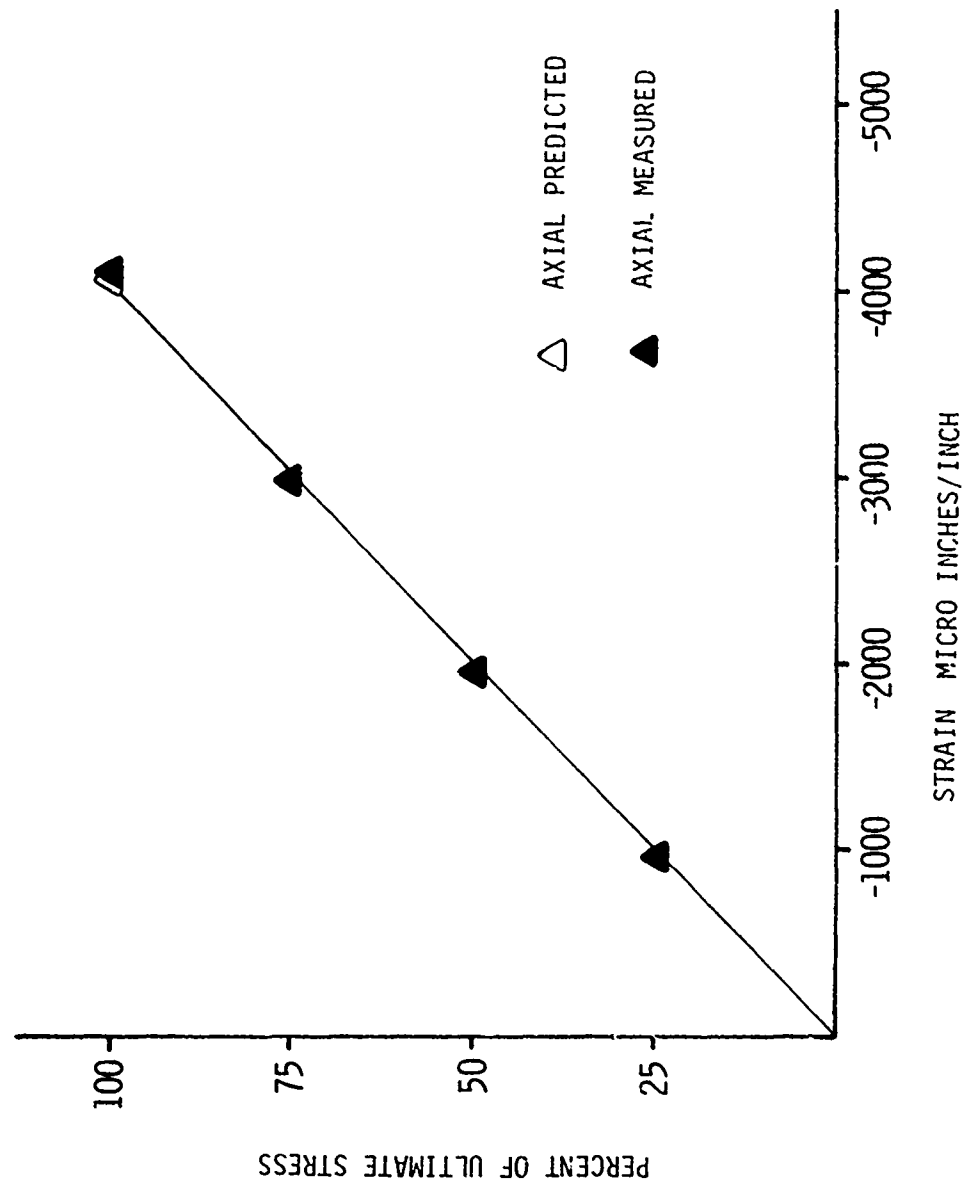
Figure 42. C/C, Involute Cylinder, 10°Arc, 0° Helix, Load: Axial Compression
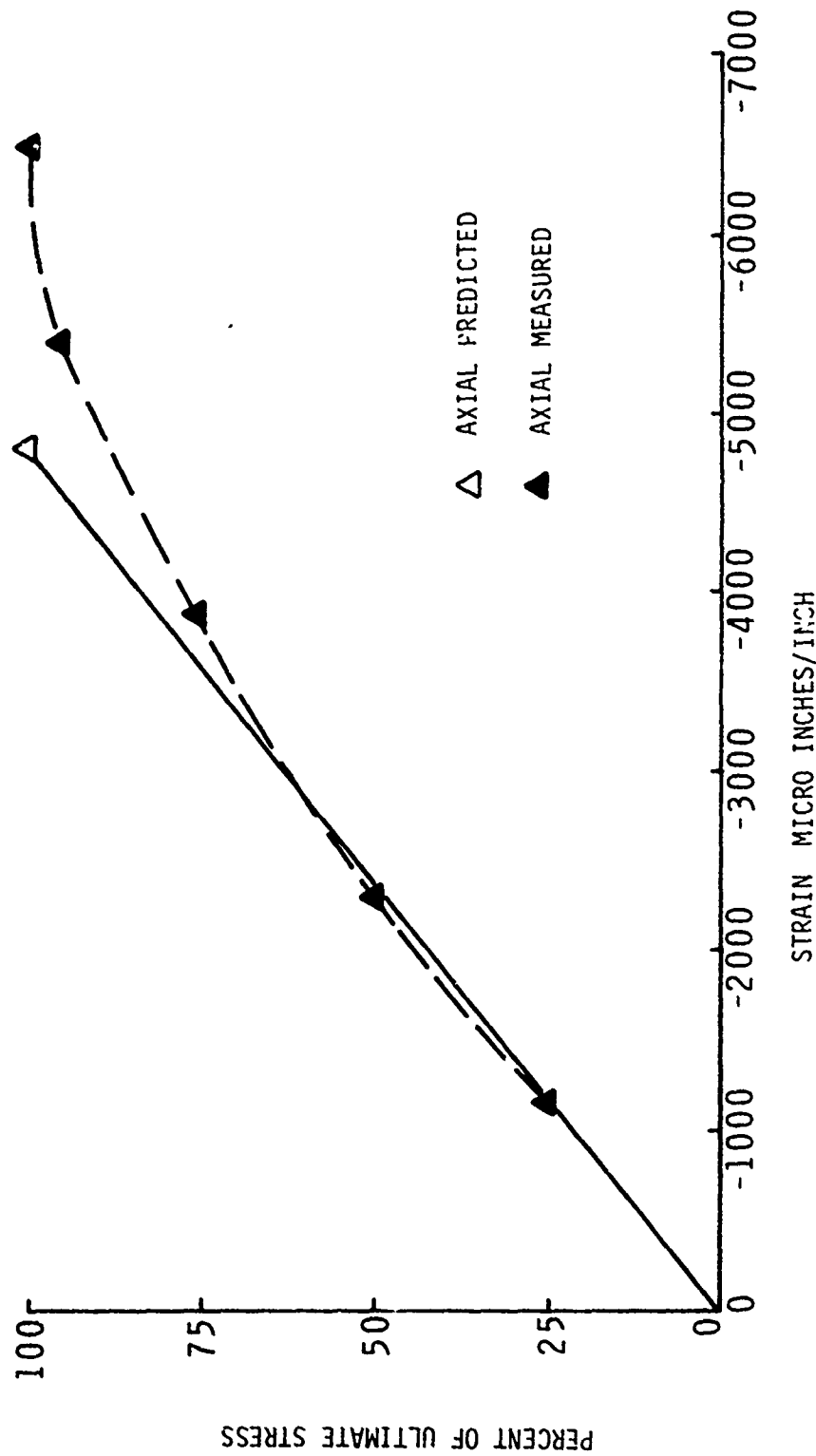
Figure 43. C/C, Involute Cylinder, 5° Arc, 45° Helix, Load: Axial Compression
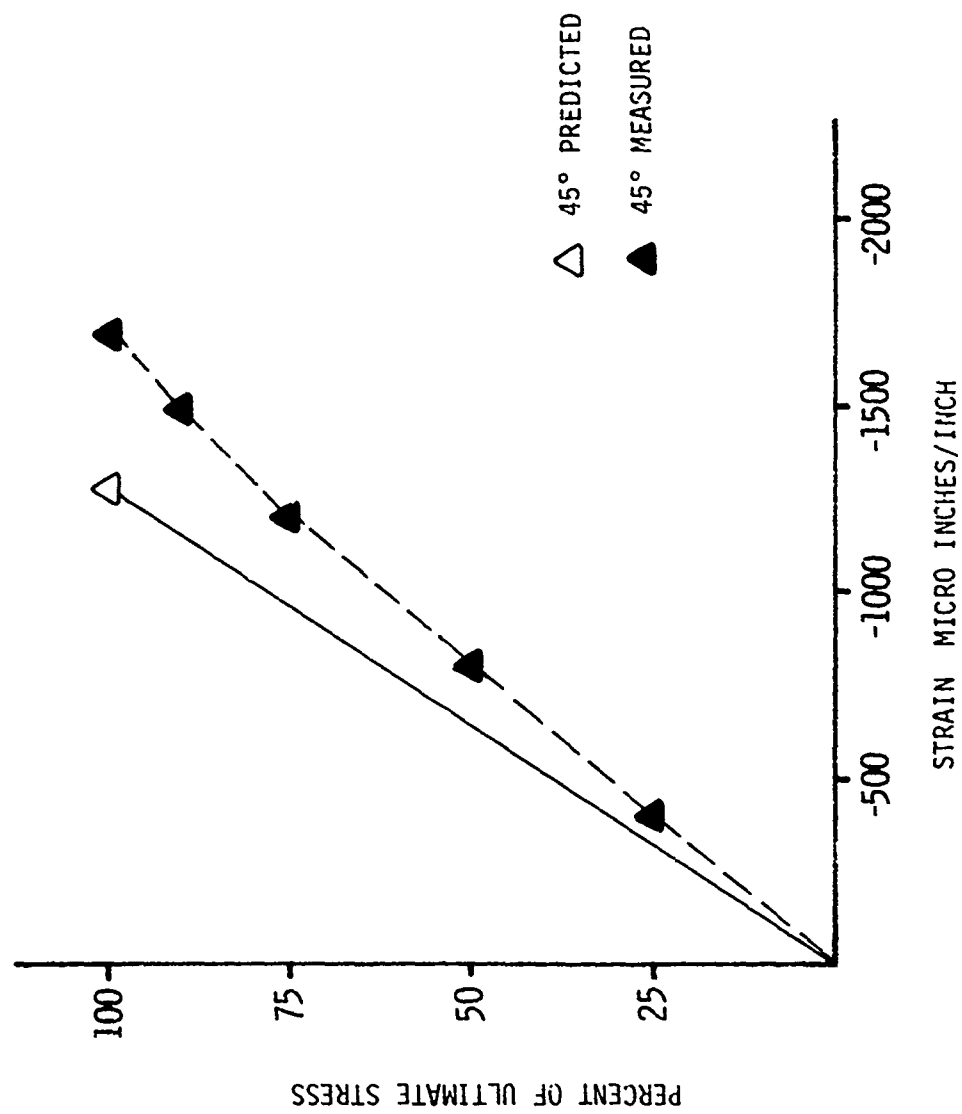
Figure 44. C/C, Involute Cylinder, 10° Arc, 45° Helix, Load: Axial Compression
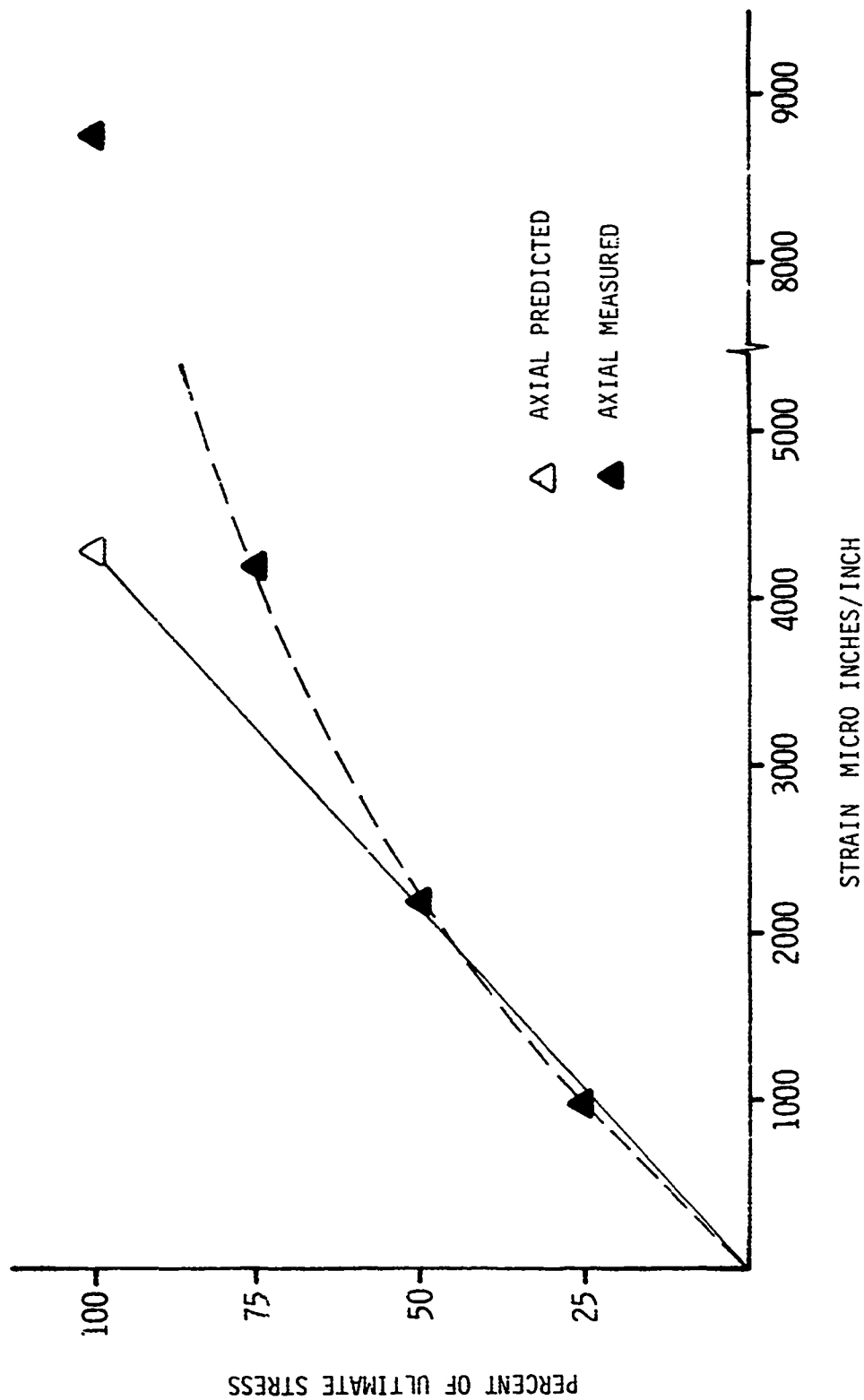
Figure 45. C/C, Involute Cylinder, 5° Arc, 45° Helix, Load: Axial Tension

Page 88

STRAIN MICRO INCHES/INCH

△ HOOP PREDICTED

▲ HOOP MEASURED
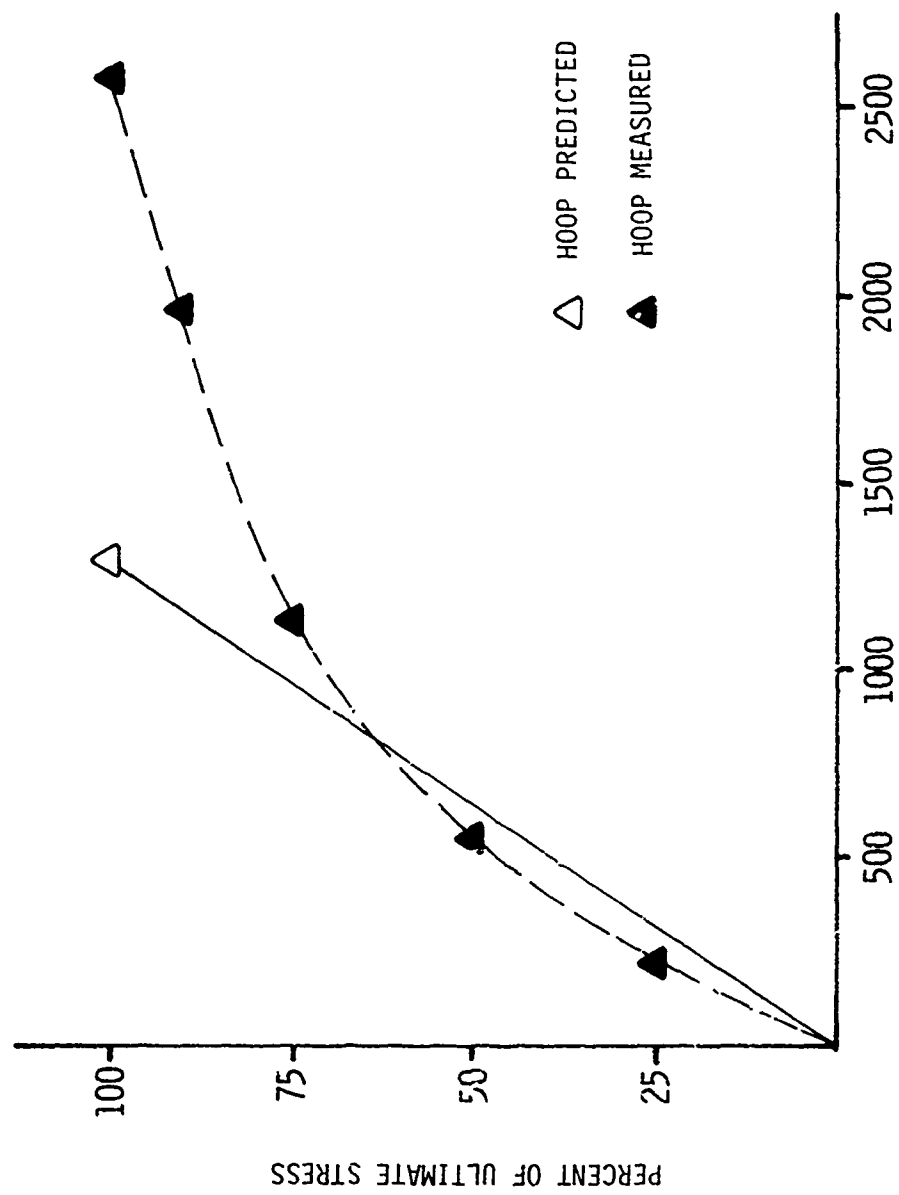
Figure 46. C/C. Involute Cylinder, 10° Arc, 45° Helix, Load: Axial Compression

Agreement for the predicted versus measured strain for tensile testing of the 5 degree arc/45 degree helix (Figure 45) is also good up to 50 percent, but deviates extremely above 50 percent of the ultimate. The measured strain is approximately twice that predicted at failure. During test, sharp sounds were produced at approximately 80 percent of ultimate, indicating local failure, but the cylinder continued to support increased load.

The measured hoop strain versus predicted strain for an axial compression test is shown in Figure 46. Agreement is satisfactory to approximately 70 percent of ultimate, but deviates by about 100 percent at failure.

Better agreement for all predicted versus measured might be achieved by using the nonlinear technique discussed in Section E.

E. PREDICTION OF CYLINDER BEHAVIOR AND CORRELATION RESULTS

The techniques used to predict the structural response of both the carbon/carbon and graphite/epoxy cylinders to tensile and compressive axial, clockwise and counterclockwise torsional, and internal pressurization applied loads are discussed in this section. For each cylinder material three conbinations of helix angle and involute arc angle were tested and analyzed. All predictions were made using the computer code received from AFML (Reference 6) converted to the UNIVAC 1108 computer.

The AFML computer code solves a one dimensional linear elasticity problem by the finite difference method. It allows orthotropic materials to be used and uses nine independent constants in the stiffness matrix. Applied loads (torque, axial load, internal and external pressure) are entered directly, after a set of influence coefficients is calculated which relate these applied loads to the displacement boundary conditions. Table 8 shows the relationship between these boundary conditions and the influence coefficients required as input to the code. The assumption of linear behavior of the code was used in all the predictive results with the exception of the nonlinear modification discussed in Section III, E.3.

For each material and cylinder configuration, unit solutions were obtained. These unit solutions were the elastic structural response to a 10,000 lbf axial load, a 10,000 in.-lbf torque, and 1000 psi internal pressure. The unit solutions were then scaled and combined to correspond to each specific test prediction. For each test "point" (cylinder load) the strain readings at the outer surface were taken as the averaged values of the three rosette strain gages located at the 0, 120, and 240 degree circumferential locations, for the axial, circumferential, and 45 degree directions. Strain

---

Reference 6: Computer Code received from N.J. Pagano, AFML, February 4, 1977.

predictions for the axial and circumferential directions are taken directly from the computer output, and the strain at 45 degrees is calculated from

$$\varepsilon_\beta = \frac{\varepsilon_z + \varepsilon_\theta}{2} + \left(\frac{\varepsilon_z - \varepsilon_\theta}{2}\right) \cos 2\beta + \frac{1}{2} \gamma_{z\theta} \sin 2\beta$$

with $\beta = 45$ degrees.

1. Graphite/Epoxy Cylinders

The ASPC 3431 graphite/epoxy cylinders were modeled using the cylinder dimensions (Appendix A). The three combinations of helix and arc angle fabricated for testing and analysis and their designations and scriptions are summarized below:

GRAPHITE/EPOXY CYLINDER DESCRIPTIONS

Specimen Designation	Helix Angle, Deg	Arc Angle, Deg	Ply Thickness, in.	Mean Number of Plys	Initial Arc Angle, α_0, Deg
A	45	5	.007	172	4.8
B	0	10	.007	324	9.06
C	45	10	.007	324	9.06

The following nine elastic constants for graphite/epoxy were used to analyze all three cylinders:

$$E_{11} = 16.8 \times 10^6 \text{ psi} \qquad G_{12} = 1.15 \times 10^6 \text{ psi} \qquad \nu_{12} = 0.04$$

$$E_{22} = 5.0 \times 10^6 \text{ psi} \qquad G_{13} = 0.70 \times 10^6 \text{ psi} \qquad \nu_{13} = 0.06$$

$$E_{33} = 1.6 \times 10^6 \text{ psi} \qquad G_{23} = 0.65 \times 10^6 \text{ psi} \qquad \nu_{23} = 0.023$$

TABLE 8.   INFLUENCE FUNCTIONS

Assume $B = D = 0$

Let P, T = Prescribed Values

σ, A, σ_0, σ_1 = Values Corresponding to P, T

P_1, T_1 = Values Corresponding to $\varepsilon = 1$, $A = \sigma_1 = \sigma_0 = 0$

P_2, T_2 = Values Corresponding to $\varepsilon = 0$, $A = 1$ $\sigma_1 = \sigma_0 = 0$

P_3, T_3 = Values Corresponding to $\varepsilon = A = 0$, $\sigma_1 = 1$, $\sigma_0 = 0$

P_4, T_4 = Values Corresponding to $\varepsilon = A = \sigma_1 = 0$, $\sigma_0 = 1$

$$\varepsilon = \frac{(P - \sigma_1 P_3 - \sigma_0 P_4)\, T_2 - (T - \sigma_1 T_3 - \sigma_0 T_4)\, P_2}{P_1 T_2 - P_2 T_1}$$

$$A = \frac{(T - \sigma_1 T_3 - \sigma_0 T_4)\, P_1 - (P - \sigma_1 P_3 - \sigma_0 P_4)\, T_1}{P_1 T_2 - P_2 T_1}$$

Where P = the applied axial load
and T = the applied torque

where the subscripts "1", "2", and "3" again refer to the warp, fill and crossply directions, respectively. The "unit" solutions corresponding to a 10,000 lbf axial load, a 10,000 in-lbf torque, and a 1000 psi internal pressure are summarized in Table 9. For comparing measured to predicted data, the data from the three strain gages were averaged at each test point and these averaged values compared to the predictions. The comparisons are shown in Table 10.

All strain measurements did not agree with the predicted strains for the graphite/epoxy. The 45° strain measurements were not in good agreement for the tension and compression loading of the 45° helix cylinders. The measured strains were consistently higher than those predicted. The sensitivity study, Section III, E.5, for a C-C 45° helix cylinder offers possible explanation, particularly for any deviation of warp-fill direction or strain gage direction.

Strain readings had different signs. For example, the compression/internal pressure combined loading of 10 degree arc 0 degree helix specimen B-2-106-1 produced a measured negative strain of -81 micro-in. and the predicted was +17 micro-in. The inaccuracies at this level are considered insignificant and are likely a result of the difficulty in obtaining reproducible strain readings at such low strains. Similar small disagreements were shown for the torsion of the 10 degree arc 0 degree helix. The Z and θ predictions, Table 10, are zero for all load increments. Measured values from 0 to 49 micro-in were obtained for the hoop direction. Measured values for Z direction ranged from 116 to 156 micro-in. These positive values are average and could be attributed to low bending loads, but the values are very low, and the differences are not considered to be significant.

There are also some relatively large discrepancies between measured and predicted strain in the 3, θ, and 45 degree directions as shown

TABLE 9. UNIT SOLUTIONS, GRAPHITE/EPOXY CYLINDERS

Speciman Designation	Predicted Item [1]	10,000 lbf Axial	10,000 in-lbf Torque	1000 psi Internal Pressure
A	ϵ_z	2681	− 296	−4569
	ϵ_θ	−1433	− 291	8475
	$\gamma_{\theta z}$	− 678	1174	−2127
	ϵ_{45}	285	294	890
	σ_L	4867	4408	13,586
	σ_T	4852	−4249	14,621
	τ_{LT}	4744	− 47	−14,723
B	ϵ_z	568	0	− 71
	ϵ_θ	− 23	0	6733
	$\gamma_{\theta z}$	0	3801	0
	ϵ_{45}	273	1900	3331
	σ_L	9540	0	13
	σ_T	− 1	0	28,850
	τ_{LT}	0	−4299	0
C	ϵ_z	2681	− 293	−4426
	ϵ_θ	−1408	− 287	8838
	$\gamma_{\theta z}$	− 672	1271	−2070
	ϵ_{45}	301	346	1171
	σ_L	4850	4370	13,428
	σ_T	4846	−4221	14,203
	τ_{TL}	4746	− 3	−14,283

(1) Units on strains are micro-in. per in. (10^{-6} in./in.)

Units on stresses are lbf per sq. in. (psi)

Subscript "L" denotes warp direction

Subscript "T" denotes fill direction

TABLE 10. ASPC 3431 GRAPHITE/EPOXY CYLINDERS COMPARISONS OF MEASURED VS PREDICTED
OUTER SURFACE STRAINS (ALL STRAINS ARE MICRO-IN./IN.), SHEET 1 OF 2

Test Type	Specimen Designation	Loading			Measured			Predicted		
		Axial, lbf	Torsion[1] in.-lbf	Pressure, psi	ε_Z (Axial)	ε_θ (Hoop)	ε_{45}	ε_Z (Axial)	ε_θ (Hoop)	ε_{45}
Tension	A,-1-106-1	6452	-	-	1991	-1461	306	1730	-925	184
	A,-1-106-1	6926	-	-	1525	-	323	1856	-	197
	B,-2-106-1	9980	-	-	646	47	323	567	-23	272
	B,-2-106-1	30,270	-	-	1929	219	1016	1719	-70	826
	C,-3-106-1	7660	-	-	2624	-	469	2054	-	231
Compression	A,-1-106-1	-7016	-	-	-2122	-	-323	-1881	1005	-200
	A,-1-106-1	-6974	-	-	-2103	-	-283	-1870	-	-199
	B,-2-106-1	-7110	-	-	-490	109	-294	-404	16	-194
	B,-2-106-1	-5775	-	-	-406	47	234	-328	13	-158
	B,-2-106-1	-29,890	-	-	-2094	251	1161	-1698	69	-816
	B,-2-106-1	-6215	-	-	-432	43	302	-353	14	-170
	B,-2-106-1	-6275	-	-	-443	32	289	-356	14	-171
	C,-3-106-1	-5000	-	-	-1678	1283	297	-1341	704	-151
	C,-3-106-1	-6000	-	-	-1442	-	352	-1609	-	-181
Torsion (+ = CCW)	A,-1-106-1	-	+7983	-	12	-143	533	-236	-232	235
	A,-1-106-1	-	-8595	-	140	82	-428	254	250	-253
	A,-1-106-1	-	-15,786	-	315	782	-	467	459	-464
	B,-2-106-1	-	-7587	-	116	49	-2100	0	0	-1441
	B,-2-106-1	-	+8352	-	156	0	2400	0	0	1587
	B,-2-106-1	-	+8334	-	145	47	2411	0	0	1583
	B,-2-106-1	-	-8532	-	152	39	-2443	0	0	-1621
	C,-3-106-1	-	+8802	-	-83	192	572	-258	-253	305
	C,-3-106-1	-	+7893	-	-76	135	555	-231	-227	273
	C,-3-106-1	-	-8136	-	+62	-144	-570	238	234	-282
	C,-3-106-1	-	-8442	-	+72	-142	-583	247	242	-292

TABLE 10. ASPC 3431 GRAPHITE/EPOXY CYLINDERS COMPARISONS OF MEASURED VS PREDICTED OUTER SURFACE STRAINS (ALL STRAINS ARE MICRO-IN./IN.), SHEET 2 OF 2

Test Type	Specimen Designation	Loading			Measured			Predicted		
		Axial, lbf	Torsion(1) in.-lbf	Pressure, psi	ε_z (Axial)	ε_θ (Hoop)	ε_{45}	ε_z (Axial)	ε_θ (Hoop)	ε_{45}
Internal Pressure	B,-2-106-1	--	--	74	32	592	313	-5	498	246
	C,-3-106-1	--	--	139	-1034	1802	291	-615	1211	160
Tension & Pressure	A,-1-106-1	9,922	--	189	1507	292	905	1796	180	451
	B,-2-106-1	30,240	--	199	1968	1433	1968	1704	1270	1489
	B,-2-106-1	5,900	--	555	381	373	410	296	3723	2009
	C,-3-106-1	7,550	--	116	1682	396	718	1511	-38	363
Compression & Pressure	A,-1-106-1	-4,982	--	95	-2253	2043	-42	-1770	1519	-57
	B,-2-106-1	-5,870	--	53	-419	472	-81	-337	371	17
	B,-2-106-1	-29,830	--	200	-2169	1925	323	-1708	1414	-148
	C,-3-106-1	-4,506	--	82	-1830	2328	149	-1571	1359	-40
Torsion & Pressure	A,-1-106-1	--	23,589	111	-600	807	-1366	191	1627	793
	B,-2-106-1	--	-7,749	288	205	2373	1029	-20	1939	-513
	B,-2-106-1	--	-8,226	288	190	2416	1139	-20	1939	-718
	C,-3-106-1	--	-3,492	210	-1556	2570	178	-1032	1756	317
	C,-3-106-1	--	-3,747	218	-1633	2493	201	-1075	1819	385

in Table 10. Tension loading of the 45 degree helix cylinders produced up to 100 percent variations in 0 strain for the 45 degrees cylinders. Measured values were higher than predicted (-1756 micro-in./in. compared with -992 micro-in./in.) and (-2033 micro-in /in. compared with -1079 micro-in./in.). Similar results were obtained for compression loading; however, the discrepancy was not as large.

The measured 3 for the 45 degree helix is in better agreement with the tension and compression loading. The effect of variation in the helix angle was not determined for the graphite/epoxy either by testing or analytically. However, based on the sensitivity discussed below for carbon/carbon, additional testing for verification and more comprehensive sensitivity studies, including helix angles other than 0 and 45 degrees, are needed to satisfactorily resolve the large differences in the measured and predicted values for the high modulus graphite/epoxy material.

The torsion and combined torsion/pressure also produced some variations between predicted and measured strains. The measured 45 degree strains were generally higher than predicted. The 45 degree helix cylinders had measured strains of ∿ 500 micro in./in. and predictions were ∿ 250 to 300 micro-in./in. The 0 degree helix cylinder had measured strains of 2000 to 2500 micro in./in. with predictions from 1441 to 1621 micro-in./in., depending on the variation in load. The individual strain indications for the 3, 0, and 45 degree direction are shown in Table 10.

Agreement for combined torsion and internal pressure was comparatively good for most data points recorded. Measured values were generally higher than predicted.

Agreement was good for the two internal pressure tests. Measured values were only slightly higher than predicted. For the combined internal

pressure/tension and internal pressure/compression loadings, agreement between
the measured and predicted strains was satisfactory. Again, measured values
were generally higher than predicted values. The measured 45 degree strains
for the 45 degree helix cylinders were relatively low, but in some instances
almost twice the predicted values. These values again indicate the sensitivity
of the gage and fiber direction for the large helix angles of the undirectional
high modulus reinforced epoxy material.

2. Carbon/Carbon Cylinders

The carbon/carbon cylinders were analyzed using the cylinder
dimensions, Appendix A. The three combinations of helix and arc angle fabri-
cated for test and their designations and descriptions are summarized in the
table below:

K408A CARBON/CARBON CYLINDER DESCRIPTIONS

Specimen Designation	Helix Angle, Deg	Arc Angle, Deg	Ply Thickness, in.	Mean Number of Plys	Initial Arc Angle α_o, Deg
A	45	5	0.0125	99.2	4.64
B	0	10	0.0125	194.4	9.12
C	45	10	0.0125	189.0	8.68

The same laminate material properties were used for all carbon/carbon cylin-
ders. These nine elastic constants were:

$$E_{11} = 2.8 \times 10^6 \text{ psi} \qquad G_{12} = 0.63 \times 10^6 \text{ psi} \qquad \nu_{12} = 0.065$$

$$E_{22} = 1.7 \times 10^6 \text{ psi} \qquad G_{23} = 0.60 \times 10^6 \text{ psi} \qquad \nu_{13} = 0.290$$

$$E_{33} = 0.75 \times 10^6 \text{ psi} \qquad G_{13} = 0.76 \times 10^6 \text{ psi} \qquad \nu_{13} = 0.185$$

where subscripts "1", "2", "3" refer to the warp, fill, and crossply directions, respectively. For each specimen, a set of unit solutions, consisting of a 10,000 lbf axial load, a 10,000 in.-lbf torque and a 100 psi internal pressure was obtained. These unit solutions are summarized in Table 11. Table 12 shows the comparisons between the averaged strain values measured during the tests and the strain values predicted by the AFML computer code.

A summary of the Z and θ calculated and measured strains for the carbon/carbon material is presented in Tables 13 through 15. The data shown are for strain at failure, and agreement is not always good between predicted and measured for those loads in the 45 degree helix cylinders. Agreement is better at the intermediate loads, less than 75 percent of the ultimate, as shown in Table 12.

At the intermediate loads, the comparison of Z strains was very satisfactory for the tension loading. Only one measured versus predicted strain comparison varied as much as 15 percent. All others were less than 10 percent with three values less than 1 percent variation. The hoop and 45 degree strains for the tension loads were also very good. One 45 degree strain varied as much as 50 percent. This was for the 5 degree arc 45 degree helix cylinder. The effects of ± 5 degree helix variation on the sensitivity of a 45 degree helix cylinder is discussed below and provides an indication of a possible cause of the large differences between measured and predicted strain values at 45 degrees.

TABLE 11. UNIT SOLUTIONS, CARBON/CARBON CYLINDERS

Speciman Designation	Predicted Item	Load Condition		
		10,000 lbf Axial	10,000 in-lbf Torque	100 psi Internal Pressure
A	ε_θ	- 403	- 106	+4126
	ε_z	+1488	- 122	-1170
	$\gamma_{\theta z}$	- 293	+1120	- 912
	ε_{45}	+ 396	+ 297	+ 618
	σ_L	+1185	+1167	+3052
	σ_T	+1218	-1095	+3392
	τ_{LT}	+1192	- 9	-3318
B	ε_θ	- 65	0	+3916
	ε_z	+ 855	0	- 145
	$\gamma_{\theta z}$	0	+1780	0
	ε_{45}	+ 395	+ 890	+1886
	σ_L	+2393	0	+ 47
	σ_T	- 11	0	+6479
	τ_{LT}	0	+1111	0
C	ε_θ	- 401	- 103	+4124
	ε_z	+1488	- 121	-1162
	$\gamma_{\theta z}$	- 209	+1130	- 886
	ε_{45}	+ 266	+ 302	+ 692
	σ_L	+1186	+1158	+3013
	σ_T	+1217	-1087	+3330
	τ_{LT}	+1192	- 9	-3260

(1)   The interlaminar shear stresses are not shown; all values are less than 100 psi.

(2)   Units on strains are micro-inches per inch (10^{-6} in/in)

Units on stresses are psi

Subscript "L" denotes warp direction

Subscript "T" denotes fill direction

TABLE 12. K408A CARBON/CARBON CYLINDERS COMPARISONS OF MEASURED VS PREDICTED
OUTER SURFACE STRAINS (ALL STRAINS ARE MICRO-IN./IN.), SHEET 1 OF 3

Test Type	Specimen Designation	Loading		Percent of Failing Load	Measured			Predicted		
		Axial, lbf	Torsion in.-lbf		ϵ_Z (Axial)	ϵ_θ (Hoop)	ϵ_{45}	ϵ_Z (Axial)	ϵ_θ (Hoop)	ϵ_{45}
Tension	A-1-101-A	10,014	-	34.8	1442	-305	706	1490	-404	+307
	A-1-103-1,A$_2$	10,610	-	36.9	1550	-371	674	1579	-428	420
	B-2-101-1B$_2$	18,785	-	57.8	1590	-158	733	1606	-122	742
	B-2-103-1-,B$_2$	18,525	-	57.0	1620	-143	695	1584	-120	732
	C-3-101-1C	10,484	-	34.9	1324	-329	373	1560	-420	418
	C-3-103-1,C$_2$	10,765	-	35.9	1470	-371	456	1602	-432	429
	C-3-103-1,C$_2$	10,525	-	35.1	1625	-402	548	1566	-422	419
Compression	A-1-101-A	-10,030	-	31.0	-1407	312	-704	-1492	404	-397
	A-1-103-1,A$_2$	-10,615	-	32.8	-1492	315	-644	-1537	428	-420
	B-2-101-1B$_2$	-20,900	-	44.1	-1735	230	-596	-1787	136	-825
	B-2-101-1B	-20,915	-	44.1	-1749	142	-802	-1788	136	-826
	B-2-103-1,B$_2$	-21,050	-	44.4	-1791	157	-812	-1800	137	-831
	C-3-101-1C	-10,443	-	32.4	-1212	447	-293	-1554	419	-416
	C-3-101-1C	-10,484	-	32.5	-1272	390	-298	-1560	420	-418
	C-3-103-1,C$_2$	-10,945	-	33.9	-1432	300	-458	-1629	439	-412
	C-3-103-1,C$_2$	-10,470	-	32.5	-1462	320	-496	-1558	420	-405
	C-3-103-1,C$_2$	-10,445	-	32.4	-1457	323	-495	-1554	419	-416
Torsion	A-1-104-1,A$_3$,*	-	+10,692	17.6	-22	124	-674	130	113	-590
	A-1-105-1,A$_4$,*	-	+42,237	69.6	330	500	-3317	515	448	-2331
	A-1-105-1,A$_4$,**	-	-9,009	14.9	46	48	562	-110	-95	497
	B-2-104-1,B$_3$,*	-	10,908	30.2	-3	-12	747	0	0	971
	B-1-105-1,B$_4$,**	-	-9,603	26.6	-115	34	727	0	0	855
	C-3-104-1,C$_3$,*	-	11,520	25.1	-183	-188	578	-139	-119	522
	C-3-105-1,C$_4$,**	-	-10,260	22.4	-83	-52	443	-124	-106	465

*   Clockwise
** Counter Clockwise

TABLE 12. K408A CARBON/CARBON CYLINDERS COMPARISONS OF MEASURED VS PREDICTED OUTER SURFACE STRAINS (ALL STRAINS ARE MICRO-IN./IN.), SHEET 2 OF 3

Test Type	Specimen Designation	Loading			Measured			Predicted		
		Axial, lbf	Pressure psi	Percent Failing Load	ε_Z (Axial)	ε_θ (Hoop)	ε_{45}	ε_Z (Axial)	ε_θ (Hoop)	ε_{45}
Internal Pressure	A-1-102-1A	-	238	N.A.	-	776	388	-278	982	486
	A-1-103-1,A$_2$	-	228	N.A.	-32	729	417	-267	941	233
	B-2-102-1,B$_1$	-	261	37.0	81	879	501	-38	1022	492
	B-2-103-1,B$_2$	-	260	36.9	68	897	508	-38	1018	490
	C-3-102-1,C$_2$	-	163	20.2	-56	653	272	-189	672	169
	C-3-103-1,C$_2$	-	163	20.2	-73	510	145	-189	672	169
Tension and Pressure	A-1-101-A	9,962	240	--	1208	596	1103	1202	589	640
	A-1-103-1,A$_2$	10,642	233	--	1448	453	1157	1310	533	659
	B-2-101-1B	18,740	251	--	1258	795	1233	1564	900	1232
	B-2-103-1,B$_2$	14,903	211	--	1370	655	983	1243	729	987
	C-3-101-1C	10,484	165	--	1185	320	560	1368	260	589
	C-3-103-1,C$_2$	10,500	166	--	1358	245	623	1370	264	588

Test Type	Specimen Designation	Loading			Measured			Predicted		
		Axial, lbf	Torsion(1) in.-lbf	Pressure psi	ϵ_Z (Axial)	ϵ_θ (Hoop)	ϵ_{45}	ϵ_Z (Axial)	ϵ_θ (Hoop)	ϵ_{45}
Compression and Pressure	A-1-101-A	-9,862	--	236	-1546	1175	-219	-1744	1371	-149
	A-1-103-1,A_2	-10,660	--	232	-1683	1175	-168	-1858	1387	-264
	B-2-101-1B	-20,850	--	263	-1785	1115	-253	-1821	1166	-328
	B-2-103-1,B_2	-14,865	--	186	-1207	732	-200	-1298	631	-236
	C-3-101-1C	-10,485	--	171	-1300	1090	-48	-1759	1125	-241
	C-3-103-1,C_2	-10,470	--	163	-1575	945	-333	-1747	1092	-248
Torsion and Pressure	A-1-102-1A,*	--	10,251	237	-182	658	-338	-152	869	-324
	A-1-104-1,A_3*	--	11,241	225	-125	640	-340	-126	809	-391
	A-1-105-1,A_4*	--	11,493	230	87	150	833	-129	827	-399
	B-2-102-1,B_1*	--	10,314	263	79	937	-391	-33	1029	-422
	B-2-104-1,B_3*	--	10,629	258	+137	1177	-80	-37	1010	-460
	B-1-105-1,B_4*	--	11,025	254	-	60	-857	-37	995	-503
	C-3-104-1,C_4*	--	11,430	157	112	848	-333	-44	766	-355
	C-3-105-1,C_3**	--	9,504	158	205	760	-237	-69	750	-267

* Clockwise
** Counter Clockwise
(1) Percent failing load not shown for combined loading. There were no combined loadings to failure

TABLE 13. PREDICTED STRAIN VS MEASURED STRAIN AT FAILURE

CARBON/CARBON

Cylinder Construction	Load	Strain Micro Inches/inch			
		Predicted z	Measured z	Predicted θ	Measured θ
10° ARC 0° Helix	Axial Tension	2779	2747	-211	-320
	Axial Comp.	-4053	-4093	308	375
	Torsion Clockwise	0	-1080	0	+100
	Torsion Clockwise	0	-376	0	-422
	Hoop Tension 750 psi	-109	-512	2937	3122

TABLE 14. PREDICTED STRAIN VS MEASURED STRAIN AT FAILURE

Carbon/Carbon

Cylinder Construction	Load	Strain Micro Inches/inch			
		Predicted z	Measured z	Predicted θ	Measured θ
5° ARC 45° Helix	Axial Tension	4278	8750	-1159	-3075
	Axial Comp.	-4821	-5680	1306	2200
	Torsion Clockwise	740	580	643	925
	Torsion Counter Clockwise	-651	-238	-566	-1133
	Hoop Tension	N/A	N/A	N/A	N/A

TABLE 15. PREDICTED STRAIN VS MEASURED STRAIN AT FAILURE
CARBON/CARBON

Cylinder Construction	Load	Strain Micro Inches/inch			
		Predicted z	Measured z	Predicted θ	Measured θ
10° ARC 45° Helix	Axial Tension	4475	7775	-1206	-2800
	Axial Comp.	-4799	-6517	1293	2583
	Torsion Clockwise	501	1288	427	1150
	Torsion Counter Clockwise	-555	-1660	-473	-557
	Hoop	-935	-408	3320	4910

The Z compression strains were also in satisfactory agreement for the intermediate loads. One of the 10 degree arc 45 degree helix cylinders produced a measured strain 20 percent below predicted. The same test load on another 10 degree arc 45 degree helix cylinder produced a 10 percent variation, with the predicted higher than the measured value. As for the axial tension load, one of the 45 degree measured strains for the axial compression was approximately 50 percent greater than predicted. The remainder of the measured versus predicted strains for the 45 degree helix cylinders varied from 10 to 30 percent. The predicted versus measured for the 45 degree strains with axial compression loading of the 0 degree helix cylinders varied by 2 to 3 percent for two loadings and 30 percent for another loading.

For the combined loading of compression/internal pressure and tension/internal pressure, strains in the Z and 0 directions produced measured versus predicted variations from 0.5 percent to 20 percent, with most variations being less than 10 percent.

The measured maximum strains, 45 degree gages, for torsion testing varied from 5 to 50 percent. Agreement of predicted versus measured for the combined loading of torsion/internal pressure was satisfactory. The measured hoop strain for torsion tests compared favorably to the predicted strains. Variations were from 3 to 24 percent. Measured strains were not consistently above or below predicted strains.

Percentage deviation comparisons for the low strain reading 150 micro-in. or less were not made. The accuracy at low strain readings is questionable.

3. Nonlinear Behavior

The AFML computer code ROSETTE is based on elastic material properties whereas many companies exhibit nonlinear behavior. The type of inelastic

response to applied loads was observed in the test data obtained during this program. Large helix angles, 45 degrees to the load produced nonlinear stress/strain curves for both compression and tension loading. In an effort to improve predictions of strain at failure a simple inelastic analysis using a secant modulus approach was performed for a cylinder loaded in compression. The results of this analysis are discussed below.

The cylinder selected for analysis, 1153769-1-101A, has a 5 degree arc and a 45 degree helix angle. The load condition analyzed was a compression failure. The ultimate load at which this cylinder failed was 32,400 obf axial compression, or 3,850 psi in the cylinder wall. Table 16 shows the axial strain reading versus percent of ultimate load. Strain reading were obtained up to 93 percent of ultimate load. The rather large variance in the β strain gage readings above 50 percent of ultimate was characteristic of the 45 degree helix cylinder.

The approach taken was to make an initial baseline run using the linear material properties. The values of stress predicted were then used to intersect the appropriate stress/strain curve and a new estimate of the material constant was made. These revised material constants were then used to make a new prediction. The set of initial material constants used are described below and were based on flat laminate test:

$$E_{11} = 2.80 \times 10^6 \text{ psi} \qquad \nu_{12} = 0.065 \qquad G_{12} = 0.63 \times 10^6 \text{ psi}$$

$$E_{22} = 1.70 \times 10^6 \text{ psi} \qquad \nu_{13} = 0.185 \qquad G_{13} = 0.760 \times 10^6 \text{ psi}$$

$$E_{33} = 0.75 \times 10^6 \text{ psi} \qquad \nu_{23} = 0.29 \qquad G_{23} = 0.60 \times 10^6 \text{ psi}$$

where:

1 = warp, 2 = fill and 3 = cross-ply directions

The following stress/strain curves were used for the nonlinear analysis:

Description	Figure
σ_W vs. ε_W $\sim$ compression	47
σ_F vs. ε_F $\sim$ compression	48
σ_{XP} vs. ε $\sim$ compression	49
σ_W vs. ν_{WF}	50
σ_W vs. ν_{W-N}	51
ε_F vs. ν_{W-N}	52
τ_{W-F} vs. γ_{W-F} $\sim$ warp axial	53
τ_{W-N} vs. γ_{W-N} $\sim$ rail shear	54
τ_{F-N} vs. γ_{F-N} $\sim$ rail shear	55

where subscripts W, F, and N refer to the warp, fill and cross-ply directions respectively, and the Poisson's ratio, ν_{ij} , is defined as the strain in the "j" direction caused by a load in the "i" direction.

The measured strains at failure, projected from the measured strains at 93 percent of ultimate, for the 5° arc/45° helix cylinder were:

$$\varepsilon_z = -5680 \; \mu in./in.$$

$$\varepsilon_\theta = +2000 \; \mu in./in.$$

$$\varepsilon_{45°} = 2600 \; \mu in./in.$$

The initial elastic analysis predictions using the linear properties yielded the following results:
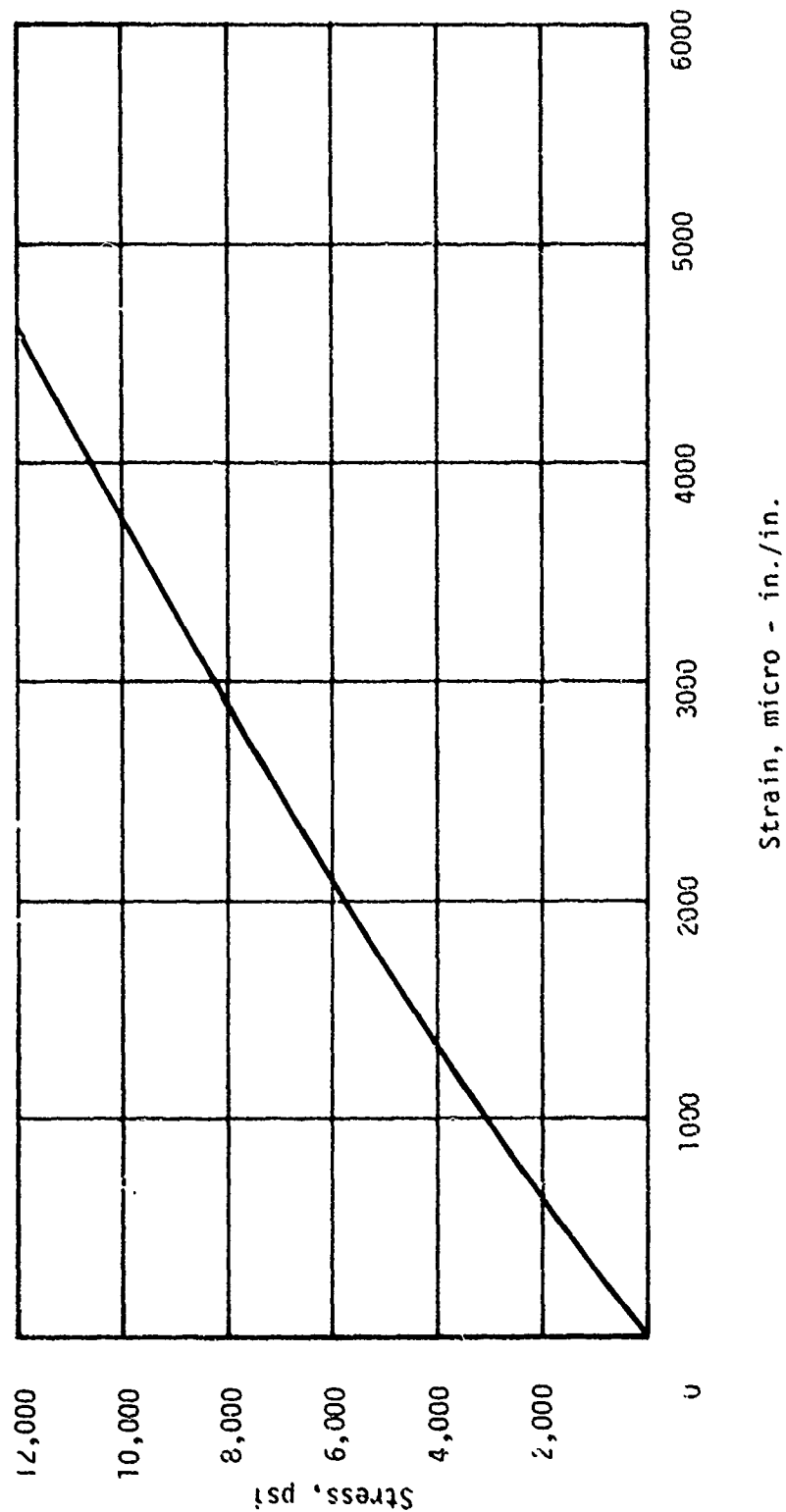
Figure 47. Typical Stress/Strain Curve for Carbon/Carbon Compression Loading – Warp Direction
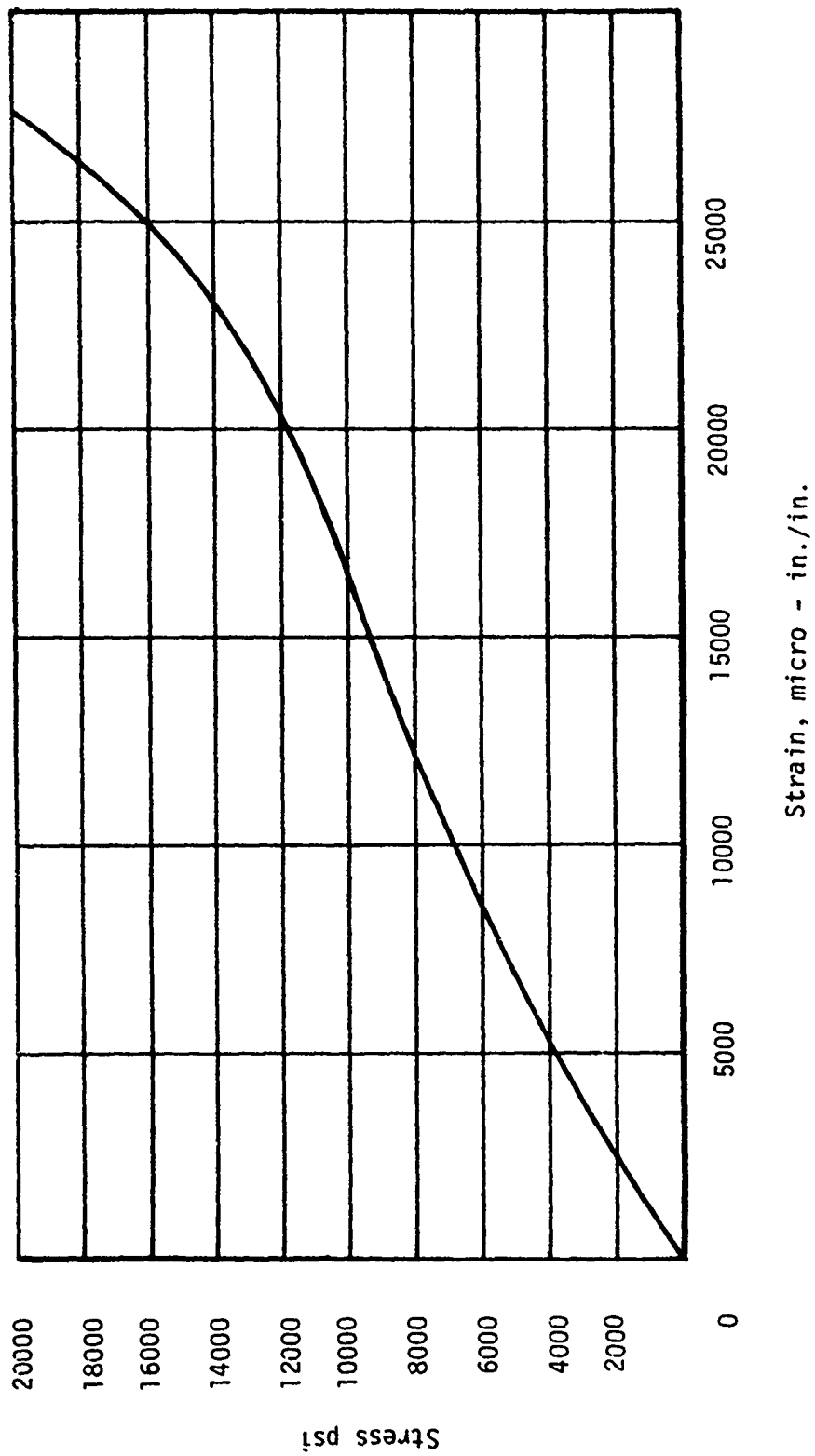
Figure 48. Typical Stress/Strain for Carbon/Carbon
Compression Loading - Cross Ply
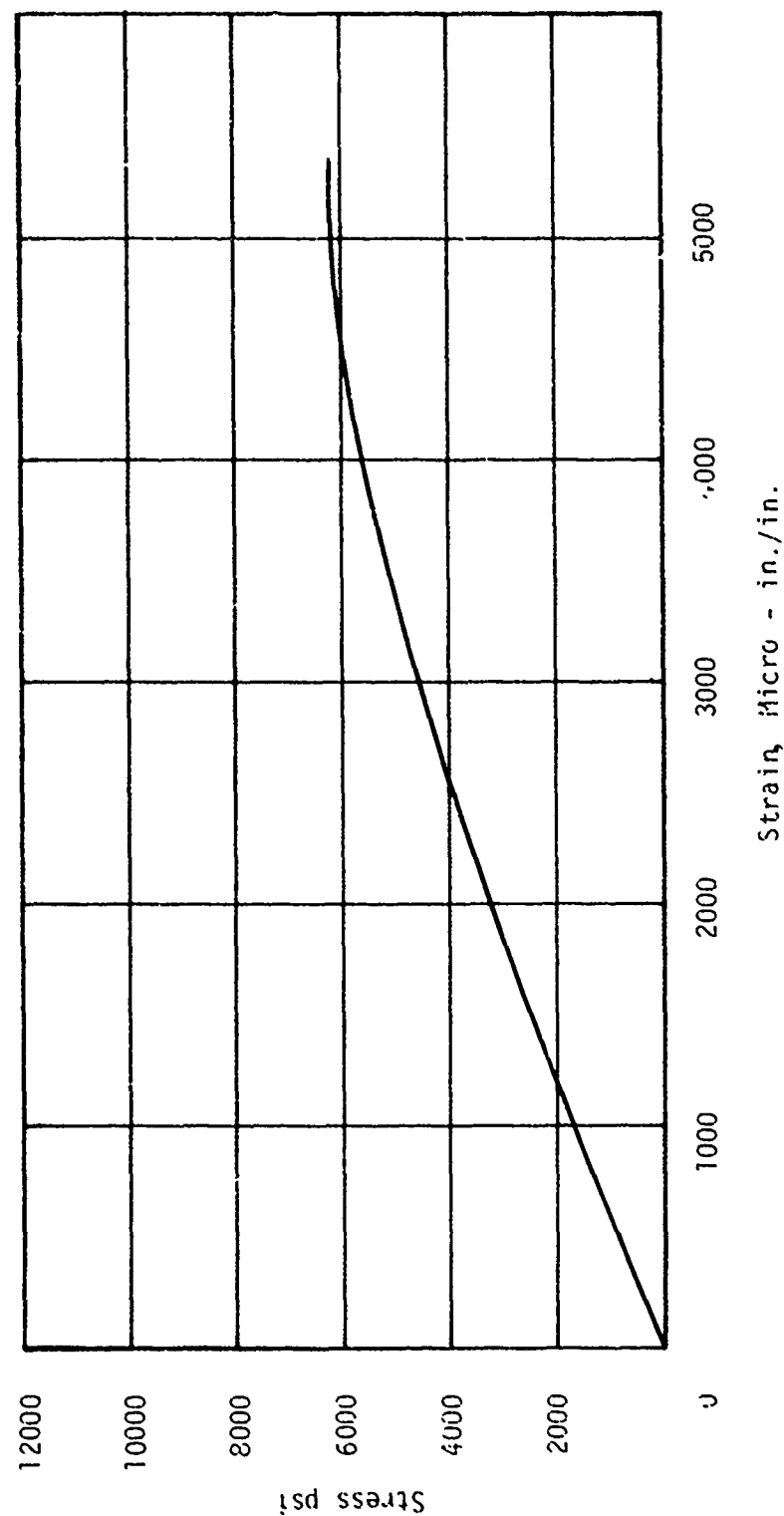
Figure 49. Typical Stress/Strain for Carbon/Carbon
Compression Loading – Fill Direction
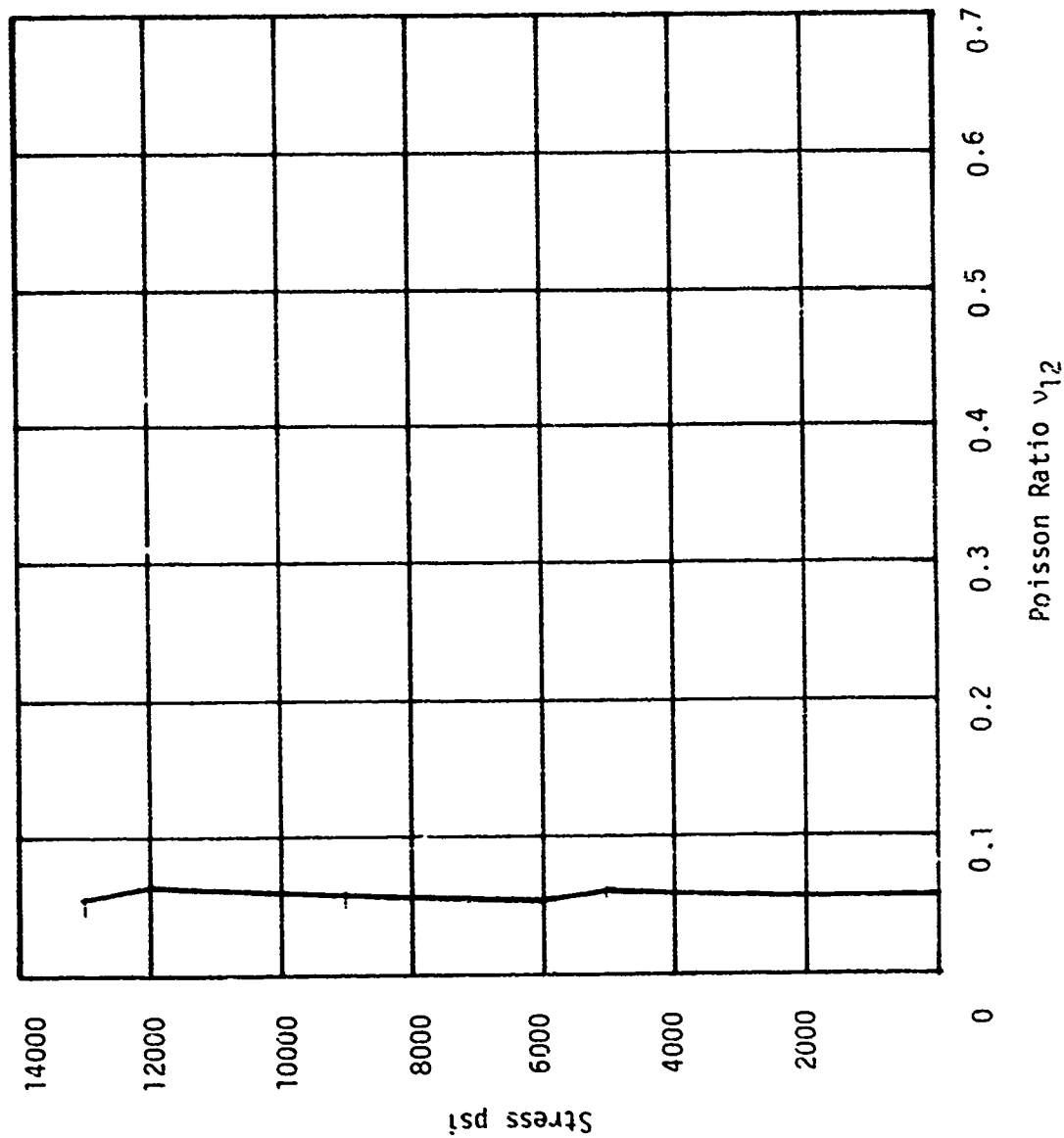
Figure 50. Poisson Ratio ν_{12} versus Stress Carbon/Carbon Compression Loading – Warp Direction
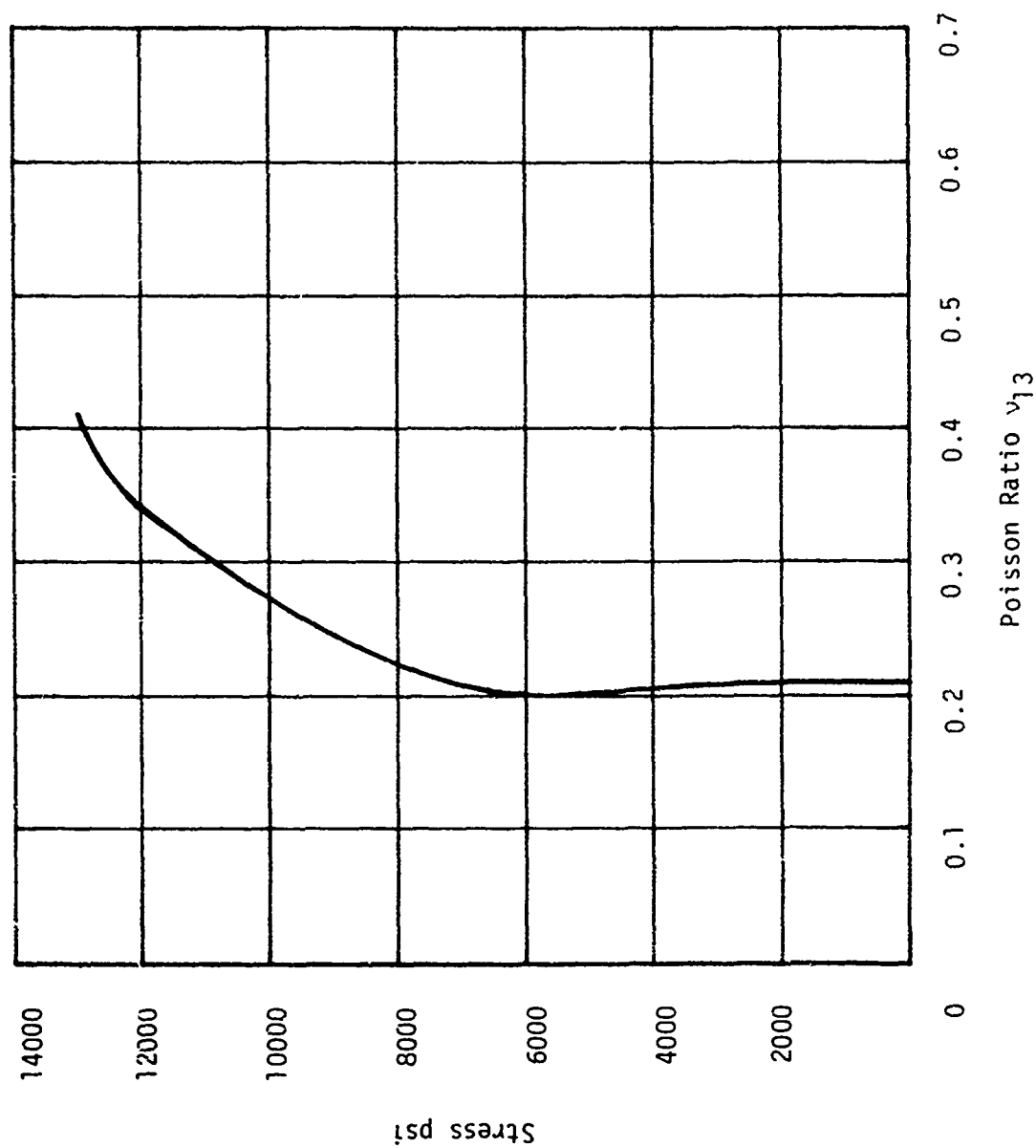
Figure 51. Typical Poisson Ratio ν_{13} versus Stress Carbon/Carbon Compression Loading – Warp Direction

Page 115
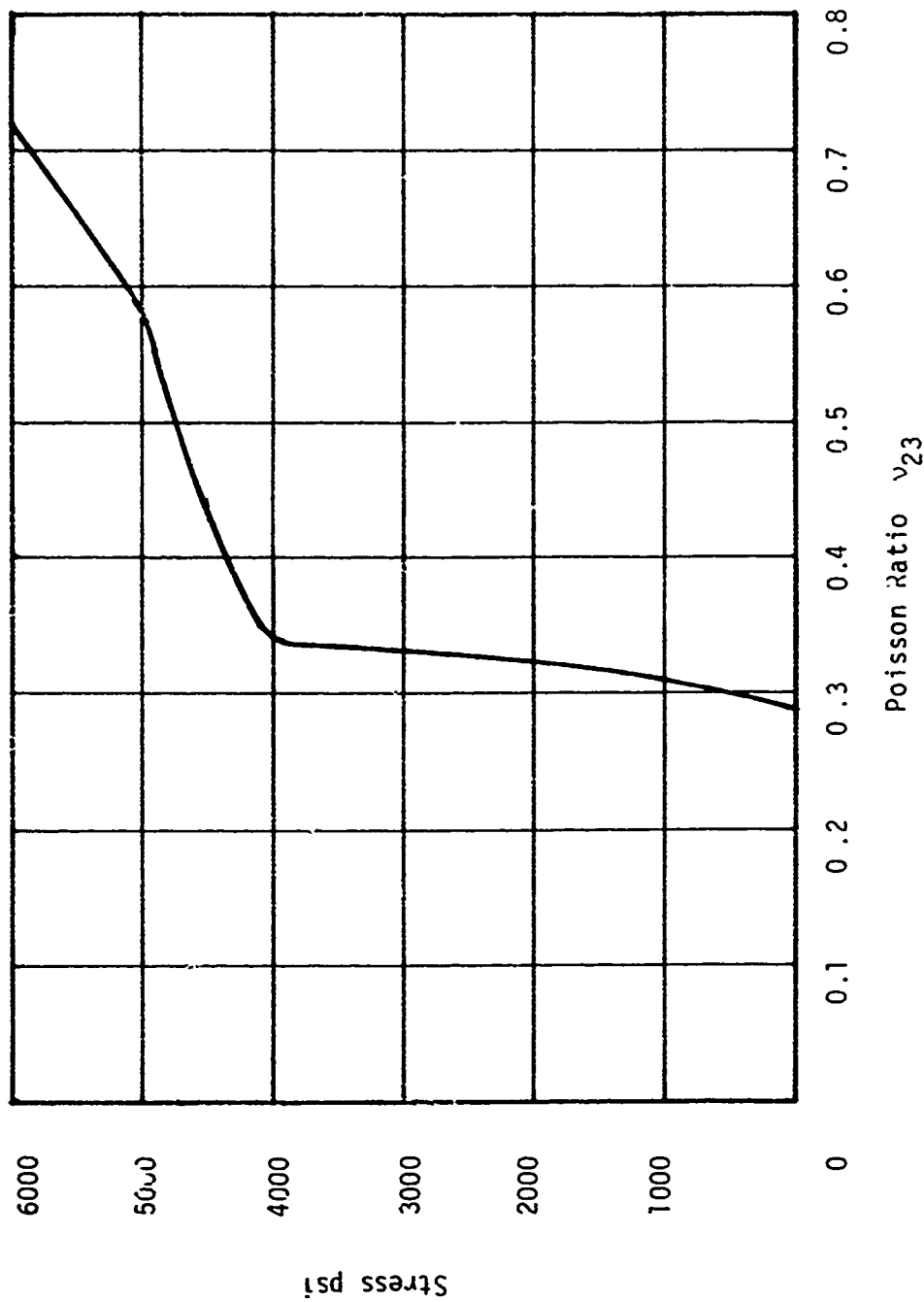
Figure 52. Typical Poisson Ratio ν_{23} Carbon/Carbon Compression Loading – Fill Direction

Figure 53. Typical Stress/Strain for Carbon/Carbon Torsion Loading – Shear Modulus Determination G_{12}
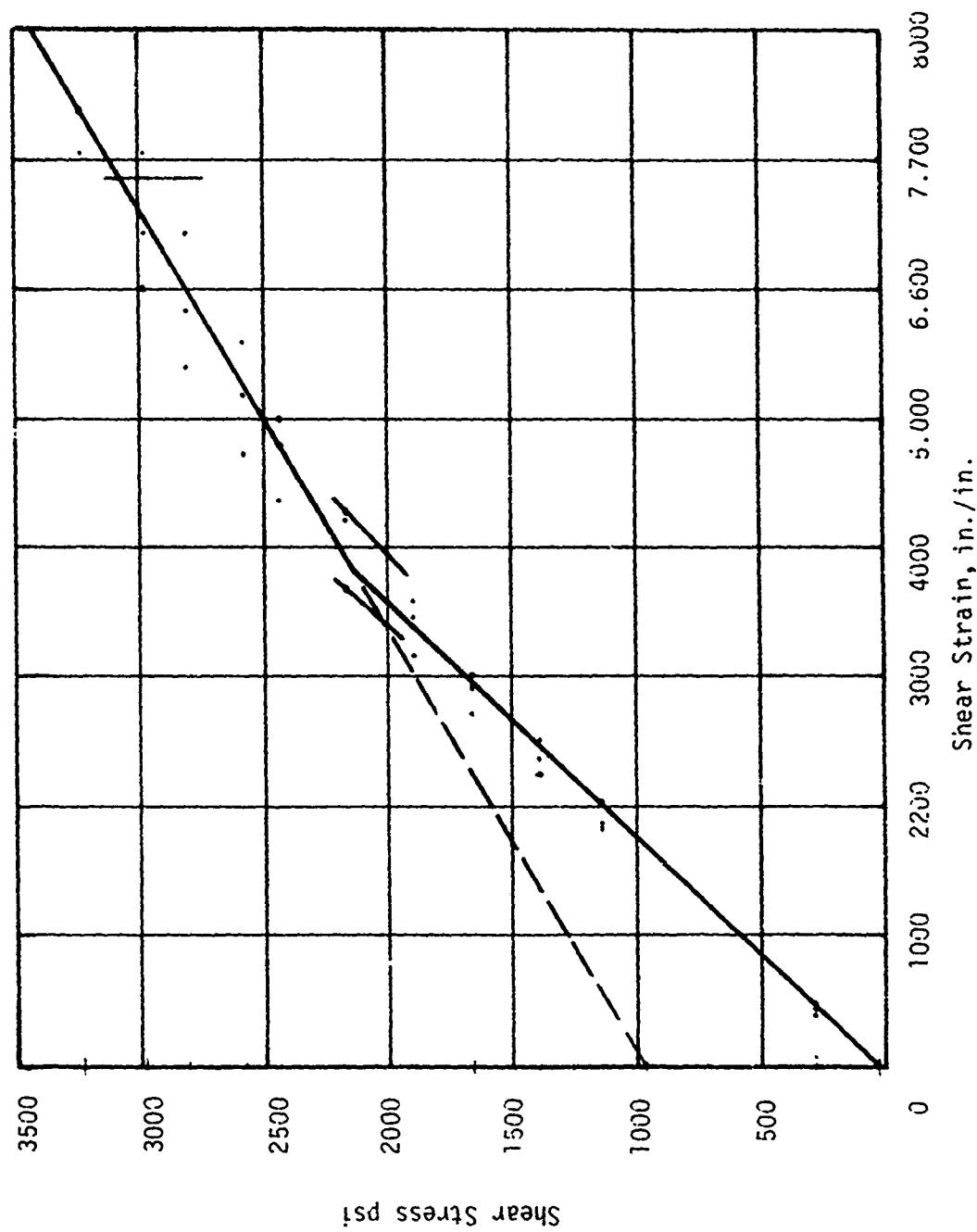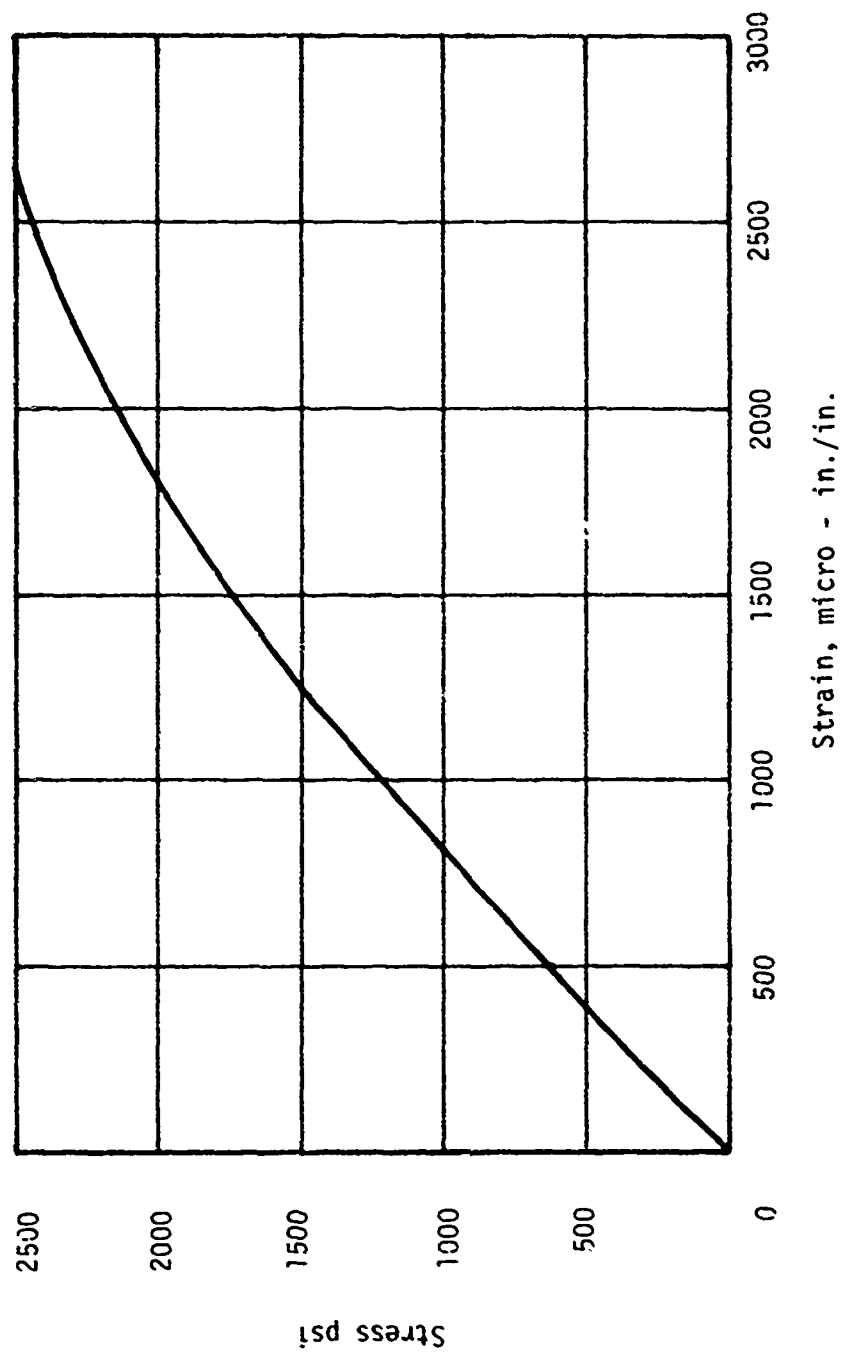
Figure 54. Typical Stress/Strain for Carbon/Carbon Interlaminar Shear (Rail Shear) loading –Warp Direction G_{13}
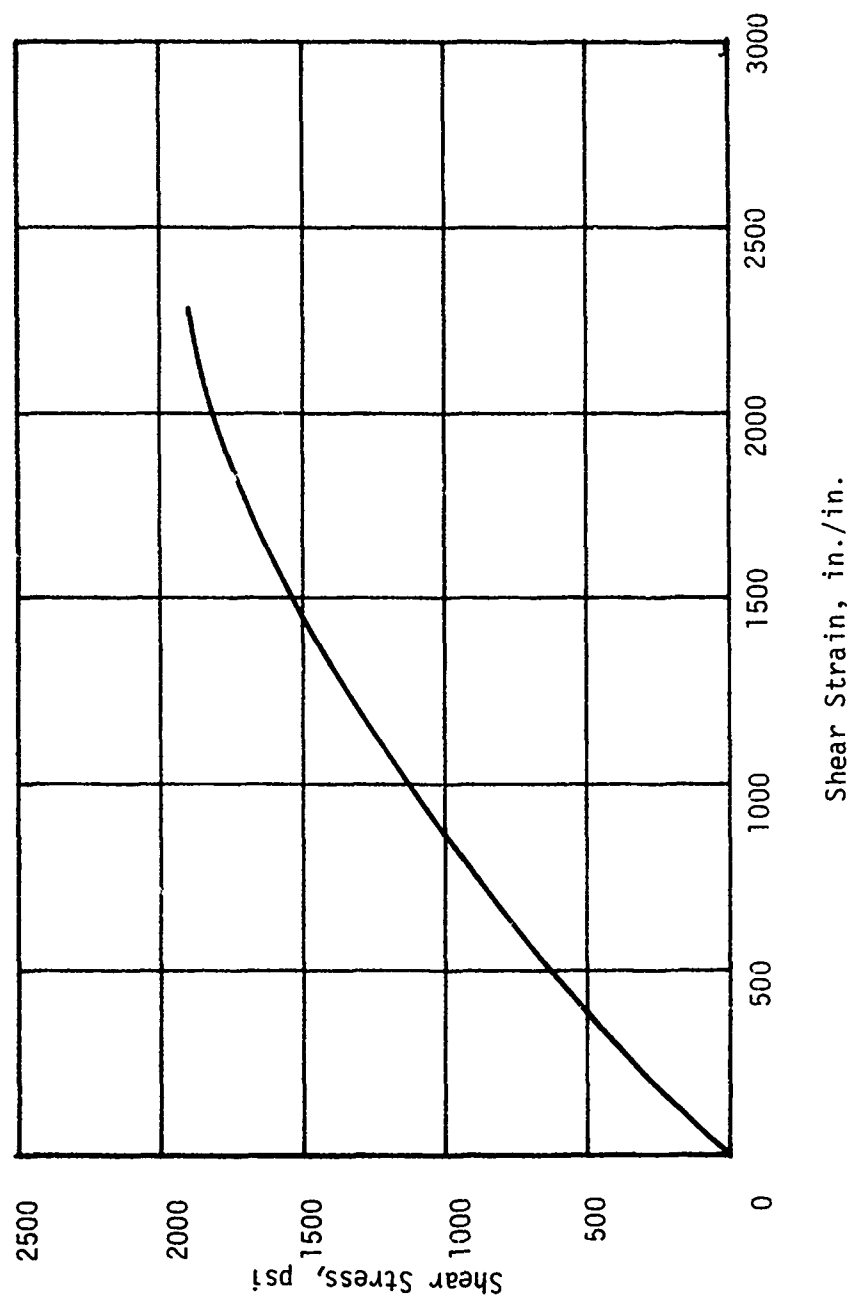
Figure 55. Typical Stress/Strain for Carbon/Carbon Interlaminar Shear (Rail Shear) Loading – Fill Direction – G_{23}

$$\sigma_W = -3847 \text{ psi} \qquad \tau_{LT} = 3859 \text{ psi}$$

$$\sigma_F = -3951 \text{ psi} \qquad \tau_{LN} = 0.70 \text{ psi}$$

$$\sigma_{XP} \simeq 0 \qquad \tau_{TN} = 5.00 \text{ psi}$$

Typical stress/strain curves for the nine material constants are shown in
Figures 47 through 55. The inspection of these figures indicates that only
the material constant G_{12}, Figure 53, requires correction based on the values
of stress. All other stress values are still in the initial portion of the
material constant curves. From Figure 53, the G_{12} stress/strain curve shows
that an τ_{LT} is approximately 8850μ"/in. The new G_{12} and the following results
obtained as interation number one.

$$\sigma_W = -3938 \text{ psi} \qquad \tau_{LT} = 3835 \text{ psi}$$

$$\sigma_F = -4009 \text{ psi} \qquad \tau_{LN} = 5.6 \text{ psi}$$

$$\sigma_{XP} \simeq 0 \qquad \tau_{TN} = 9.5 \text{ psi}$$

Again, the only material constant falling outside the linear range was G_{12}
(Figure 53). However, the difference between the initial solution (τ_{LT} = -3895
psi) and the first iteration (τ_{LT} = -3935 psi) does not result in a signifi-
cant change in G_{12} based on Figure 53. Therefore, an attempt was made to use
the predicted strains rather than stresses to obtain a better shear modulus
value. The initial run yielded the following values for strain:

$$\varepsilon_z = -5195 \text{ μin./in.}$$

$$\varepsilon_\theta = +1597 \text{ μin./in.}$$

$$\gamma_{z\theta} = 949 \text{ μin./in.}$$

From this the maximum strain is computed as:

$$\gamma_{max} = 6858 \ \mu in./in.$$

which from Figure 53 corresponds to a shear modulus of

$$G_{12} = 448,000 \ psi$$

Using this value of G_{12} for the revised iteration number one, yielded the following predictions:

$$\epsilon_z = -6105 \ \mu in./in.$$

$$\epsilon_\theta = +2445 \ \mu in./in.$$

$$\gamma_{z\theta} = 950 \ \mu in./in.$$

$$\gamma_{max} = 8603 \ \mu in./in., \ \tau_{LT} = 3837 \ psi$$

from which:

$$G_{12} = 446,000 \ psi,$$

or approximately the input, and approximately the same result obtained from using the predicted stress values. The comparison of measured to predicted results is shown below:

Interation Number	G_{12} (psi)	STRAINS $\sim \mu in./in.$			
		Predicted		Measured	
		ϵ_z	ϵ_θ	ϵ_z	ϵ_θ
0	568,000	-5195	+1597	-5690	+2000
1	448,000	-6105	+2445	-5690	+2000

These results show that the initial value used for G_{12} was too high, thus under-predicting the actual values while the attempt to force G_{12} to be on the stress/strain curve at the higher load levels resulted in values of strain too large. However, the use of the non-linear G_{12} improved the predictions and, in fact, made them conservative for both the Z and θ strains.

As discussed in Section III. E, the measured strain values at failure show significantly more variation than at one third or one half the failing load; therefore, the one data point obtained at failure cannot be assumed to be exact. This limited attempt at a non-linear analysis does not represent a sufficient sample size of the material properties and their normal variabilities to provide a valid test of the nonlinear analysis technique. An increase in the cylinder properties data base at failure is needed to validate any nonlinear analyses at failing loads.

This is shown as an example. Other configurations and loads would involve other nonlinear properties.

TABLE 16. STRAIN GAGE READING VS PERCENT OF ULTIMATE LOAD

(Ultimate Load = 32,400 lbf)

Load $\sim$ %	Strain Gage Readings $\sim 10^{-6}$ in./in.			
	#3	#7	#11	Averaged
0	0	0	0	0
25	-1050	-1200	-1000	-1083
50	-2025	-2500	-2130	-2218
75	-3120	-4130	-3500	-3583
85	-3870	-5033	-4556	-4486
92.6	-4339	-4183	-6608	-5377

4. Prediction of Cylinder Failure

This section discusses the methods used to predict various failures in both the carbon/carbon and graphite/epoxy test cylinders. For each of the three helix/arc angle combinations, a carbon/carbon cylinder was failed in tension, compression, internal pressure, and clockwise and counterclockwise torsion. For the graphite/epoxy, two cylinders were failed in compression only.

The same set of unit solutions were used to predict the cylinder failure as to predict its elastic response, only now the stress values were used to predict whether or not failure had occurred. One failure criterion was employed, maximum stress theory. The maximum stress theory simply states that the stresses in the principal material directions must be less than the respective laminate strengths. Otherwise, failure is assumed to have occurred. This theory is actually three subcriteria and does not account for any interaction between modes of failure in a specimen.

a. Graphite/Epoxy Cylinders

The ultimate strengths for the graphite/epoxy material are summarized below:

Strength Component	Ultimate Stress, psi
Fill-Tension	41,500
Fill-Compression	73,000
Warp-Tension	190,000
Warp-Compression	140,000
Warp/Fill Shear	17,200

For the graphite/epoxy cylinder, only two were tested to failure, both in compression. No other failure tests were run of the graphite/epoxy cylinders. The results of these two compression failure tests are shown in Table 17. Similar to the carbon/carbon failure data, Table 18, margins of safety are calculated for each stress in the principal material directions. As can be seen

TABLE 17. AEROJET 3431 GRAPHITE/EPOXY CYLINDERS COMPARISON OF MEASURED VERSUS
PREDICTED FAILURE (ALL STRESSES ARE LBS PER SQ IN. PSI) (2)

Type of Failure	Specimen Designation & Ultimate Load	% Load	Warp			Fill			Warp-Fill-Shear		
			Stress	Allowable	MS[1]	Stress	Allowable	MS[1]	Shear Stress	Allowable	MS[1]
Compression	A-1-106-1	25	-3261	-140,000	+42.0	-5251	-73,000	+21.0	3178	17,200	+4.4
		50	-6522	-140,000	+20.0	-6502	-73,000	+10.0	6357	17,200	+1.7
		75	-9783	-140,000	+13.0	-9753	-73,000	+6.0	9535	17,200	+0.8
	-26,800	100	-13949	-140,000	+10.0	-13003	-73,000	+4.0	12714	17,200	+0.35
Compression	C,-3-106-1	25	-3383	-140,000	+40.0	-3380	-73,000	+20.0	3310	17,200	+4.0
		50	-6766	-140,000	+19.0	-6760	-73,000	+9.0	6621	17,200	+1.5
		75	-10149	-140,000	+12.0	-10140	-73,000	+6.0	9931	17,200	+0.7
	-27,900	100	-13532	-140,000	+9.0	-13520	73,000	+4.0	13241	17,200	+0.3

(1) Negative values indicate failure

(2) Interlaminar Shear Stress (NL) was less than 50 psi for the compressive load at failure.

TABLE 18. K408A CARBON/CARBON CYLINDERS COMPARISON OF MEASURED VERSUS PREDICTED FAILURE, SHEET 1 OF 5

Type of Designation & Failure Ultimate Load	% Load	Warp			Fill			Warp-Fill-Shear			Interlaminar Shear (NL) (2)		
		Stress	Allowable	MS(1)	Stress	Allowable	MS(1)	Shear Stress	Allowable	MS(1)	Shear Stress	Allowable	MS
Tension A-1-103-1,A₂													
28,750 lbf	25	852	9951	+10.7	875	5670	+5.5	857	3487	+3.1	-	1420	-
	50	1703	9951	+4.8	1751	5670	+2.2	1714	3487	+1.03	-	1420	-
	75	2555	9951	+2.9	2626	5670	+1.2	2570	3487	+0.36	-	1420	-
	100	3407	9951	+1.9	3502	5670	+0.6	3427	3487	+0.018	-	1420	-
B-2-101-1B													
32,500 lbf	25	1944	9951	+4.12	9	5670	++	0	3487	-	-	1420	-
	50	3889	9951	+1.56	18	5670	++	0	3487	-	-	1420	-
	75	5833	9951	+0.71	27	5670	++	0	3487	-	-	1420	-
	100	7777	9951	+0.28	36	5670	++	0	3487	-	-	1420	-
C-3-101-1C													
30,074	25	892	9951	+10.2	915	5670	+5.2	896	3487	+2.89	-	1420	-
	50	1783	9951	+4.6	1830	5670	+2.1	1792	3487	+0.95	-	1420	-
	75	2675	9951	+2.72	2745	5670	+1.07	2689	3487	+0.3 (0.0 at 97.3% of ultimate)	-	1420	-
	100	3567	9951	+1.79	3660	5670	+0.55	3585	3487	-0.027	-	1420	-

(1) Negative values indicate failure
(2) Values for Interlaminar less than 50 psi are not shown.

TABLE 18. K408A CARBON/CARBON CYLINDERS COMPARISON OF MEASURED VERSUS
PREDICTED FAILURE, SHEET 2 OF 5

Type of Designation & Failure Ultimate Load	Load	Warp			Fill			Warp-Fill-Shear			Interlaminar Shear (IL)		
		Stress	Allowable	MS(1)	Stress	Allowable	MS(1)	Shear Stress	Allowable	MS(1)	Shear Stress	Allowable	MS
Compression													
A-1-101-4 32,400 lbf	25	-960	-13,727	+13.3	-987	-6333	+5.4	966	3487	+2.6	-	1420	-
	50	-1920	-13,727	+6.2	-1973	-6333	+2.2	1931	3487	+0.81	-	1420	-
	75	-2880	-13,727	+3.8	-2960	-6333	+1.1	2897	3487	+0.20	-	1420	-
	100	-3839	-13,727	+2.6	-3946	-6333	+0.6	3862	3487	-0.097	-	1420	-
		(0.0 at 121% of ultimate)						(0.0 at 90.3% of ultimate)					
B-2-103-1,E$_2$ 47,400 lbf	25	-2836	-13,727	+3.84	-13	-6333	++	0	3487	-	-	1420	-
	50	-5671	-13,727	+1.42	-26	-6333	++	0	3487	-	-	1420	-
	75	-8507	-13,727	+0.61	-39	-6333	++	0	3487	-	-	1420	-
	100	-11343	-13,727	+0.21	-52	-6333	++	0	3487	-	-	1420	-
C-3-103-1,C$_2$ 32,250 lbf	25	-956	-13,727	+13.4	-981	-6333	+5.5	961	3487	+2.63	-	1420	-
	50	-1912	-13,727	+6.2	-1962	-6333	+2.23	1922	3487	+0.81	-	1420	-
	75	-2869	-13,727	+3.8	-2944	-6333	+1.15	2883	3487	-0.21	-	1420	-
	100	-3325	-13,727	+2.6	-3925	-6333	+0.61	3844	3487	-0.093	-	1420	-
								(0.0 at 91% of ultimate)					

(1) Negative values indicate failure

Type of Designation & Failure Ultimate Load	Load	Warp			Fill			Warp-Fill-Shear			Interlaminar Shear (ILL)		
		Stress	Allowable	MS[1]	Stress	Allowable	MS[1]	Shear Stress	Allowable	MS[1]	Shear Stress	Allowable	MS[1]
Internal Pressurization Test Not Run, A	25	-	9951		-	5670		-	3487		-	1420	-
	50	-	9951		-	5670		-	3487		-	1420	-
	75	-	9951		-	5670		-	3487		-	1420	-
	100	-	9951		-	5670		-	3487		-	1420	-
B-2-102-1, 750 psi	25	+9	9951		1215	5670	+3.7	0	3487	-	-	1420	-
	50	+18	9951		2430	5670	+1.33	0	3487	-	-	1420	-
	75	+27	9951		3644	5670	+0.56	0	3487	-	-	1420	-
	100	+35	9951		4859 (0.0 at 117% of ultimate)	5670	+0.17	0	3487	-	-	1420	-
C-3-102-1,C, 805 psi	25	606	9951	+15.4	670	5670	+7.5	-656	3487	+4.3	139	1420	-
	50	1213	9951	+7.2	1370	5670	+3.23	-1312	3487	+1.66	279	1420	-
	75	1819	9951	+4.5	2010	5670	+1.82	-1968	3487	+0.77	418	1420	-
	100	2425	9951	+3.1	2681	5670	+1.1	-2624	3487	+0.33	558	1420	+1.5

(1) Negative values indicate failure

TABLE 18. K408A CARBON/CARBON CYLINDERS COMPARISON OF MEASURED VERSUS
PREDICTED FAILURE, SHEET 4 OF 5

Type of Failure	Designation & Ultimate Load	Load	Warp			Fill			Warp-Fill-Shear			Interlaminar Shear (iL)		
			Stress	Allowable	MS[1]	Stress	Allowable	MS[1]	Shear Stress	Allowable	MS[1]	Shear Stress	Allowable	MS[1]
Clock-wise Torsion (fill fiber in tension)	A-1-105-1, A$_4$ 60,660 in-lbf	25	-1770	13727	+6.7	1661	5670	+2.4	14	3487	++	103	1420	-
		50	-3540	13727	+2.8	3321	5670	+0.71	27	3487	++	205	1420	-
		75	-5309	13727	+1.6	4982	5670	+0.14	41	3487	++	308	1420	-
		100	-7079	13727	+0.94	6642 (0.0 at 85% of ultimate)	5670	-0.15	55	3487	++	410	1420	+2.4
	B-1-105-1, B$_4$ 36,090 in-lbf	25	0	13727	-	0	5670	-	1003	3487	+2.4	162	1420	-
		50	0	13727	-	0	5670	-	2005	3487	+0.74	323	1420	-
		75	0	13727	-	0	5670	-	3007	3487	+0.16	485	1420	-
		100	0	13727	-	0	5670	-	4010 (0.0 at 87% of ultimate)	3487	-0.13	646	1420	+1.2
	C-3-105-1, C$_4$ 45,900 in-lbf	25	-1329	13727	+9.3	1247	5670	+3.5	11	3487	++	148	1420	-
		50	-2658	13727	+4.2	2495	5670	+1.2	21	3487	++	296	1420	-
		75	-3986	13727	+2.4	3742	5670	+0.51	31	3487	++	444	1420	-
		100	-5315	13727	+1.6	4989	5670	+0.14	41	3487	++	592	1420	+1.4

(1) Negative values indicate failure

Page 128

TABLE 18. K408A CARBON/CARBON CYLINDERS COMPARISON OF MEASURED VERSUS
PREDICTED FAILURE, SHEET 5 OF 5

Type of Failure	Specimen Designation & Ultimate Load	Load	Warp			F111			Warp-Fill-Shear			Interlaminar Shear (TtL)		
			Stress	Allowable	MS(1)	Stress	Allowable	MS(1)	Shear Stress	Allowable	MS(1)	Shear Stress	Allowable	MS(1)
Counter Clockwise Torsion (Warp fiber in tension)	A-1-104-1,A₃ 53,370 in-lbf	25	1557	9951	+5.4	-1461	-6333	+3.3	-12	3487	++	91	1420	-
		50	3114	9951	+2.1	-2922	-6333	+1.2	-24	3487	++	182	1420	-
		75	4671	9951	+1.1	-4383	-6333	+0.44	-36	3487	++	273	1420	-
		100	6228	9951	+0.6	-5844 (0.0 at 108% of ultimate)	-6333	+0.08	-48	3487	++	363	1420	+2.9
	B-2-104-1,B₃ 39,474 in-lbf	25	0	9951	-	0	-6333	-	-1096	3487	+2.1	177	1420	-
		50	0	9951	-	0	-6333	-	-2193	3487	+0.59	353	1420	-
		75	0	9951	-	0	-6333	-	-3289	3487	+0.06	530	1420	-
		100	0	9951	-	0	-6333	-	-4386 (0.0 at 80% of ultimate)	3487	-0.20	707	1420	+1.0
	C-3-104-1,C₃ 41,436 in-lbf	25	1200	9951	+7.3	-1126	-6333	+4.6	-9	3487	++	134	1420	-
		50	2399	9951	+3.1	-2252	-6333	+1.8	-19	3487	++	267	1420	-
		75	3599	9951	+1.7	-3378	-6333	+0.87	-28	3487	++	401	1420	-
		100	4798	9951	+1.07	-4504 (0.0 at 141% of ultimate)	-6333	+0.4	-37	3487	++	535	1420	+1.6

(1) Negative values indicate failure

Page 129

from Table 17 the predictions were very unconservative in that they showed positive margins of safety at the test failure load. The most likely failure mode, based on the analysis, is warp-fill shear. The agreement was not satisfactory for the graphite/epoxy. Failure loads were lower than anticipated because of possible buckling and the low fiber volume. Therefore, the analysis was not continued.

b. Carbon/Carbon Cylinders

The ultimate stresses and strains for the carbon/carbon materials are summarized below. All values shown are averaged values.

Strength Component	Ultimate Stress, psi	Ultimate Strain, 10^{-6} in./in.
Fill-Tension	5,670	3,900
Fill-Compression	6,333	4,983
Warp-Tension	9,951	3,915
Warp-Compression	13.727	5,758
Warp/Fill Shear	3,487	7,305

Table 19 shows the measured and predicted stress levels for the carbon/carbon material at failure for each cylinder configuration for each type of failure. Stresses shown are in the plane of the laminate (warp-fill plane) at the outer radius of the cylinder. Analysis showed that maximum stresses do not always occur at the outer surfaces. However, measurements were taken on the outer surfaces, and warp, fill, and warp-fill shear stresses are shown and each is compared with the allowable values shown above, and a margin of safety (M.S.) is computed. If the margin of safety is less than or equal to zero, failure is predicted. Table 18 shows a comsiderable variation of the accuracy of the failure predictions. For example, for Cylinder C, in the tension test, the predicted failure was at 97 percent of the actual ultimate load whereas, in the compression test, the maxiumu stress theory predicted

failure at 91 percent of ultimate. Within a given test type, the accuracy of the prediction varied with the cylinder layup. For example, in the counter-clockwise torsion test, the predicted load at failure, based on a maximum stress theory, was 108 percent of ultimate for the fill fiber in Cylinder A, 141 percent of ultimate for Cylinder C, and 80 percent of ultimate warp-fill shear for Cylinder B. The worst agreement was for the internal pressurization test and for Cylinder B, while the best agreement for all tests was obtained on Cylinder C.

In those cases where any criteria indicated failure at a level lower than the actual, the predictions were interpolated to indicate what the predicted value would be at failure. The values are noted in Table 18 below the 10 percent load prediction.

5. Sensitivity Studies for a C-C Cylinder

Sensitivity studies were limited; however, some sensitivity studies were made to show effects of elastic constant variation and helix angle variation. The variations selected for evaluation were ± 20 percent for the elastic constants and ± 5 degrees for the helix angle.

The number of cylinders tested to failure was limited to one for each type of uniaxial load. The comparison of measured versus predicted values used elastic constants based on the averages from laminate and tube tests. Furthermore, these average values were generally obtained from stress values; therefore, statistical range of property variation could not be ascertained with any confidence. An arbitrary range of ± 20 percent was selected to determine effects of variation about the average for all nine material constants.

The results compared with the nominal prediction of stress in the warp and fill yarn of the 5 degree arc 45 degree helix cylinder

are shown in Table 19. Also shown are the nominal shear stress warp-fill
(W-F) and the interlaminar shear at the measured failing load of 32,000 lb.

The variation in warp fiber compressive stress at the
load of 32,000 lb. for a +20 percent E_{11}, E_{22}, or E_{33} is rather small. Max-
imum variation in warp fiber stress is +92 psi for a 20 percent reduction in
E_{22} and -61 psi for a 20 percent increase in E_{22}. Similar results, although
with less variation, were obtained for the fill stress with ± 20 percent
change in E_{22} and E_{11}. The ± 20 percent change in E_{33} produced no change in
warp or fill fiber stress. Changes in warp-fill shear and interlaminar shear
stresses were insignificant for the ± 20 percent change in E_{11}, E_{22}, and E_{33}.

The ± 20 percent variation of ν_{12}, ν_{13}, and ν_{23} produced
less than 20 psi change in warp and fill compressive stress. The warp-fill
shear stress and interlaminar shear had even less variation for the ± 20 per-
cent variation in Poisson's ratio. G_{12} was the only shear modulus which
showed any effect on warp or fill compressive stress from the ± 20 percent
variation. Changes were small, less than 100 psi. Variation in G_{12} also
produced very small changes in warp-fill shear stress and interlaminar shear
stress.

From these determinations, it appears that the computed
stress of the 5 degree arc 45 degree helix is rather insensitive to ± 20 per-
cent change in any of the elastic constants. The G_{12} at -20 percent of the
obtained average reduced the warp-fill shear stress from -3837 to -3820 psi.
Although the warp-fill shear stress is the most likely failure mode, the 17
psi decrease in stress is less than 1 percent of the total warp-fill stress.
It would be difficult to isolate any effects on ultimate compressive strength
of the cylinder from this small change.

It is believed that results similar to those shown in Table 19 would be obtained for tensile testing of the 5 degree arc 45 degree helix cylinder and also for both compression and tension testing of the 10 degree arc 45 degree helix cylinder.

The sensitivity of model predictions of fiber compressive stress, warp-fill shear stress, and interlaminar shear stress is more for a ± 10 percent change in helix angle than for the ± 20 percent change in elastic constants. The stress values for the fiber stress in the warp and fill direction are shown in Table 20. The +5 degree helix angle change produces approximately 600 psi decrease in warp fiber stress and the -5 degree helix angle change produces approximately 600 psi increase in warp fiber stress. Similar results were obtained for the predicted fill fiber stress.

The warp-fill iber shear stress and interlaminar shear stress are affected much less by the +5 degree helix change as shown in Table 20.

As discussed in Section III, D2, closer control than ±5 degree helix angle on the fill yarns is not likely feasible using current fabric conversion, prepreg, and lay-up processing procedures. As the warp-fill fiber shear stress approaches the allowable stress level, control of the helix angle effects becomes significant.

Current designs using graphite/epoxy and C-C material should take into account the effects of this degree of non-uniformity.

Some empirical verification of this predicted phenomenon is needed, particularly at the 45 ± 5 degree helix angle and also at the 15 ± 5 degree helix angle, as this might be a steeper part of the curve for both materials. Furthermore, the current trend in fabrication of exit cones

TABLE 19. EFFECTS OF ± 20 PERCENT CHANGES IN CONSTANTS ON CALC -
LATED STRESS VALUES AT FAILING COMPRESSION LOAD FOR
DEGREE ARC 45 DEGREE HELIX CARBON/CARBON CYLINDER (1)

	σ_L (warp)	σ_T (fill)	τ_{LT} (W-F shear)	τ_{NL} (ILS)
Nominal	-3926	-4001	-3837	-5.0
C_{11} +20%	-3028	-4022	-3832	-5.0
C_{11} -20%	-3924	-3970	-3844	-4.0
C_{22} +20%	-3988	-4024	-3828	-8.0
E_{22} -20%	-3834	-3978	-3851	-1.0
C_{33} +20%	-3926	-4001	-3837	-5.0
E_{33} -20%	-3926	-4001	-3837	-5.0
ν_{12} +20%	-3928	-4002	-3837	-5.0
ν_{12} -20%	-3924	-4000	-3837	-5.0
ν_{13} +20%	-3921	-3998	-3839	-5.0
ν_{13} -20%	-3932	-4005	-3835	-5.0
ν_{23} +20%	-3912	-3993	-3842	-4.0
ν_{23} -20%	-3940	-4010	-3832	-6.0
G_{12} +20%	-3863	-3961	-3853	-0.5
G_{12} -20%	-4021	-4062	-3820	-11.0
G_{13} +20%	-3926	-4001	-3837	-5.0
G_{13} -20%	-3926	-4001	-3837	-5.0
G_{23} +20%	-3926	-4001	-3837	-5.0
G_{23} -20%	-3926	-4001	-3837	-5.0

(1) The nominal values used are from laminate moduli and poissons
ratio at failing loads.

TABLE 20. EFFECTS OF ± 5 DEGREE CHANGE IN HELIX ANGLE ON CALCULATED
STRESS VALUES AT FAILING COMPRESSION LOAD FOR 5 DEGREE
ARC 45 DEGREE HELIX CYLINDER

Helix Angle Degrees	σ_L (warp)	σ_T (fill)	τ_{LT} (W-F shear)	τ_{NL} (ILS)
45	-3926	-4001	-3937	-5.0
40	-3330	-4613	-3738	-9.0
50	-4513	-3381	-3787	-0.0

has been toward complicated ply pattern with a significant change (45 degree) in helix angle ID to OD. Techniques for analyzing these effects are needed.

Work is in progress by AFML and PDA to extend this work to involute exit cones that will aid in the analysis of the changing helix angle for the more complicated ply patterns.

SECTION IV

CONCLUSIONS

Notwithstanding variability of individual solutions, the AFML involute computer code was verified as a useful tool for predicting behavior of involute composite cylinders under uniaxial and combined loads using linear elastic laminate properties. Specific differences in the predicted versus measured strains were as high as 100 percent; however, the general variability was less than ±10 percent.

Development of photomicrograph standards appears to be feasible for both test panel and tag-end samples.

A tentative but promising non-linear analysis has been presented.

The thin wall tubes were not satisfactory for obtaining ultimate compressive strengths. Values obtained were from 30 to 40 percent lower than the laminate for both graphite/epoxy and carbon/carbon tubes loaded parallel to warp fibers.

The program test matrix did not provide empirically supported sensitivity studies; however, limited analytical studies indicate warp and fill fiber stress, warp-fill shear stress, and interlaminar shear stress are sensitive to ±5 degree variation in the 45 degree helix angle.

A ±20 percent variation in material elastic constants makes relatively small (less than 3 percent) differences in the predicted warp or fill fiber stress, warp-fill shear, and interlaminar shear stress for compression loading of a 45 degree helix cylinder.

Prediction of cylinder behavior from laminate properties requires the following:

1. Warp and fill alignment be within ±5 degrees or better.

2. Load be transmitted uniformly into the specimen.

3. Preloading and checkout to assure uniform loading for the cylinders. (Less than 10 percent variation for initial loading was achieved; however, some variation at failure was greater than 10 percent.)

4. Laminate and cylinder material should have the following:

   a. Same density
   b. Ply thickness
   c. Fiber volume factor
   d. Matrix condition

The cylinder test length was questionable for the internal pressure loading and required sensitive alignment of pins to prevent non-uniform strain in compression and tension loading.

SECTION V

RECOMMENDATIONS

Additional sensitivity evaluation should be conducted. All types of loading and variation of elastic constants and currently used arc and helix angles should be analyzed with empirical validation of selected parameters.

Further evaluation of the use of photomicrographs is recommended as a technique to assure reproducibility for both in-processing steps and the final processing for carbon/carbon materials.

The increase of cylinder length should be considered for any subsequent cylinder testing where loading is introduced by shear pins in the cylinder wall. This would reduce or eliminate effects of misalignment caused by pin/hole mismatch.

Further examination for non-linear behavior similar to that reported herein should be conducted to verify the applicability of the AFML involute computer code at involute structures experience in solid rocket applications.

Additional analysis and methods of treatment for the non-linear behavior of involutes, particularly with high arc and helix angles, should be conducted for all types of loading.

The program for cylinders should be expanded and continued to include combined loading to failure of involute cylinders.

REFERENCES

1. Pagano, N.J., "Elastic Response of Rosette Cylinders Under Axi-symmetric Loading" AIAA Journal, Vol. 15, No. 2, Feb. 1977 pp. 159-166.

2. AFML TR-69-311

3. MX Upper Stage Motor Advanced Development Program, Volume XI, Part 2, Material Properties, Composites, Plastics, Elastomers

4. MX Upper Stage Motor Advanced Development Program, Volume XI, Part 1, Material Properties, Carbon/Carbon

5. Data Reported by G. Lucido, Kaiser Aerotech, Telephone Conversation February 1979.

6. Computer Code received from N.J. Pagano, AFML, Feb. 4, 1977

APPENDIX

TEST SPECIFICATION CONFIGURATION

The uniaxial test specimens, tube, cylinder configuration and an example of a cutting plan are contained in this section. The same specimen design was used for the graphite/epoxy and carbon/carbon material. In some instances thickness was reduced for the stronger and stiffer graphite/epoxy material.

A.   CUTTING PLAN

The cutting plan for the 6 by 3 by 3 in. laminates is shown in Figure A-1. The plan shown is for warp yarns in the 6 in. direction. Similar plans were used for the fill direction and the 0.250 in. laminates.

B.   LAMINATE AND TUBE UNIAXIAL TEST SPECIMENS

The tensile specimen is shown in Figure A-2. The specimen is a standard dog-bone shape and is 9 in. in length. The ends are tab with glass/epoxy for testing.

The compression specimen is also shown in Figure A-2, and is dog-bone in shape. It is 6 in. shorter with a reduced tab and section, which is mounted into the compression test fixture. This specimen produced good results for both graphite/epoxy and carbon/carbon laminates.

The crossply tensile specimen, Figure A-3, is 3 in. in length and is subsequently bond into end supports for attaching in the test machine. Alignment into these supports is very critical toward obtaining good crossply tensile results. A modification of this specimen was also used. A straight section of 0.5 by 0.5 by 3.0 in. was bonded into the end supports. Results were good, and the specimen machining losses were eliminated.

The crossply compression specimen is not shown. The standard ASTM D695, D3410 (AFML TR-67-332) was used. Crossply compression was not obtained for the graphite/epoxy.

The rail shear specimen is shown in Figure A-4. The specimen was designed in accordance with AFML-TR-69-311. The specimen was used to test shear and measure shear modulus in the G_{13} and G_{23} direction for both the graphite/epoxy and the carbon/carbon materials.

The notched shear specimen is shown in Figure A-7. The standard ASTM-D2345 specimen was used. The specimen and test procedure are also shown in AFML-TR-332, Supplement I, Structural Plastics Application Handbook. Both the graphite/epoxy and carbon/carbon materials were tested with warp and fill parallel to the load direction. Supports were used to reduce bending.

The tube specimen, shown in Figure A-8 was the same for both of the materials. The specimen was satisfactory for the torsion test and fill compression testing of the carbon/carbon. It was not satisfactory for ultimate compression strength of the graphite/epoxy or the warp strength of the carbon/ carbon. The specimen was used as the source for G_{12} and G_{21} shear moduli. Poisson's ratio ν_{12} and ν_{21} were also determined from compression loading of the tube.

C.   CYLINDER SPECIMENS

The cylinder test specimens for the graphite/epoxy and carbon/carbon materials are shown in Figures A-7 and A-10, respectively. The only difference between the two specimens is the test section wall thickness. The graphite/epoxy has a nominal wall thickness of 0.074 in. The carbon/carbon wall was made thicker, nominal 0.295 in.
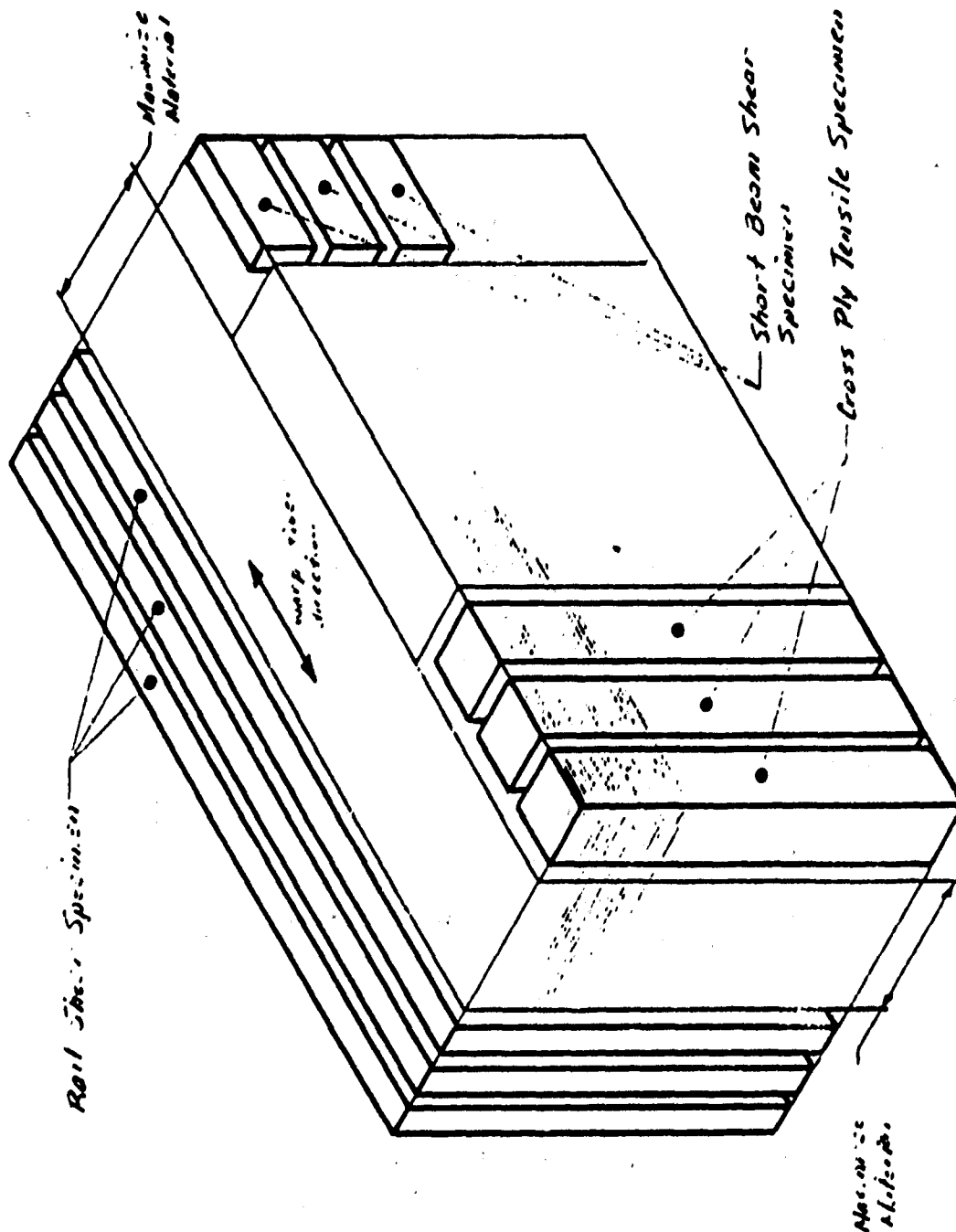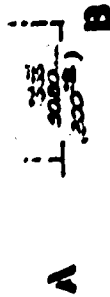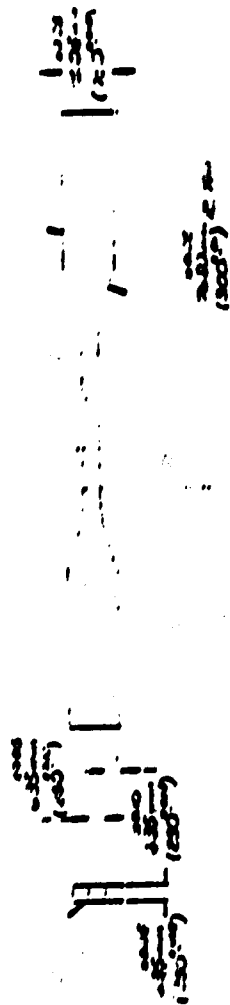
Figure A-1. Cutting Plan for Carbon/Carbon Laminate — Warp in 6 inch Direction.

Figure A-2. Laminate Tension and Compression Test Specimen
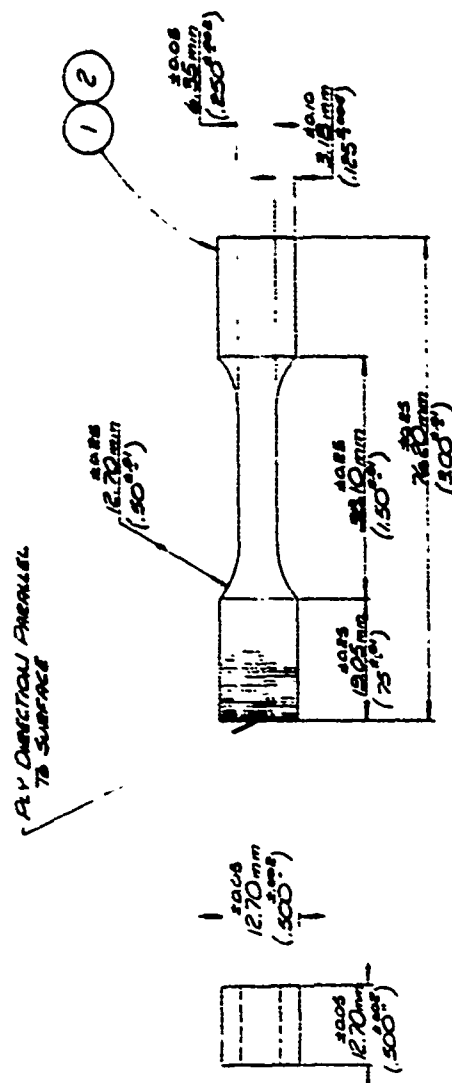Used for Both Warp and Fill Direction Testing

Figure A-3. Crossply Tensile Specimen Used for Graphite/
Epoxy and Carbon/Carbon Materials

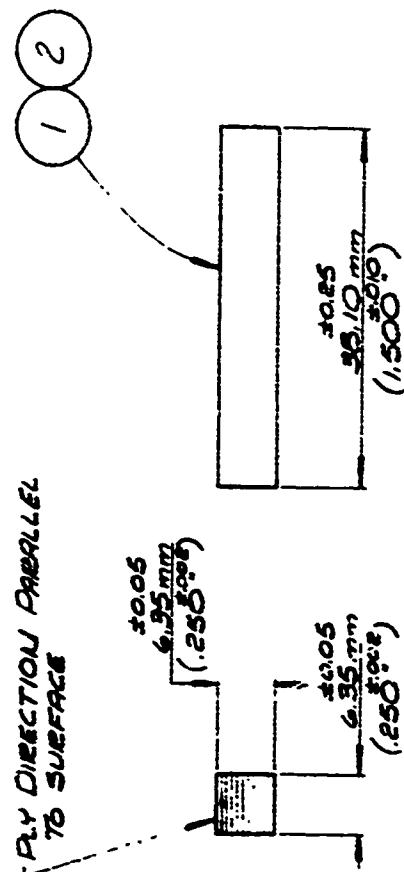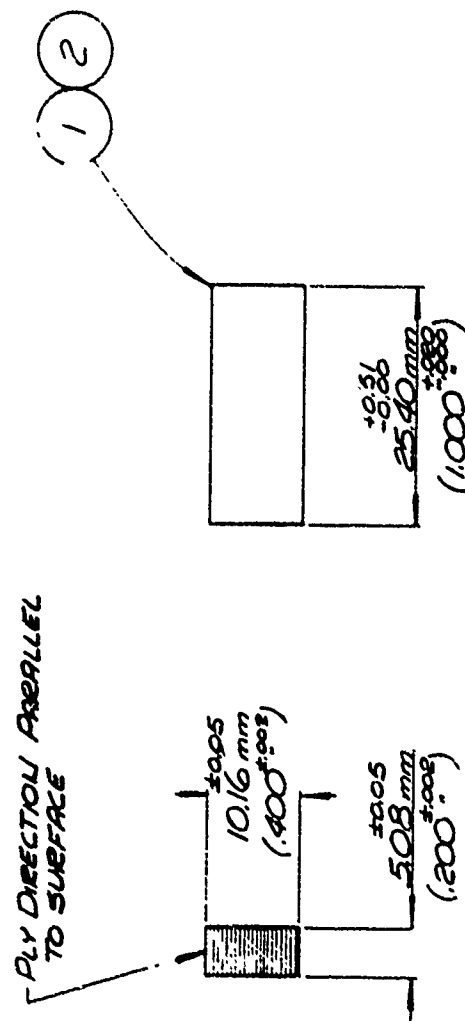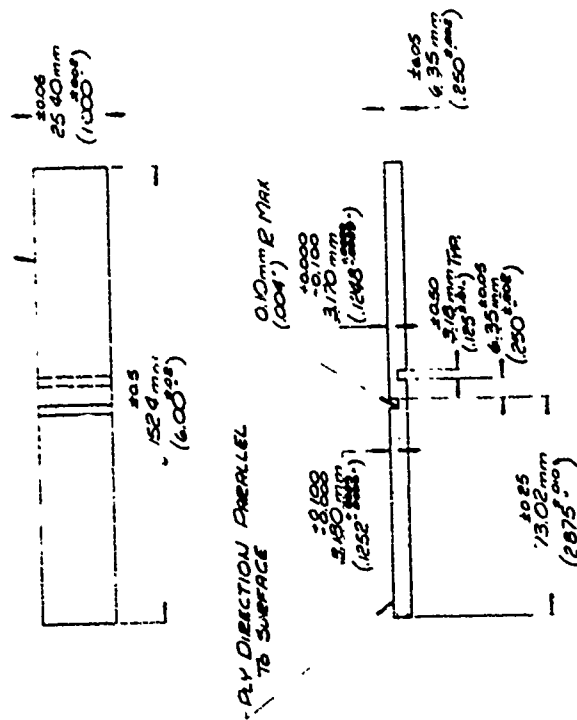Figure A-4. Rail Shear Specimen Used for Graphite Epoxy and Carbon/Carbon Materials — Source of G_{13} and G_{23} and Ultimate Shear Stress

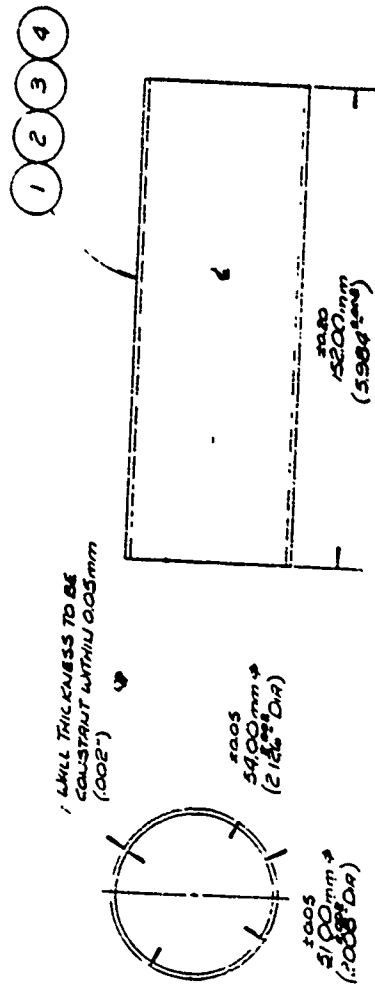Figure A·5. Short Beam Shear Specimen for Graphite/Epoxy Laminate Test

Figure A-6. Short Beam Specimen Shear for Carbon/Carbon Laminate Test

Figure A-7. Notched Interlaminar Shear Specimen Used
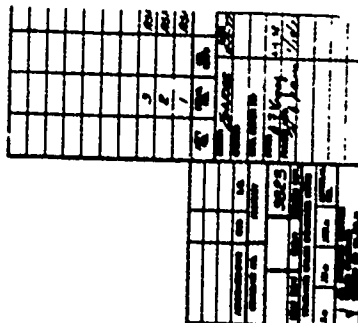for Graphite/Epoxy and Carbon/Carbon
Materials

Figure A-8. Thin Wall Tube Specimen for Graphite/
Epoxy and Carbon/Carbon Materials

Figure A-9. Test Cylinder Configuration for Graphite/
Epoxy Involute Structure

Figure A-10. Test Cylinder Configuration for Carbon/Carbon Involute Structure